NASA Tech Briefs

Transferring Technology to American Industry and Government

October 1989
Volume 13 Number 10

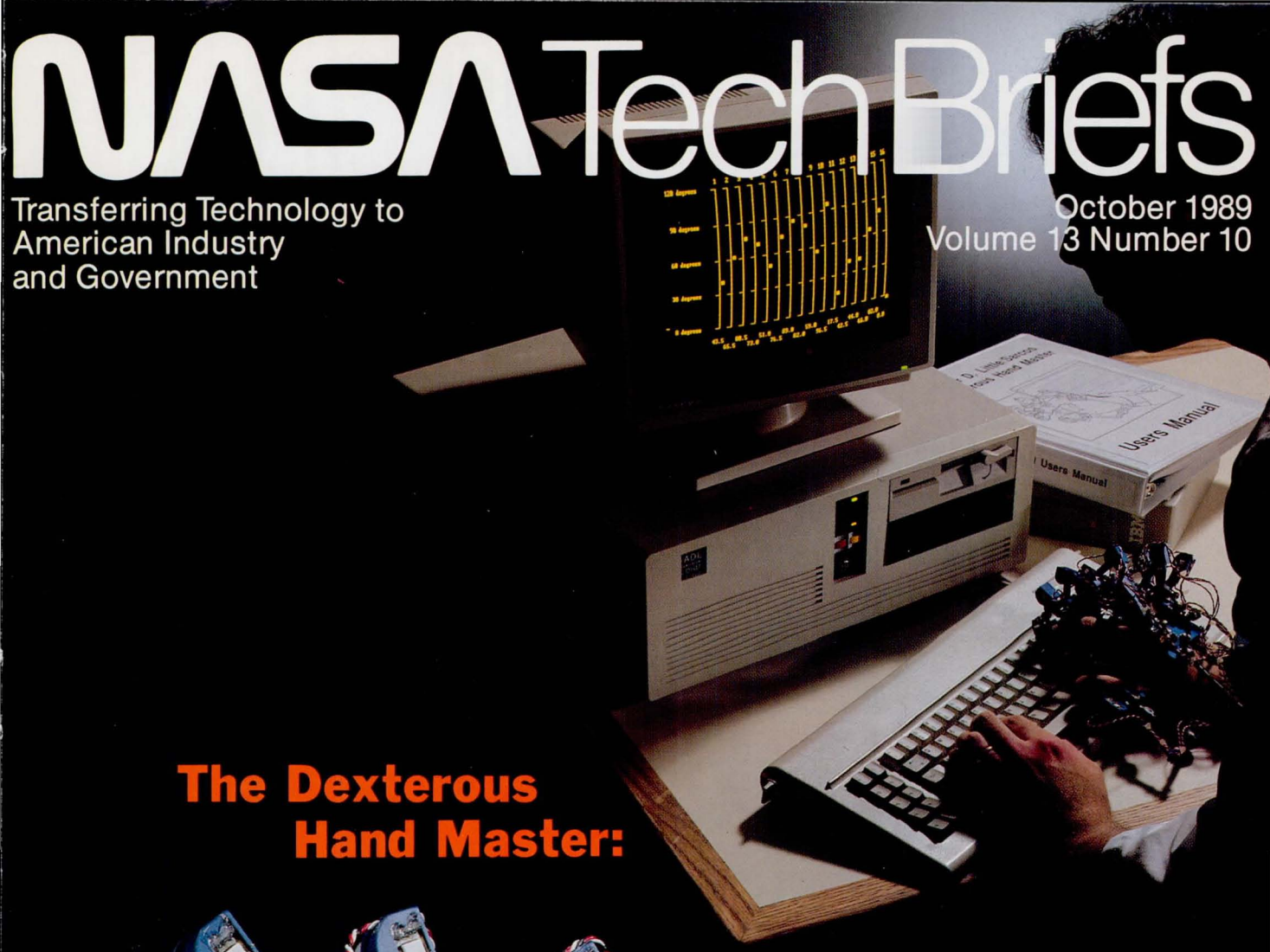

The Dexterous Hand Master:

New Invention Enables Machines To Simulate Human Actions

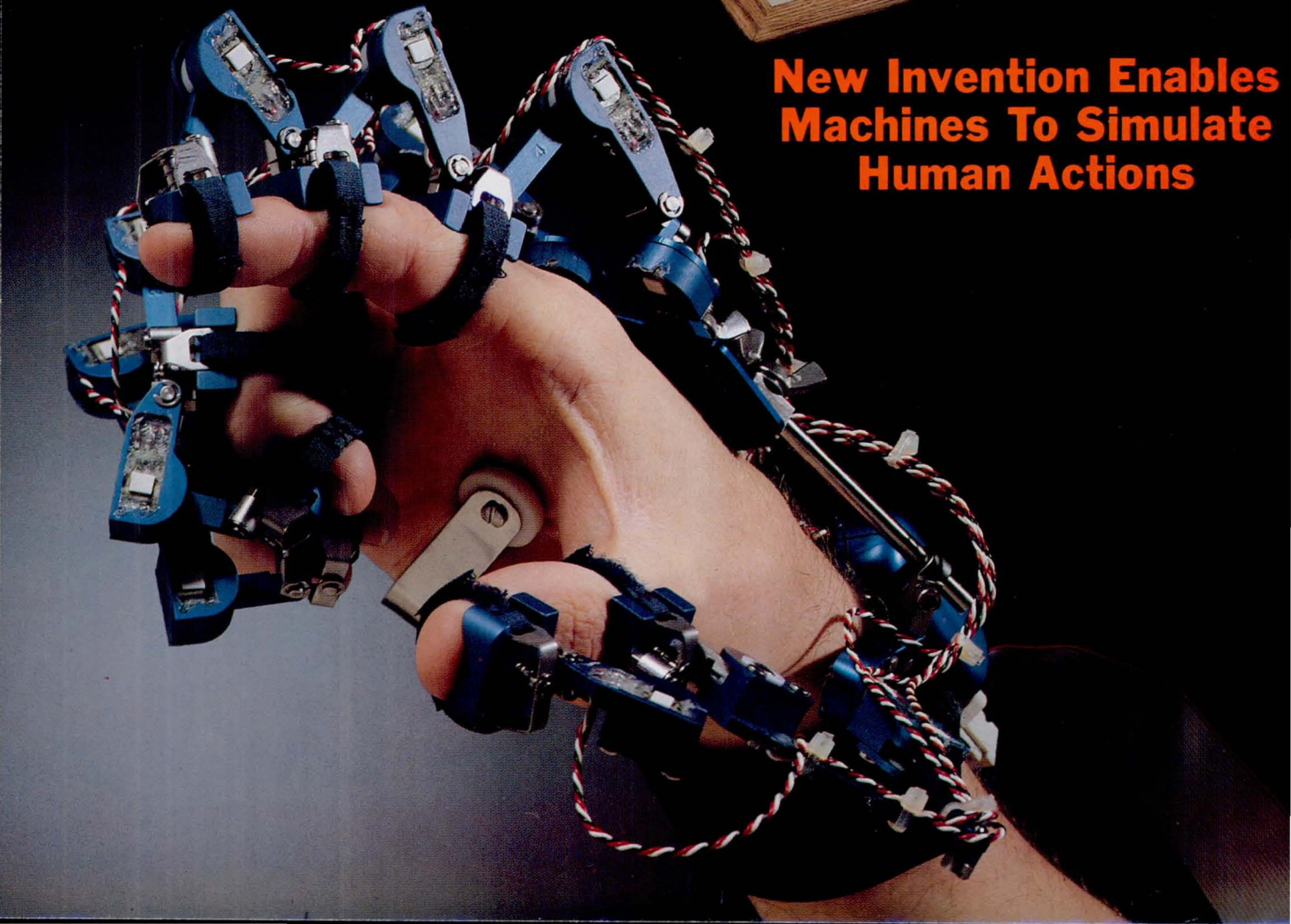

We Take Great Ideas…
& Make Them Even Better™

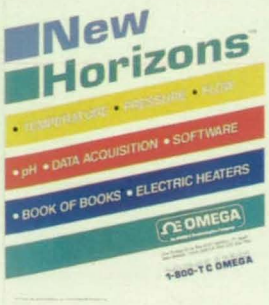

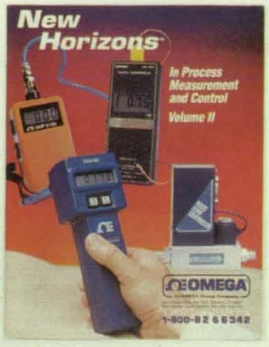

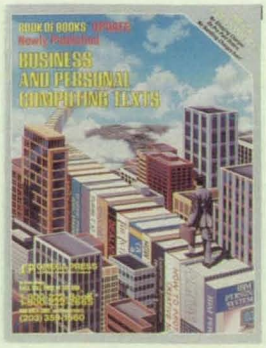

FREE! MONTHLY! NEW!
PRODUCT UPDATE!

Call or Write Today, and Add Your Name to Receive All Future Issues.

Circle Reader Action No. 617

OMEGA
An OMEGA Technologies Company

One Omega Drive, Box 4047, Stamford, CT 06907
Telex 996404 Cable OMEGA FAX (203) 359-7700

Ask For Your FREE Qualification Form!

Dial (203) 359-RUSH
(203) 359-7874

Selected for NASA's MCC

The next step in TELEMETRY SYSTEMS

System 500

ORAL SETS EW STANDARDS OR POWER, SPEED, ND PERFORMANCE

ur next step in telemetry stems is the System 500 om Loral Instrumentation. hind our easy-to-use terface is more capability to erge diverse data streams d process and display data real-time, making this the w standard in telemetry stems.

The System 500's distributed pen architecture disperses al time processing and high-eed Gigabyte storage *within* e system, eliminating host mputer bottlenecks. ultiple color graphics orkstations simultaneously onitor data on-the-fly.

Advanced color graphics, pop-up windows, pull-down menus, and mice make it easy to set up and view data acquisition from multiple data streams and sources, including

- PCM (up to 20 Mb/s)
- PAM
- MIL-STD-1553
- DMA
- Analog and Digital

More real-time processing power.

Each processor provides up to 730K measurements per second using a single 20-MFLOPS numerics processor. A single System 500 can handle a *minimum* of 4M measurements per second, for greater real-time processing.

Escape laborious microcode development with your choice of algorithm development languages: C, Fortran, and direct algebraic entry, and a large algorithm library that includes data compression, EUC, FFT, and PSD.

A system designed for you and your future.

Buy only the capability you need today, and rely on our library of acquisition, storage, and distribution modules when your needs change.

The System 500 is the new standard for

- power
- speed
- performance
- ease of use
- flexibility

Call us at **800-351-8483, ext. A500** (619-560-5888, ext. A500) to see why Loral's System 500 is your next telemetry system. We're located at 8401 Aero Drive, San Diego, California 92123-1720.

LORAL

Instrumentation

Circle Reader Action No. 309

Wide range.

MIL-C-24308. Every type you need to cover the territory. All the support you need, right up front.

Take the initiative, with complete design flexibility backed by in-depth technical support and on-the-mark delivery.

Our full AMPLIMITE 24308 line of MIL D connectors offers all the options you need—including .108″ or .090″ centerlines, or double-density .075″ centerlines. Crimp/snap, solder cup, and posted terminals. Standard or non-magnetic shells. "Rugged Ds" with stainless steel shells. All in a wide range of sizes and insert styles.

Star examples: our versions with coax/power cavities offer—in addition to standard signal contacts—power contacts with free-air current ratings to 45 amperes, and blind-mate coax contacts that cover the range to 26GHz.

There's much more, and you don't have to range very far to get it. To request technical literature or local distribution, just call the AMP Product Information Center at 1-800-522-6752. AMP Federal Systems Business Group, Harrisburg, PA 17105-3608.

AMP Interconnecting ideas

Circle Reader Action No. 657

MATLAB™ Version 3.5

Introducing the Signal Processing Toolbox

- **Faster Matrix Computation**
- **Digital Filter Design**
- **Spectrum Estimation**
- **Parametric Modelling**
- **Time Series Analysis**
- **New 2-D and 3-D Graph Types**

MATLAB v3.5 is the latest version of the premier interactive system for numerical analysis and signal processing. Problems and solutions are expressed just as they are written mathematically — ***without traditional programming***.

MATLAB has rapidly become an industry standard for digital signal processing research. Its unique interactive interface, algorithmic foundation, easy extensibility, and speed make MATLAB the software system of choice for ***high productivity*** and ***high creativity*** research at thousands of universities, laboratories, and companies.

Over 200 Built-in Functions

- eigenvalues
- least squares
- cubic splines
- convolution
- complex arithmetic
- IIR and FIR filters
- curve fitting
- singular value decomposition, ***and more***
- 1-D and 2-D FFTs
- matrix arithmetic
- multivariate statistics
- polynomial arithmetic
- nonlinear optimization
- linear equation solving
- differential equations

Version 3.5 adds new 2-D and 3-D plot types, including feather plots, error bars, automatic contour labelling, and optimized VGA support.

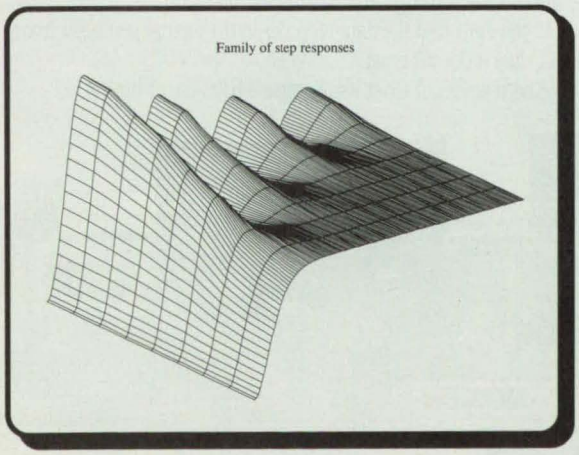

Computers

- ✓ PC and AT Compatibles
- ✓ 80386 Computers
- ✓ Macintosh
- ✓ Sun Workstations
- ✓ Apollo Workstations
- ✓ VAX/VMS and Unix
- ✓ Ardent Titan
- ✓ Convex C-Series
- ✓ Alliant FX/Series
- ✓ Other Computers

Open and Extensible

Create functions and programs rapidly — without the time-consuming compiling, linking, and complex syntax of traditional languages. Our open-system philosophy gives you access to algorithms so you can edit functions or add your own.

Optional Toolboxes extend MATLAB with application-specific capabilities, such as control system design, parametric modelling, and chemometrics.

Benchmarks (20 MHz 386-based PC)

50 x 50 matrix multiply	0.71 sec
50 x 50 matrix inverse	1.32 sec
50 x 50 eigenvalues	1.21 sec
4096-point complex FFT	1.16 sec

Fast, Accurate, and Reliable

MATLAB can handle lots of data and do it fast, fully utilizing all available floating point hardware for maximum performance. You won't have to question the results either — the algorithms have been programmed by leading experts in mathematical software and are used by leading researchers around the world.

Please provide additional information!

Name _____
Company _____
Dept. _____
Address _____
City, State, Zip _____
Country _____
Telephone _____
Computer _____

The MATH WORKS Inc.
21 Eliot Street
South Natick, MA 01760
(508) 653-1415
Telex: 910-240-521

NASA 10/89

Circle Reader Action No. 503

TEAC.
BECAUSE IT TAKES ALL KINDS.

If you need to measure the bumps, the shakes, the beats, the pressure, or the heat, TEAC makes a data recorder in the right size and format to meet your needs. In fact, we make so many different kinds of data recorders you almost need a data recorder to keep track of them all.

We made the first, and we offer the most extensive line of VHS data recorders. For ease of operation, economy, and convenience of media, the VHS format is the best.

We make the world's smallest 9-channel portable Philips cassette data recorder.

And we make a comprehensive line of reel-to-reel data recorders with extended recording times and up to 28 channels available.

We offer the widest selection of cassette data recorders from 1- to 9-channel models, from pocket-sized to sturdy laboratory and field systems.

Our new portable data recorders incorporating DAT technology are the leading edge in instrumentation recorders.

If you can't find the data recorder in the format you need from TEAC, then it doesn't exist.

And if it doesn't exist it's because TEAC hasn't built it yet.

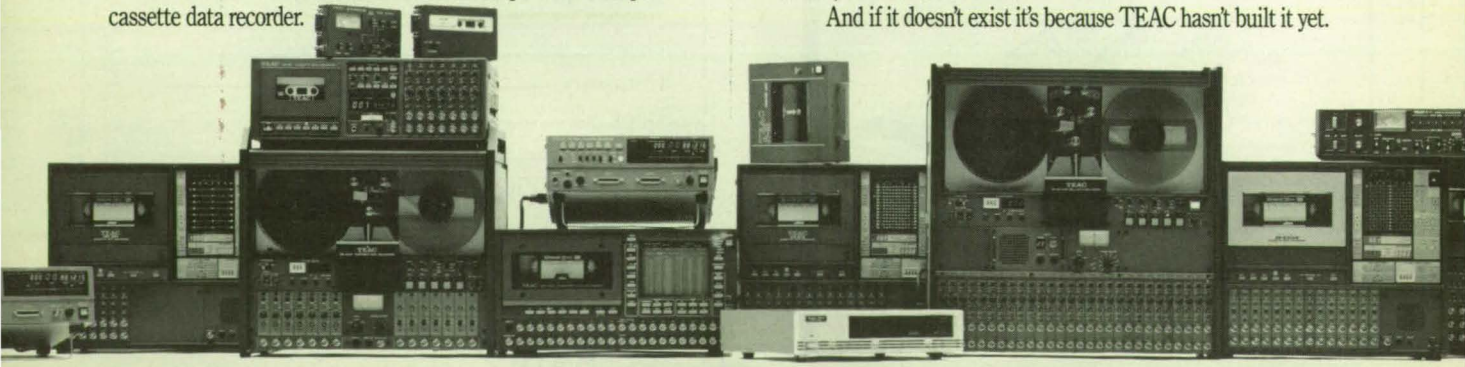

TEAC®

Instrumentation Data Recorder Division.

Circle Reader Action No. 344

Tough enough to position the heavy stuff.

KLINGER'S TCB LINEAR STAGE POSITIONS UP TO 450 POUNDS OVER 40 INCHES WITH PINPOINT ACCURACY.

The rugged, TCB stage features a rolling carriage with two rows of pre-loaded recirculating balls for smooth, precise travel under heavy loads and over long distances. Choose either ball-screw drive for high thrust and low friction. Or a lead-screw drive for high friction and increased accuracy. An optional incremental encoder can be incorporated for position verification. Easily assembled for XY or complex multiaxis positioning, the TCB is available in two module widths. With the wider stage on the bottom of an XY, twist is significantly reduced.
For more information call or write Klinger Scientific Corporation, 999 Stewart Ave., Garden City, NY 11530. (516) 745-6800.

KLINGER SCIENTIFIC

U.S.A. Headquarters:
999 Stewart Avenue, Garden City, NY 11530 (516) 745-6800.
In California: (415) 969-0247.

Worldwide distribution network: Contact Micro-Controle, Evry, France.
Tel. 33(1)64.97.98.98.
Fax 33(1)60.79.45.61.

Circle Reader Action No. 368

NASA Tech Briefs
Transferring Technology to
American Industry and Government

OCTOBER 1989
Volume 13 Number 10

SPECIAL FEATURE

TECHNICAL SECTION

Researchers at NASA's Johnson Space Center are developing "smart hands" for the Extravehicular Activity (EVA) Retriever, an experimental free-flying robot designed to retrieve equipment or a spacewalking astronaut drifting in separated flight near the Space Station. Turn to page 12.

DEPARTMENTS

On The Cover: The Dexterous Hand Master™, a sensor-lined exoskeleton that enables remote control of robots and computers. The device, described on page 12, may also be used by clinicians to diagnose and treat diseases and injuries affecting the hand. *(Photo courtesy EXOS Inc.)*

For Your Convenience
We have combined the Subscription/Technical Support Package Form and the Reader Action Card into a single, easy-to-use form (page 65).

ABP BPA

NASA Tech Briefs, ISSN 0145-319X, USPS 750-070, copyright © 1989 in U.S., is published monthly by Associated Business Publications Co., Ltd. 41 E. 42nd St., New York, NY 10017-5391. The copyrighted information does not include the individual Tech Briefs which are supplied by NASA. Editorial, sales, production and circulation offices at 41 E. 42nd Street, New York, NY 10017-5391. Subscriptions for non-qualified subscribers in the U.S., Panama Canal Zone, and Puerto Rico, $75.00 for 1 year; $125.00 for 2 years; $200 for 3 years. Single copies $10.00. Remit by check, draft, postal or express orders. Other remittances at sender's risk. Address all communications for subscriptions or circulation to NASA Tech Briefs, 41 E. 42nd Street, New York, NY 10017-5391. Second-class postage paid at New York, NY and additional mailing offices.

POSTMASTER: please send address changes to NASA Tech Briefs, 41 E. 42nd Street, Suite 921, New York, NY 10017-5391.

Build Your Future with Newport

With up to 90 dB isolation, there's no better insurance against laser diode failure

Up to 1,000,000 times the protection of ordinary, 30 dB isolators

How important is laser diode isolation? If it's inadequate, you risk frequency instability, poor modulation bandwidth, even laser failure.

All our isolators give you the highest level of protection from optical feedback damage, yet they're very easy to use.

High performance

For critical experiments, our high performance H Series isolators eliminate cumbersome cascaded setups. They consistently deliver 60 dB (0.0001% retroreflection) isolation in a single, compact package. Beam polarization is preserved so you need no additional optics. For even more protection, an optional snap-in waveplate retarder boosts isolation 1,000-fold, to an incredible 90 dB.

Fiber

At long last there's a connectorized isolator for quick, convenient attachment to fiber optic equipment. Just plug it in. FIB Series isolators deliver up to 40 dB isolation, with less than 2 dB insertion loss, in the convenience of a sealed pigtail package.

Tuneable IR and NIR

For multi-wavelength applications, ISO Series tuneable isolators provide safe, 35 dB isolation levels for the major laser diode wavelength ranges: 1.3-1.5 micron and 700-950 nm. Pre-calibrated, engraved wavelength scales and a large aperture simplify alignment and tuning.

They're everything you'd want in optical isolators: the most protection for your diode laser, the most convenience for you. Call Newport at **(714) 965-5406.**

Newport

Unshakeable Quality

Newport Corporation
18235 Mt. Baldy Circle
Fountain Valley, CA 92708
Europe: Newport GmbH
Ph. 06151-26116
U.K.: Newport Ltd.
Ph. 05827-69995

Circle Reader Action No. 510

NASA Tech Briefs
National Aeronautics and Space Administration

ABP BPA

NASA Tech Briefs:

Published by ..... **Associated Business Publications**
Editor-in-Chief/Publisher ..... **Bill Schnirring**
Associate Publisher ..... **Frank Nothaft**
Managing Editor ..... **R. J. Laer**
Senior Editor ..... **Joseph T. Pramberger**
Technical Advisor ..... **Dr. Robert E. Waterman**
Production Manager ..... **Rita Nothaft**
Traffic Manager ..... **James E. Cobb**
Circulation Director ..... **Anita Weissman**
Advertising Coordination Manager ..... **Maya Falek**
Telecommunications Specialist ..... **Evelyn Mars**
Reader Service Manager ..... **Sylvia Ruiz**

Briefs & Supporting Literature:
Provided to National Aeronautics and Space Administration by **International Computers & Telecommunications, Inc.**, NY, NY with assistance from **Logical Technical Services**, NY, NY
Technical/Managing Editor ..... **Ted Selinsky**
Art Director ..... **Ernest Gillespie**
Administrator ..... **Elizabeth Texeira**
Chief Copy Editor ..... **Lorne Bullen**
Staff Writers/Editors ..... **Dr. James Boyd, Dr. Larry Grunberger, Dr. Theron Cole, Jordan Randjelovich, George Watson, Oden Browne**
Graphics ..... **Luis Martinez, Vernald Gillman, Charles Sammartano**
Editorial & Production **Bill Little, Ivonne Valdes, Frank Ponce, Susan Finelli**

NASA:
NASA Tech Briefs are provided by the National Aeronautics and Space Administration, Technology Utilization Division, Washington, DC:
Administrator ..... **Richard H. Truly**
Assistant Administrator for Commercial Programs ..... **James T. Rose**
Deputy Assistant Administrator (Programs) ..... **Henry J. Clarks**
Deputy Director TU Division (Publications Manager) ... **Leonard A. Ault**
Manager, Technology Utilization Office, NASA Scientific and Technology Information Facility ..... **Walter M. Heiland**

Associated Business Publications
41 East 42nd Street, Suite 921, New York, NY 10017-5391
(212) 490-3999 FAX (212) 986-7864
President ..... **Bill Schnirring**
Executive Vice President ..... **Frank Nothaft**
Vice President ..... **Domenic A. Mucchetti**
Operations Manager ..... **Rita Nothaft**
Controller ..... **Felecia Lahey**

Advertising:
New York Office: (212) 490-3999 FAX (212) 986-7864
National Sales Manager ..... **James G. McGarry**
Regional Sales Manager (Mid-Atlantic) ..... **Michelle Larsen**
Account Executive ..... **Debby Crane** at (201) 967-9838
Account Executives (Midwest) ..... **Jack Cartwright** or **Paul Lesher** or **Michael Salberg** at (312) 501-4140
Account Executives (Eastern MA, NH, ME, RI) ..... **Paul Gillespie** at (508) 429-8907; **Bill Doucette** at (617) 894-7931
Account Executives (Western MA, CT, VT) ..... **George Watts** or **David Haggett** at (413) 253-9881
Account Executives (Southeast) ..... **Newton Collinson** or **Jonathan Kiger** or **Lawrence Mischik** at (404) 939-8391
Account Executive (No. Calif., WA, OR) ..... **Janice Richey King** at (415) 656-3613
Account Executives (So. Calif., AZ, NV, NM) for Area Codes 818/213/805 **Thomas Stillman** and for Area Codes 619/714 —**Karen Mock** at (213) 372-2744

NTBM-Research Center
Account Supervisor ..... **Lourdes Del Valle**

Get a close look at the big picture.

With the new HI JetPro™ printer/plotter.

Select your drawing. Preview it on your monitor. Zoom in on the tightest detail. Clip it, scale it, mark a "window." Then press a key to get a high-quality hardcopy of the segment you want.

You can do all of this—*plus* high-speed draft and letter-quality printing—with one machine: the HI JetPro printer/plotter.

The flexible hardcopy control system

Whether it's an E-size drawing or a scanned data file, HI JetPro delivers the flexibility you need and the image you want. With HI's JetPro, you have a complete hardcopy control system that includes hardware and software for high-speed, high-resolution printing and plotting—in both vector and raster environments.

Convenient, quiet, and precise

HI JetPro produces your images on ordinary paper, in sizes up to 16.5 × 23.3 inches (DIN A2), with the incredibly sharp clarity of 360 dpi. And because it's a bubble-jet, it prints and plots quickly and quietly.

Simple to use and easy to maintain, the HI JetPro printer/plotter is fully backed by Houston Instrument's reputation for price-performance, quality, and support.

To get a closer look, call *1-800-444-3425* or 512-835-0900.

HOUSTON INSTRUMENT™
A DIVISION OF AMETEK

8500 Cameron Road, Austin, TX 78753

Houston Instrument and HI JetPro are trademarks of AMETEK, Inc.

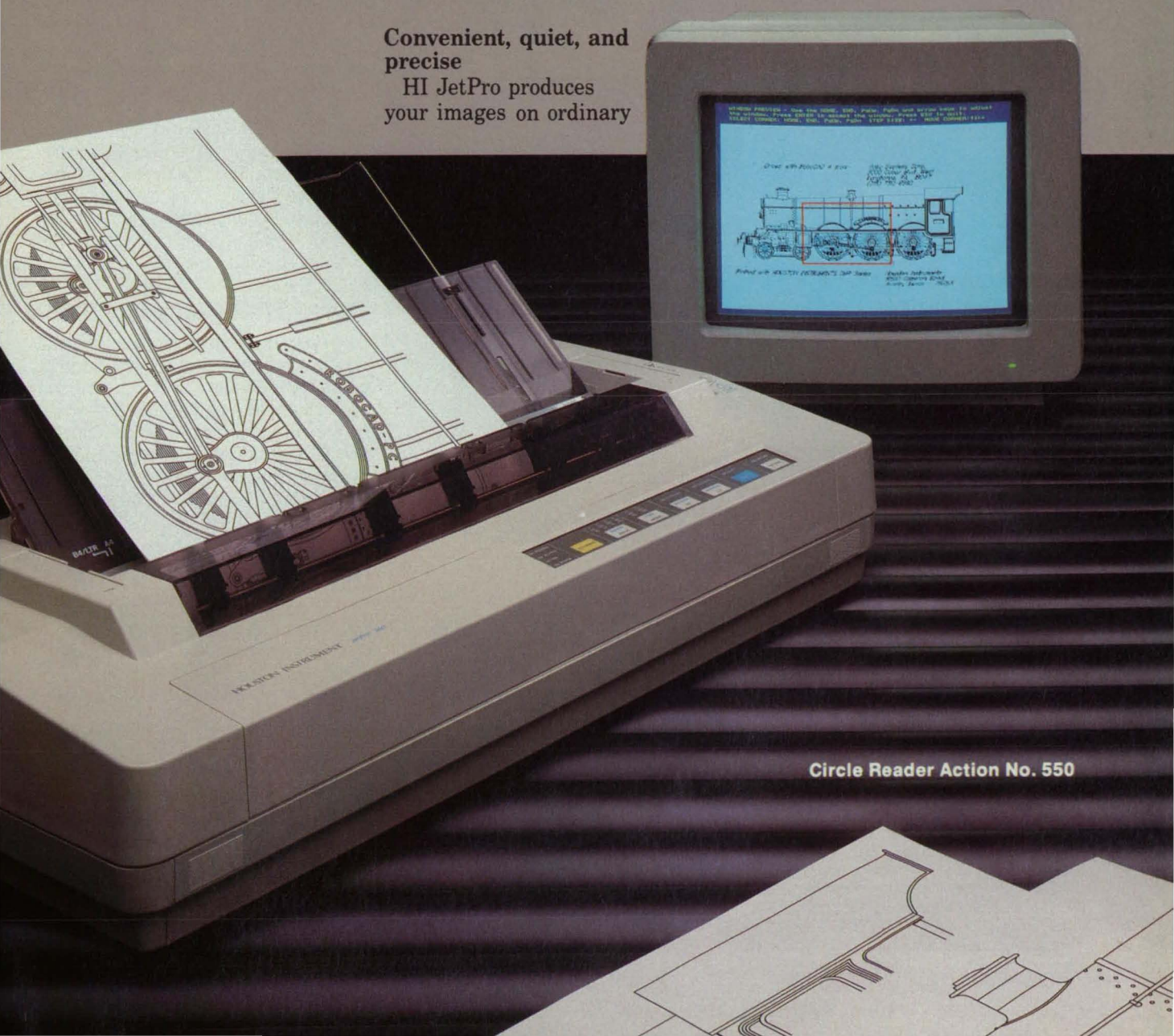

Circle Reader Action No. 550

New Product Ideas

New Product Ideas are just a few of the many innovations described in this issue of *NASA Tech Briefs* and having promising commercial applications. Each is discussed further on the referenced page in the appropriate section in this issue. If you are interested in developing a product from these or other NASA innovations, you can receive further technical information by requesting the TSP referenced at the end of the full-length article or by writing the Technology Utilization Office of the sponsoring NASA center (see page 16). NASA's patent-licensing program to encourage commercial development is described on page 16.

Aligning Plasma-Arc Welding Oscillations

A tool aids in the alignment of the oscillator probe on a variable-polarity plasma-arc welding torch. This simple, easy-to-use tool improves weld quality. (See page 68).

Subminiature Hot-Wire Probes

A class of improved subminiature hot-wire flow-measuring probes has been developed. The sensing portions of the wires in the new probes have a typical diameter of 0.63 μm and lengths of 200 μm. The smaller sizes yield improved resolution in measurements of practical aerodynamic flows. (See page 40).

Jig Aligns Shadow Mask on CCD

An alignment jig positions a shadow mask on a charge-coupled device so that a metal film can be deposited on it precisely. The jig holds the device securely and isolates it electrostatically while providing electrical contact to each of its pins. (See page 70).

Ozone/Ultraviolet-Photo-oxidation Reactor

An experimental chemical-processing system destroys waste hydrazine in water by use of ozone in an ultraviolet-photo-oxidation reactor. The new process reduces the concentrations of hydrazines and intermediate decomposition products in the effluent liquid and gas to below the limit of detectability. (See page 50).

Gland With Cantilever Seal

A single-piece gland forms a tight seal on a probe or tube that contains liquid or gas at high pressure. The gland and probe align themselves as they are assembled by a simple torquing procedure. Conventional pressure fittings for probes consist of two to four pieces and require more-complicated assembly. (See page 56).

Caldron for High-Temperature Alloys

An induction-heated caldron melts high-temperature alloys. The caldron can liquefy 200 grams of the solid metal components of an alloy like niobium aluminum and make the alloy homogeneous in less than 3 minutes. (See page 69).

Controlled-Turbulence Bioreactors

Two versions of a bioreactor vessel provide steady supplies of oxygen and nutrients with little turbulence. One has kept human kidney cells alive for as long as 11 days. This version cultures mammalian cells to a density of 1.4×10^6 cells/cm^3 for as long as 15 days. (See page 74).

Sarnoff's Centers of Excellence Offer Innovative Research Answers. Let Our Contract Research Solve Your Problems.

The powerful new laser pictured here — called a Grating Surface Emitting Array (GSE) — is 100 times brighter than any previous device.

This new semiconductor diode laser technology was developed at the David Sarnoff Research Center, which has been in the forefront of major advances in diode laser devices for the past 25 years.

Some day circuits will talk to each other by means of light because of what Sarnoff researchers in interdisciplinary "centers of excellence" have accomplished in optoelectronics.

The Sarnoff Research Center, today a thriving contract research facility in Princeton, NJ, and a subsidiary of SRI International, had its genesis as RCA Laboratories. Internationally known for its pioneering development of all-electronic, compatible color television, it has a worldwide reputation in electronics, communications, and solid state physics. Many of the electronic advances of the past 45 years had their birth in Sarnoff's Princeton laboratories.

The GSE laser is but one example of the creativity of Sarnoff scientists. We at Sarnoff are in the problem-solving business. What others may consider problems, our researchers consider as challenges to their imagination and ingenuity.

We perform innovative contract research and development on the frontiers of technology. So, challenge us with your problems and let us transform them into solutions!

To learn more about us, contact Market Development, at the David Sarnoff Research Center, CN 5300, Princeton, NJ 08543-5300, or call (609) 734-2553.

DAVID
Sarnoff
RESEARCH CENTER
Subsidiary of SRI International

Heads in the clouds, feet on the ground.

The Dexterous Hand Master: A sensor-lined exoskeleton that measures the joint movements of the human hand. Each exoskeleton finger senses three bending motions and radial-ulnar deviation (side-to-side motion).

Photo courtesy EXOS Inc.

Hand Master Controls "Smart" Machines

Using the latest computer and sensor technologies, scientists are creating "smart" robotic hands that can grasp and manipulate objects with human-like finesse. To make these machines widely and commercially applicable, a simple, easy-to-use method for controlling them is needed. Presently, dexterous devices such as the Utah/MIT and Stanford/JPL robot hands are controlled through software programs, which are often difficult and time-consuming to develop.

One promising alternative is the Dexterous Hand Master™ (DHM), a high-precision sensor system that enables robots to emulate human hand gestures. Marketed by EXOS Inc. of Lexington, MA, the DHM is the first commercial system that accurately tracks the complex motions of the human finger joints. It consists of a metal exoskeleton that fits over the user's hand and connects to an AT-compatible microcomputer. Attached to each finger joint is a Hall Effect sensor, a tiny semiconductor device that changes its signal output voltage in proportion to the magnetic field it is experiencing. As the hand moves, the sensors measure the joint angles. The computer translates the sensor data into position control commands which are transmitted to the robot.

"The exoskeleton master will allow researchers to study robotic tasks before they invest the time, effort, and resources in developing autonomous programs," said Dr. Beth Marcus, President of EXOS. "If I want a robot hand to pick up a glass, for instance, it could take me six months to write the software to do that one task, and I don't even know if it will work until I'm finished and turn it on. Whereas with the exoskeleton, on day one I can pick up the glass and the robot will do the same. I might discover that the shape of the robot's fingers is such that it can only pick up the glass in a certain way. If I then decide to go ahead and program the robot to be autonomous, at least I won't be working in the dark; I'll already know the robot's capabilities and limitations."

A Handy Tool

The first DHM system was developed in 1986 at Arthur D. Little (ADL) Inc., under Dr. Marcus' direction. She conceived the idea for the exoskeleton while designing an anthropomorphic robot hand for use with a NASA space suit. "I thought it would be extremely useful to have a master controller that would allow the robot to perform many different tasks," Marcus recalled. "Our research group found that there were no devices like this available for purchase, so we decided to build our own." Using the NASA design project as a knowledge base, ADL researchers created a two-finger prototype, followed by a four-finger model with 16 degrees of freedom.

In 1988, Dr. Marcus formed EXOS and began marketing the Dexterous Hand Master under license from ADL. Initial customers included NASA, the Department of Defense, and AT&T Bell Laboratories.

NASA's Johnson Space Center acquired a DHM to manipulate the end-effectors of an Extravehicular Activity (EVA) Retriever, a free-flying robot now in the early stages of development that will "fetch" equipment and tools, as well as astronauts, that accidently separate from the Space Station. "The exoskeleton is helping us learn how to move the robot's fingers so that it can grab a floating object and hold it securely," explained Cliff Hess of the Johnson Center's Special Projects Branch.

Scientists at NASA's Ames Research Center plan to use a new five-fingered version of the DHM in conjunction with the Virtual Workstation, a head-mounted display system that combines three-dimensional graphics and sound to produce an "artificial reality." The DHM will serve as an input device, enabling the wearer to manipulate the graphic images as if they were real objects. Applications include cockpit simulation, in which pilots fly virtual aircraft by maneuvering computer-generated instruments, and telepresence, the projection of human capability to distant locations. In one scenario, Space Station astronauts would use the Virtual Workstation and DHM system to remotely control robots on the moon. Explained Scott Fisher of Ames' Human Interface Research Branch:

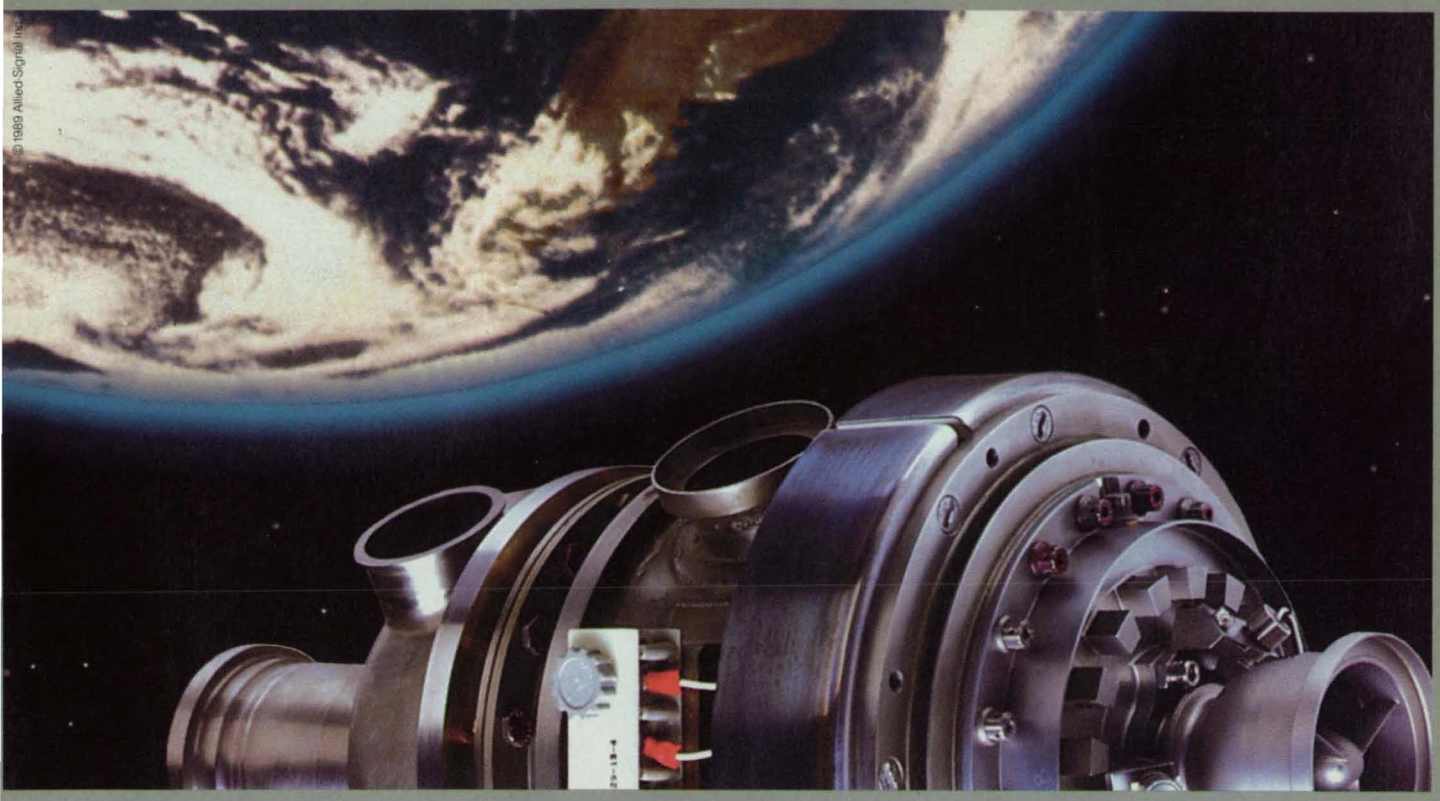

AFFORDABLE POWER FOR THE FINAL FRONTIER.

OVER THE 30-YEAR PLANNED GROWTH OF THE SPACE STATION, A SOLAR DYNAMIC POWER SYSTEM CAN SAVE OVER $3 BILLION, COMPARED TO CONVENTIONAL SYSTEMS.

TRANSLATION: AFFORDABLE POWER FOR A WIDE SPECTRUM OF MILITARY AND COMMERCIAL APPLICATIONS. DEVELOPED WITH NASA. A CLOSED BRAYTON CYCLE DESIGN SUPPORTED BY 220 MILLION HOURS OF TURBINE EXPERIENCE. UNAFFECTED BY ZERO GRAVITY OR THE COLD EMPTINESS OF SPACE. UNRIVALED FOR EFFICIENT ENERGY CONVERSION.

A LIGHTER PAYLOAD SPECIFIC WEIGHT AT LAUNCH, THE POTENTIAL FOR MORE KILOWATTS IN ORBIT. LESS SURFACE AREA FOR LESS DRAG AND RELIABILITY THAT EXCEEDS THE LIFE OF ANY SPACE STATION OR SPACE PLATFORM.

GARRETT FLUID SYSTEMS DIVISION 1300 WEST WARNER ROAD TEMPE AZ 85284 (602) 893-4421. WHERE THE ULTIMATE EFFICIENCY IS RELIABILITY.

Allied-Signal Aerospace Company

Circle Reader Action No. 415

Allied Signal

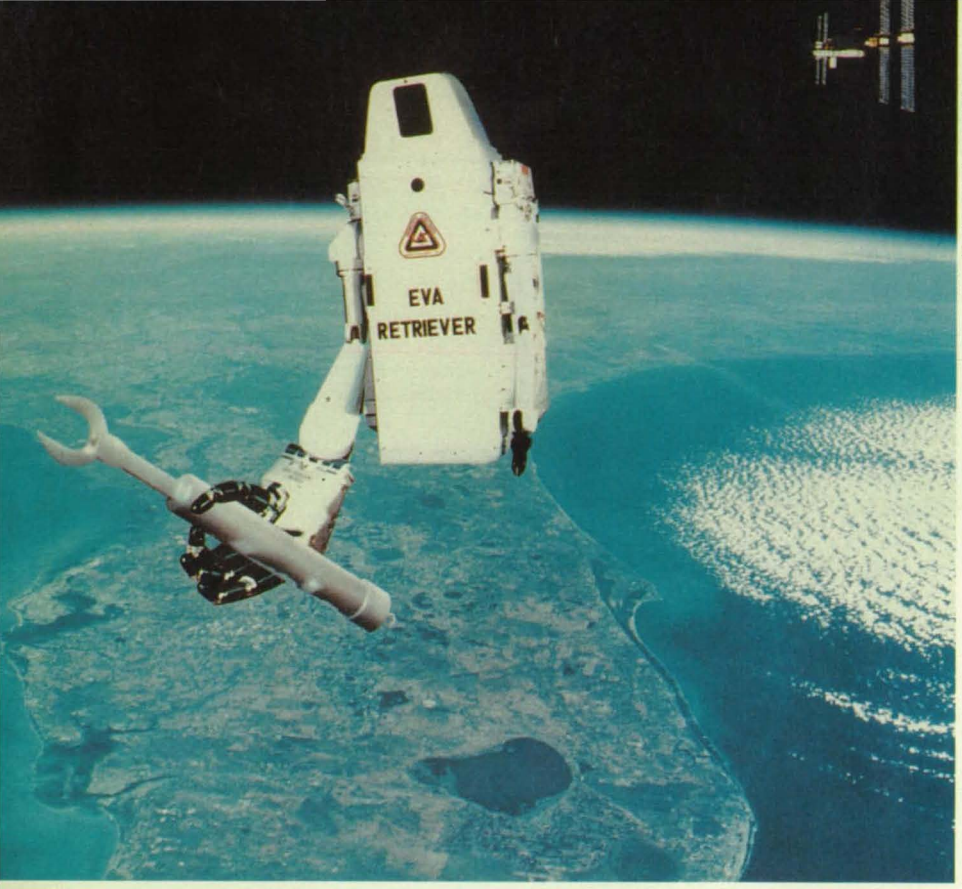

Photo courtesy NASA

The EVA Retriever would "fetch" astronauts and tools that become separated from the Space Station during EVA maneuvers.

"The astronaut would feel as if he were right there beside the robot, guiding its hands to collect rock samples or to operate a piece of mining equipment."

The Hand Master's utility as an input device extends to CAD workstations and PCs. Dr. Marcus hopes to produce a lightweight plastic exoskeleton that would allow computer users to bypass the keyboard and manipulate screen images directly, using hand movements. "You'd be able to perform complex maneuvers that aren't possible with a mouse," said Marcus. "You could rotate a graphic object in two directions at the same time and change its color — all with a single gesture."

The exoskeleton can be used to study the interaction of products with the hand.

Photo courtesy EXOS Inc.

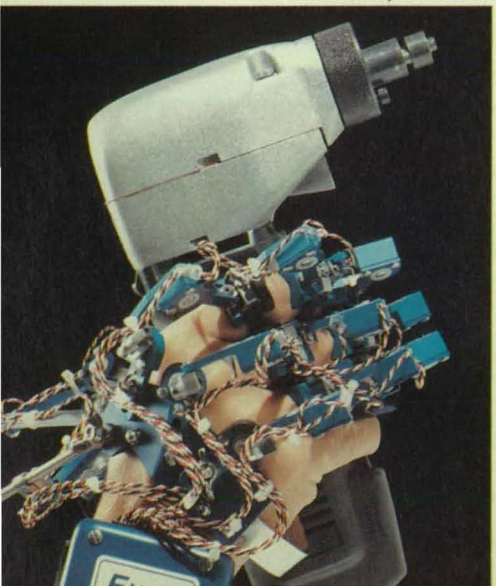

A New Invention

EXOS has developed a spinoff of the DHM technology which employs Hall Effect sensors to measure wrist motion and thin-film force sensors to map pressure distribution on the hand. Called the GripMaster™, this system will aid clinicians in diagnosing and treating diseases and injuries affecting the hand. It may also prove useful for studying the interaction of the hand with tools, machinery, and consumer products — from aerosol sprays to toothpaste.

"Designers could apply the GripMaster data to improve the packaging of products so they're easier for the elderly or impaired to open and handle," said Marcus, "and they could develop tools that are just the right size and shape to fit comfortably in the hand."

Analysis of the hand and its interplay with various objects will benefit future robotics research, according to Dr. Marcus. "As we learn more about the human hand and its capabilities," she said, "we'll be able to build better, smarter mechanical hands." □

For further information on smart robot hands, see NASA Tech Briefs *Vol. 11, Num. 9. For more on Virtual Workstation technology, see NTB Vol. 12, Num. 7.*

Circle Reader Action No. 313

THERE'S ONLY ONE THING TO SAY ABOUT TOTAL INFORMATION SOLUTIONS.

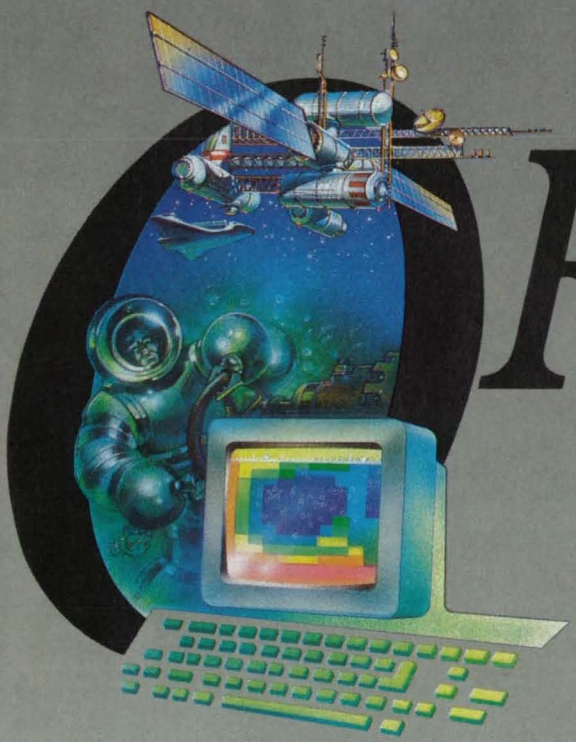

ORACLE

Whether the application involves space exploration, earthquake detection, oceanic engineering, or just about anything related to information management, Federal information resource managers know who to turn to.

Oracle.

That's because Oracle software performs on virtually all types of hardware and operating systems. Fully compatible with industry standards, Oracle software makes information transparent, and helps you avoid costly conversions.

But there's more to Oracle than simply software. Our staff and consultant network support you every step of the way, from requirements analysis and training to system and network design and implementation. That's what total solutions are all about.

For more information and a free brochure, call **1-800-345-DBMS, ext. 6768.**

By the way, there's one more thing to say about total information solutions: Authorized ADP Schedule Price List Contract No. GS00K 88 AGS 5937.

ORACLE®

FEDERAL DIVISION

Compatibility. Portability. Connectability. Capability.

Oracle Federal Division
3 Bethesda Metro Center, Suite 1400
Bethesda, MD 20814

Circle Reader Action No. 313

HOW YOU CAN BENEFIT FROM NASA'S TECHNOLOGY UTILIZATION SERVICES

If you're a regular reader of TECH BRIEFS, then you're already making use of one of the low- and no-cost services provided by NASA's Technology Utilization (TU) Network. But a TECH BRIEFS subscription represents only a fraction of the technical information and applications/engineering services offered by the TU Network as a whole. In fact, when all of the components of NASA's Technology Utilization Network are considered, TECH BRIEFS represents the proverbial tip of the iceberg.

We've outlined below NASA's TU Network—named the participants, described their services, and listed the individuals you can contact for more information relating to your specific needs. We encourage you to make use of the information, access, and applications services offered by NASA's Technology Utilization Network.

How You Can Utilize **NASA's Industrial Applications Centers**—A nationwide network offering a broad range of technical services, including computerized access to over 100 million documents worldwide.

You can contact NASA's network of Industrial Applications Centers (IACs) for assistance in solving a specific technical problem or meeting your information needs. The "user friendly" IACs are staffed by technology transfer experts who provide computerized information retrieval from one of the world's largest banks of technical data. Nearly 500 computerized data bases, ranging from NASA's own data base to Chemical Abstracts and INSPEC, are accessible through the ten IACs located throughout the nation. The IACs also offer technical consultation services and/or linkage with other experts in the field. You can obtain more information about these services by calling or writing the nearest IAC. User fees are charged for IAC information services.

Aerospace Research Applications Center (ARAC)
Indianapolis Center for Advanced Research
611 N. Capitol Avenue
Indianapolis, IN 46204
Dr. F. Timothy Janis, Director
(317) 262-5036

Rural Enterprises, Inc. Central Industrial Applications Center/NASA (CIAC)
P.O. Box 1335
Durant, OK 74702
Steve R. Hardy, President
(405) 924-5094

North Carolina Science and Technology Research Center (NC/STRC)
Post Office Box 12235
Research Triangle Park, NC 27709
H. Lynn Reese, Director
(919) 549-0671

NASA Industrial Applications Ctr. 823 William Pitt Union
University of Pittsburgh
Pittsburgh, PA 15260
Dr. Paul A. McWilliams, Exec. Director
(412) 648-7000

NASA/Southern Technology Applications Center
Box 24
Progress Ctr., One Progress Blvd.
Alachua, FL 32615
J. Ronald Thornton, Director
(904) 462-3913
(800) 354-4832 (FL only)
(800) 225-0308 (toll-free US)

NASA/UK Technology Applications Program
University of Kentucky
109 Kinkead Hall
Lexington, KY 40506-0057
William R. Strong, Director
(606) 257-6322

NERAC, Inc.
One Technology Drive
Tolland, CT 06084
Dr. Daniel U. Wilde, President
(203) 872-7000

Technology Application Center (TAC)
University of New Mexico
Albuquerque, NM 87131
Dr. Stanley A. Morain, Director
(505) 277-3622

NASA Industrial Applications Center
University of Southern California
Research Annex
3716 South Hope Street
Los Angeles, CA 90007-4344
Robert Stark, Director
(213) 743-6132
(800) 642-2872 (CA only)
(800) 872-7477 (toll-free US)

NASA/SU Industrial Applications Center
Southern University Department of Computer Science
P.O. Box 9737
Baton Rouge, LA 70813-9737
Dr. John Hubbell, Director
(504) 771-6272

If you represent a public sector organization with a particular need, you can contact NASA's Application Team for technology matching and problem solving assistance. Staffed by professional engineers from a variety of disciplines, the Application Team works with public sector organizations to identify and solve critical problems with existing NASA technology. **Technology Application Team, Research Triangle Institute, P. O. Box 12194, Research Triangle Park, NC 27709. *Doris Rouse, Director,* (919) 541-6980**

How You Can Access Technology Transfer Services At NASA Field Centers: **Technology Utilization Officers & Patent Counsels**—Each NASA Field Center has a Technology Utilization Officer (TUO) and a Patent Counsel to facilitate technology transfer between NASA and the private sector.

If you need further information about new technologies presented in *NASA Tech Briefs,* request the Technical Support Package (TSP). If a TSP is not available, you can contact the Technology Utilization Officer at the NASA Field Center that sponsored the research. He can arrange for assistance in applying the technology by putting you in touch with the people who developed it. If you want information about the patent status of a technology or are interested in licensing a NASA invention, contact the Patent Counsel at the NASA Field Center that sponsored the research. Refer to the NASA reference number at the end of the Tech Brief.

Ames Research Ctr.
Technology Utilization Officer: Laurance Milov
Mail Code 223-3
Moffett Field, CA 94035
(415) 694-4044
Patent Counsel: Darrell G. Brekke
Mail Code 200-11
Moffett Field, CA 94035
(415) 694-5104

Lewis Research Center
Technology Utilization Officer: Harvey Schwartz (acting)
Mail Stop 7-3
21000 Brookpark Road
Cleveland, OH 44135
(216) 433-5567
Patent Counsel: Gene E. Shook
Mail Code 301-6
21000 Brookpark Road
Cleveland, OH 44135
(216) 433-5753

John C. Stennis Space Center
Technology Utilization Officer: Robert M. Barlow
Code GA-00
Stennis Space Center, MS 39529
(601) 688-1929

John F. Kennedy Space Center
Technology Utilization Officer: Thomas M. Hammond
Mail Stop PT-PMO-A
Kennedy Space Center, FL 32899
(407) 867-3017
Patent Counsel: James O. Harrell
Mail Code PT-PAT
Kennedy Space Center, FL 32899
(407) 867-2544

Langley Research Ctr.
Technology Utilization Officer: John Samos
Mail Stop 139A
Hampton, VA 23665
(804) 864-2484
Patent Counsel: George F. Helfrich
Mail Code 279
Hampton, VA 23665
(804) 864-3523

Goddard Space Flight Center
Technology Utilization Officer: Donald S. Friedman
Mail Code 702.1
Greenbelt, MD 20771
(301) 286-6242
Patent Counsel: R. Dennis Marchant
Mail Code 204
Greenbelt, MD 20771
(301) 286-7351

Jet Propulsion Lab.
NASA Resident Office
Technology Utilization Officer: Gordon S. Chapman
Mail Stop 180-801
4800 Oak Grove Drive
Pasadena, CA 91109
(818) 354-4849
Patent Counsel: Paul F. McCaul
Mail Code 180-801
4800 Oak Grove Drive
Pasadena, CA 91109
(818) 354-2734
Technology Utilization Mgr. for JPL: Dr. Norman L. Chalfin
Mail Stop 156-211
4800 Oak Grove Drive
Pasadena, CA 91109
(818) 354-2240

George C. Marshall Space Flight Center
Technology Utilization Officer: Ismail Akbay
Code AT01
Marshall Space Flight Center,
AL 35812
(205) 544-2223
Fax (205) 544-3151
Patent Counsel: Bill Sheehan
Mail Code CC01
Marshall Space Flight Center,
AL 35812
(205) 544-0021

Lyndon B. Johnson Space Center
Technology Utilization Officer: Dean C. Glenn
Mail Code IC-4
Houston, TX 77058
(713) 483-3809
Patent Counsel: Edward K. Fein
Mail Code AL3
Houston, TX 77058
(713) 483-4871

NASA Headquarters
Technology Utilization Officer: Leonard A. Ault
Code CU
Washington, DC 20546
(202) 453-8377
Assistant General Counsel for Patent Matters: Robert F. Kempf, Code GP
Washington, DC 20546
(202) 453-2424

A Shortcut To Software: **COSMIC®**—For software developed with NASA funding, contact COSMIC, NASA's Computer Software Management and Information Center. New and updated programs are announced in the Computer Programs section. COSMIC publishes an annual software catalog. For more information call or write: **COSMIC®** 382 East Broad Street, Athens, GA 30602 *John A. Gibson, Dir.,* (404) 542-3265

If You Have a Question . . . **NASA Scientific & Technical Information Facility** can answer questions about NASA's Technology Utilization Network and its services and documents. The STI staff supplies documents and provides referrals. Call, write or use the feedback card in this issue to contact: **NASA Scientific and Technical Information Facility,** Technology Utilization Office, P.O. Box 8757, Baltimore, MD 21240-0757. *Walter M. Heiland, Manager,* (301) 859-5300, Ext. 242, 243

Call for HP's new Spectrum Analyzer Selection Guide. Or, mail the reply card today.

1-800-752-0900.
Ask for **Ext. 123B.**

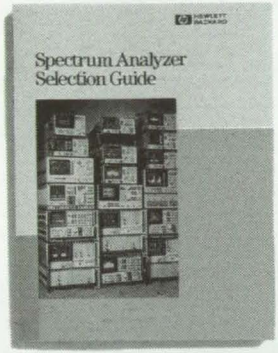

Yes, send me HP's FREE selection guide on spectrum analyzers.

Phone ( ) _____

Name _____

Title _____

Company _____ Mail Stop _____

Address _____

City _____ State _____ Zip _____

123B

NO POSTAGE
NECESSARY IF
MAILED IN THE
UNITED STATES

BUSINESS REPLY MAIL

FIRST-CLASS MAIL PERMIT NO. 609 CUPERTINO, CA

POSTAGE WILL BE PAID BY ADDRESSEE

HEWLETT-PACKARD CO.
Inquiry Manager
Customer Information Center
19310 Pruneridge Ave. M/S 49AM
Cupertino, CA 95014

To make the right choice in spectrum analyzers, you can collect all this

or call for this.

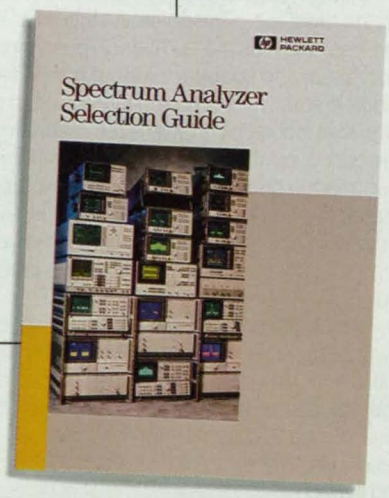

You simply wouldn't make a spectrum analyzer decision without up-to-date information. But a lot has happened since your last look at spectrum analyzers. And it's not easy to get all the data.

The best way to catch up is to get HP's new Spectrum Analyzer Selection Guide. It gives you side-by-side comparisons of HP's full line. Including 10 new analyzers. You'll find details on our new built-in tracking generators, memory cards, and a new color display. All in a format for comparing price and performance in terms of your applications.

Make sure your next analyzer decision is based on the latest facts. Call **1-800-752-0900** today.

Ask for **Ext. 123B** and we'll send your **FREE** selection guide right away. Or, mail the reply card today.

There is a better way.

HEWLETT PACKARD

Circle Reader Action No. 594

Electronic Components & Circuits

Q-Switch for Self-Injection Locking of Laser

The spectral width and pulse time would be regulated.

Langley Research Center, Hampton, Virginia

A proposed scheme for improved electro-optical switching (Q switching) of a pulsed, self-injection-locked laser involves the sensing of and compensation for the level of the pumping light. The scheme would decrease the spectral width of a laser pulse and make it independent of the pumping level, at least to first order. Such independence is desirable because the degree of spectral narrowing of the emitted radiation is heavily dependent on the level of the pumping light, which is usually highly variable. Because the time of evolution of the pulse also depends heavily on the pumping level, the proposed scheme would also be beneficial in reducing jitter.

As in other Q-switched, self-injection-locking schemes, the laser is operated in a high-loss condition during the initial evolution of the pulse. During this time, the light makes many round trips through the laser resonator. On each round trip, the spectrum-narrowing optical elements operate on the radiation in the pulse. An increase in the loss, and thus the number of round trips, decreases the spectral width of the pulse. Once a small laser pulse has evolved in a high-loss condition in the laser resonator, the optical configuration of the resonator is switched to one of low loss. In the low-loss state, the majority of the energy is extracted in an efficient manner while retaining the narrow spectral width of the initial pulse.

The problem is to control the moment of switching and/or the level of loss during the initial high-loss period. In the new scheme, the solution is to regulate the amount of loss during the initial high-loss period in response to the measured level of pumping in such a way that the time of evolution of the pulse and the number of round trips is maintained nearly constant from pulse to pulse.

As shown in the figure, a photodiode or other detector would be exposed to the fluorescence emitted by the laser medium. This fluorescence would be directly proportional to the population of the upper laser level and, thus, to the effective pumping level. A spectral filter could be used in front of the optical detector to reject the unwanted background radiation. The output of the detector would be amplified, typically by an amplifier that has a large voltage gain.

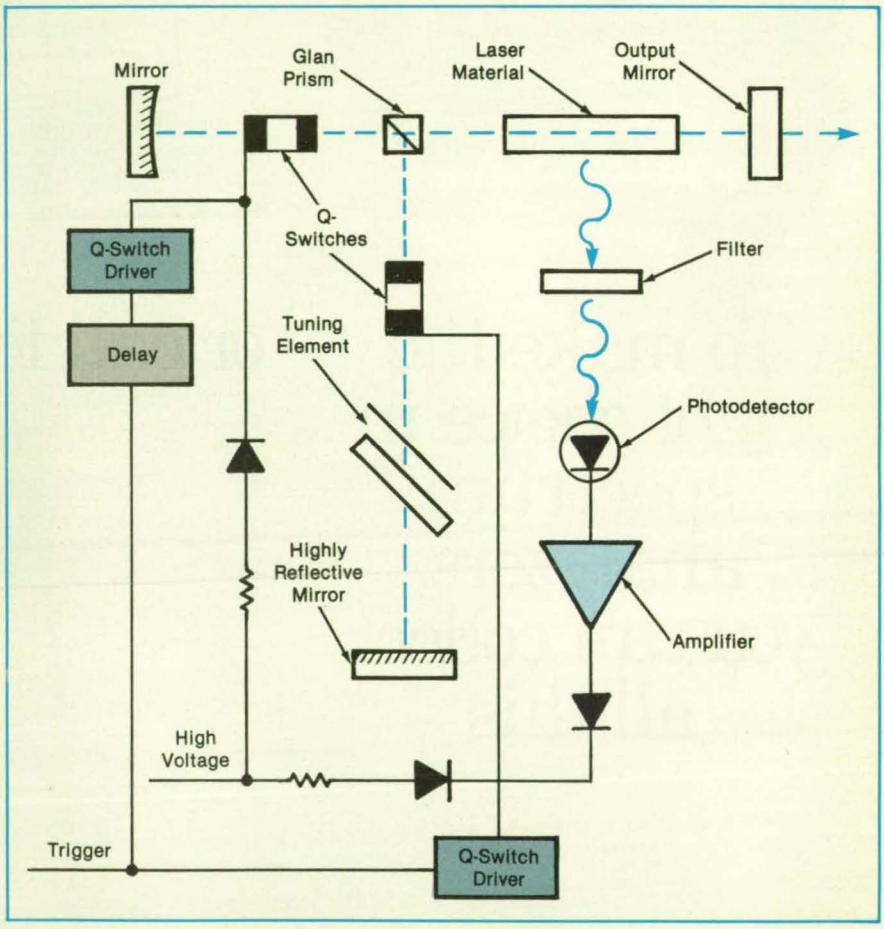

The **Amplified Output of the Photodetector** would be applied to the Q-switch to regulate the level of loss in response to the level of pumping light.

The output from the amplifier would be applied directly to an electro-optical Q-switch in addition to the main Q-switch-driving voltage to obtain a total Q-switch-driving voltage that varies the level of loss. To increase the accuracy of control, the amplified voltage could be applied in addition to a dc voltage. With this arrangement, the loss could be approximated by a linear relationship rather than a direct proportionality. If better regulation of loss were required, a nonlinear amplifier could be used.

This work was done by Norman P. Barnes of **Langley Research Center**. *For further information, Circle 94 on the TSP Request Card.*

This invention is owned by NASA, and a patent application has been filed. Inquiries concerning nonexclusive or exclusive license for its commercial development should be addressed to the Patent Counsel, Langley Research Center [see page 16]. Refer to LAR-13772

ANOTHER ASTRO-MED FIRST IN 8-CHANNEL RECORDERS

LASER PRINTER RESOLUTION!

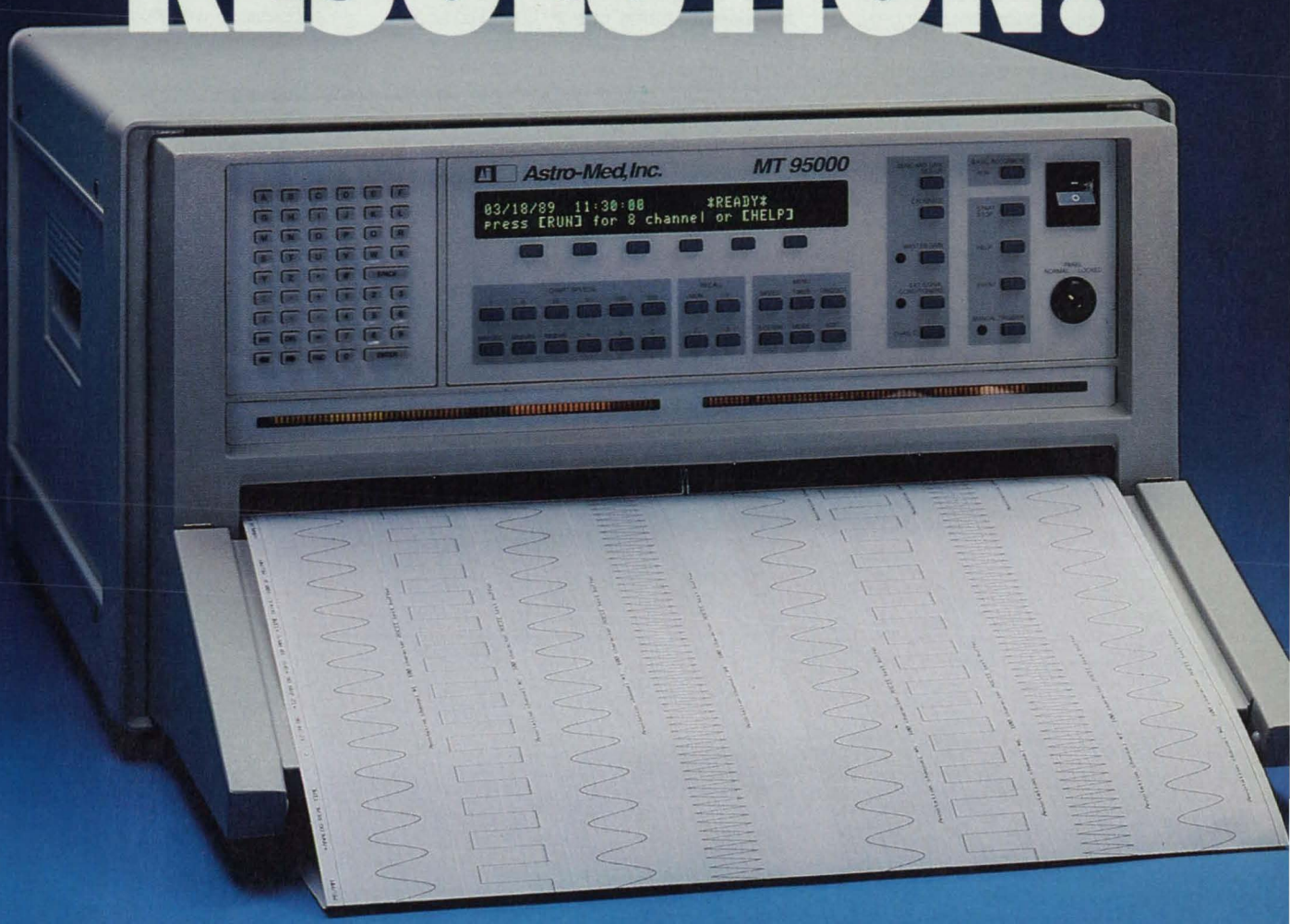

- **Laser Quality Writing–300 dpi**
- **20 kHz Frequency Response**
- **Automatic Self-Calibration–Traceable to NBS**
- **Expandable to 16 Channels**
- **Data Capture with 200 kHz Sample Rate Per Channel**
- **Built-In Programmable Signal Conditioners**

From its laser-sharp charts to its unparalleled frequency response, this remarkable new 8-channel recorder brings you the technology of the Twenty-First Century today! It outperforms even Astro-Med's MT-9500, which in 1987 was heralded as the first breakthrough in 8-channel recorders in 20 years. It has 50% more resolution, 4 times higher frequency response, and 8 times more memory than the MT-9500. With automatic self-calibration traceable to NBS, expandability to 16 channels, and a host of other important features. We call it the MT-95000, a product so unique that it is protected by U.S. Patent No. 4,739,344.

Phone, Fax or Write for details!

Astro-Med, Inc.®

Astro-Med Industrial Park, West Warwick Rhode Island 02893
Telephone (401) 828-4000 • Toll Free 800-343-4039
Telex No. 710-382-6409 • Fax (401) 822-2430

Circle Reader Action No. 405

Integrated Semiconductor/Optical Information Processors

Optical, electro-optical, and electronic devices would be integrated into three-dimensional structures.

NASA's Jet Propulsion Laboratory, Pasadena, California

Optical information processors of a proposed new type would be made of integrated three-dimensional devices that would include optical, electro-optical, and electronic devices. The integration would be achieved by a combination and extension of advanced semiconductor (integrated-circuit) and integrated-optics technology. The development of the new processors could lead to the miniaturization of sophisticated optical information-processing systems.

The figure illustrates the concept of an integrated device that would perform matrix•vector multiplication. This device would combine two separate components of a previously demonstrated system for matrix•vector multiplication: an electrically-addressable spatial light modulator that generated the light-and-dark matrix pattern, and a thin chip of GaAs, in which the multiplication was performed by degenerate four-wave mixing via the photorefractive effect. In the integrated device, the spatial light modulator would be fabricated on the surface of the chip.

Because the photorefractive portion of the device would constitute an all-optical processor, its inputs and control signals would have to be spatially modulated beams of light, which could be generated by other optical processors or by the electrically addressable spatial light modulator on its surface. Several types of spatial light modulators could satisfy the requirements for speed (a frame rate ⩾ 1,000 Hz) and compatibility with lasers that have wavelengths suited to the photorefractive effect. The logical choice for integration is semiconductor spatial light modulators on semiconductor processors. Candidate superlattice spatial light modulators of this type include GaInAs/GaAs, GaInAs/InP, and HgCdTe/CdTe.

The simplistic approach to integration is to miniaturize the established components, but this is not likely to exploit the full potential of the new concept. A more promising approach would be to use holographic patterns generated by computers and electron-beam lithography to make holographic patterns on surfaces and interfaces. These patterns could not only provide the functions of conventional optical components but could also create novel applications.

This work was done by Li-Jen Cheng of Caltech for **NASA's Jet Propulsion Laboratory**. *For further information, Circle 154 on the TSP Request Card.*

In accordance with Public Law 96-517, the contractor has elected to retain title to this invention. Inquiries concerning rights for its commercial use should be addressed to

Edward Ansell
Director of Patents and Licensing
Mail Stop 305-6
California Institute of Technology
1201 East California Boulevard
Pasadena, CA 91125

Refer to NPO-17533, volume and number of this NASA Tech Briefs *issue, and the page number.*

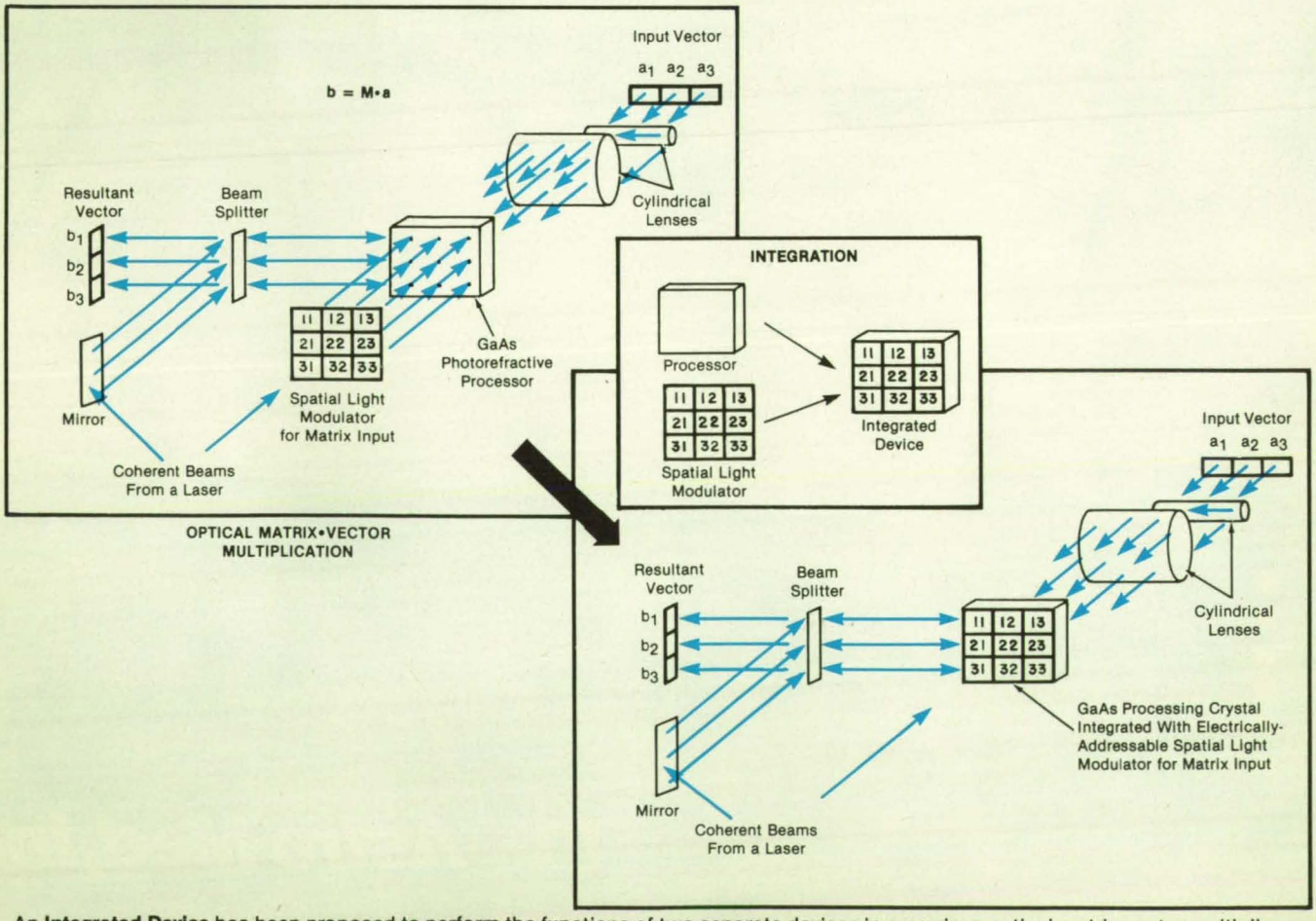

An **Integrated Device** has been proposed to perform the functions of two separate devices in a previous optical matrix•vector multiplier.

"IT'S SLIPPERIER THAN TEFLON"®

WHY BUY A NEW CAR WHEN YOU DON'T HAVE TO?

USE Tufoil® AND YOUR ENGINE WILL LAST... AND LAST...AND LAST!

You've seen the price of new cars...they go up every year! Cars get flimsier ... prices get higher...it never seems to end. There are lots of reasons to keep that nice car of yours on the road as long as possible.

Now it's easy to make your engine run better, last longer. Just add TUFOIL to the crankcase. You don't have to shake the container or add an engine flush. Just pour it in and drive away.

Your throttle will get silky smooth ...acceleration will improve. One customer said his car "takes off like a scared rabbit!"

TUFOIL works wonders for all known engine oils. It's actually slipperier than Teflon®. (according to a famous US goverment laboratory.)

You'll get astonishingly fast starts on cold mornings with both diesels and gas engines. The Canadian government tested TUFOIL at it's cold regions lab. They showed faster cranking and significant fuel savings with TUFOIL.

I keep getting telephone calls from owners of very expensive German diesels wanting to buy stock in our company. They say their diesels are accelerating like nothing they've ever seen before. One said he doesn't have to down shift any more on an annoying hill in his area.

Your car can have more power like that too.

What about additives that claim to be one time treatments that will last the life of an engine? Well, I've been following the scientific literature on lubrication for a very long time. As far as I know, there isn't a shred of scientific evidence for such a claim. So don't believe it!

TRY ONE 8 OZ BOTTLE OF TUFOIL FOR 30 DAYS OR 1000 MILES

If you don't notice quieter-smoother operation,quicker starting,snappy acceleration.Just send us proof of purchase with a note describing the year and make of your car.We'll refund your money immediately-

Send for TUFOIL today and prove to yourself the amazing increase in your car's performance. Fill in the coupon today or call TOLL-FREE any time, 24 hours a day.

1-800-922-0075.
(in New Jersey, call 201-825-8110.)

Stay in tune with your car!

Engines last longer with TUFOIL.. Our 1976- 476 T-Bird is now at 190,000 miles and purring.

A bunch of customers' cars have now passed 250,000 miles.

Several months ago, a nice man I'd never seen before walked into my office, big smile on his face, sat down and said, "Would you believe 340,000 miles on a Tufoil engine?" He went on to rave about how well his engine has been running all these years. I couldn't get a word in edgewise.

It made me very proud.

Recently, a truck driver called in with over 1,000,000 miles on a diesel using TUFOIL - Wow!

A customer from Vermont added 10% TUFOIL to his sticky mechanical transmission, called in and said he couldn't believe it..."Shifting is like slicing butter now!", he said.

SAAB owners are writing letters praising TUFOIL in their "NINES" magazine. They report spectacular improvements in their engines and transmissions!

Don't forget! TUFOIL is the result of over 15 years of research and development. The U.S. government has awarded us 6 patents so far...so have Germany, England, France and Canada.

No other lubricant even comes close.

One customer put it nicely when he said, "You can hear it...you can feel it!"

PS--Our loyal customers wrote this ad for us. Its full of their comments !

Thanks !

FREE . . . Products based on TUFOIL technology. Check one with each order of 2 bottles or a quart. Check 2 for each gallon order. Values range from $3.98 to $9.95.

- ☐ TUFOIL Gun-Coat — Super rust inhibited, smooth action
- ☐ TUFOIL Compu-Lube — Low viscosity for computer mechanisms
- ☐ TUFOIL Lightning Grease — Easily sheared grease for instruments
- ☐ TUFOIL Lubit-8 — General purpose, household use lubricant

FREE brochures . . .

- ☐ 30 Questions/Answers about TUFOIL
- ☐ "Fun with Superconductors"—we're leading that field too!

See NASA Tech Briefs for technical details, 1986, 1987 and 1988.

When POPULAR MECHANICS tested TUFOIL, it reported "TUFOIL is absolutely spectacular!"

YES **rush my TUFOIL order:**

- ☐ ONE 8 oz. bottle . . . treat one car for $14.25 (plus $3.50 shipping and handling). See money back guarantee.
- ☐ TWO 8 oz. bottles . . . treat two cars for $25.00 (plus $4.00 shipping and handling) **SAVE $6.00**
- ☐ ONE Quart bottle . . . treat 4 cars for $34.95 (plus $4.00 shipping and handling)
- ☐ ONE GALLON . . . treat 16 cars for $125.00 (plus $6.00 shipping and handling.)

We ship within days!

*over the single bottle price **BIG SAVINGS**

Fluoramics, Inc. NTB-109
103 Pleasant Avenue
Upper Saddle River, N.J. 07458

My check or money order for $ _____ is enclosed.
Charge my credit card:
☐ Am.Express ☐ MasterCard ☐ Visa

Card No. _____
Exp. Date _____
Signature _____
Name _____
Address _____ UPS Shipping Address
City _____
State _____ Zip _____

(N.J. residents please add 6% sales tax).
Canadian Distributor: 1-800-363-7753

Circle Reader Action No. 364

Piezoelectrostatic Generator

High voltage is generated by compact, lightweight equipment.

Marshall Space Flight Center, Alabama

An improved variable-capacitance electrostatic generator puts out high pulsed direct (in effect, rectified alternating) voltages at currents greater than those usually obtainable from electrostatic generators. The generator is light in weight and relatively compact because it relies on the piezoelectric effect to convert mechanical energy directly into electrical energy and contains neither transformers nor bulky high-voltage rectifiers. Unlike some other variable-capacitance electrostatic generators, the piezoelectrostatic generator requires neither an external power supply to charge, nor a vacuum to insulate, its electrodes.

The heart of the piezoelectrostatic generator is a stator composed of multiple piezoelectrostatic capacitive elements shaped somewhat like slices of pie (see Figure 1). Each element contains two piezoceramic

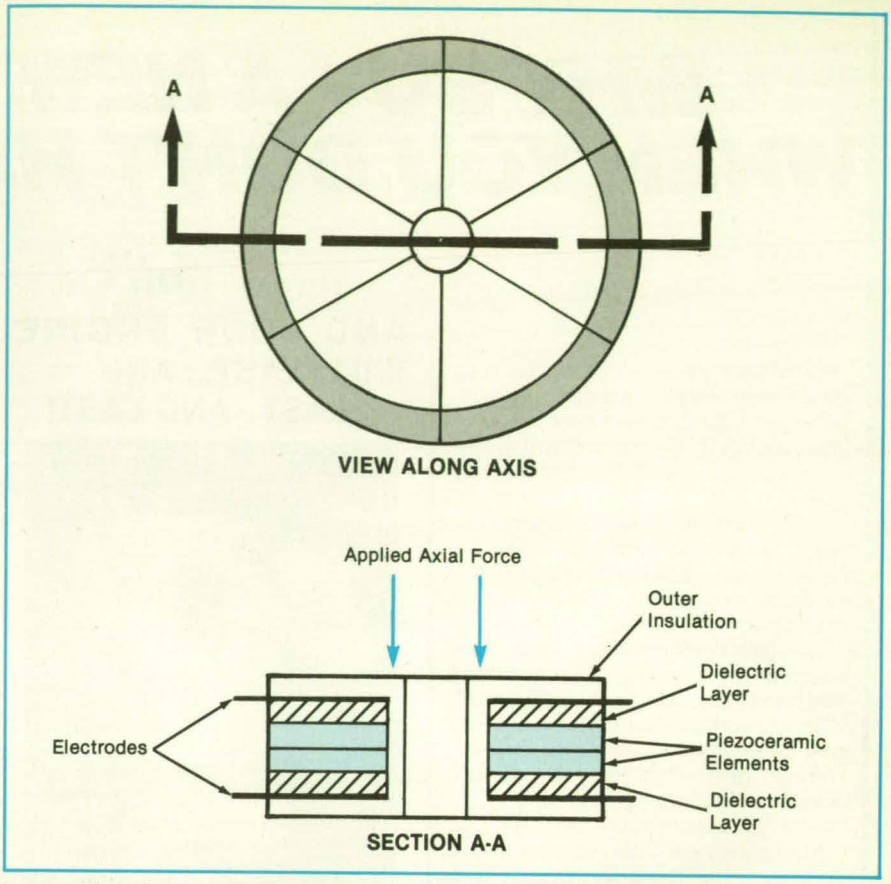

Figure 1. **Piezoelectrostatic Elements** are, in effect, capacitors that generate their own voltages when stressed. They are connected in parallel and cyclically stressed at their inner tips to produce electricity.

3D Laser Imaging in a Practical Package

The Odetics 3D Laser Imaging System provides versatile machine vision for a variety of applications.

The system provides high quality concurrent range and video images with an all digital output.

The compact, lightweight, low power-consumption unit is self contained and ready for immediate installation. Its robust construction and reliable performance independent of ambient illumination, make it suitable for many demanding applications.

To learn more about the Odetics 3D Laser Imaging System, call our vision experts today.

Circle Reader Action No. 346

Odetics

Advanced Intelligent Machines Division

1515 South Manchester Avenue, Anaheim, California 92802-2907
✆ 714 758-0300 TLX 3716642 Fax 714 491-9885

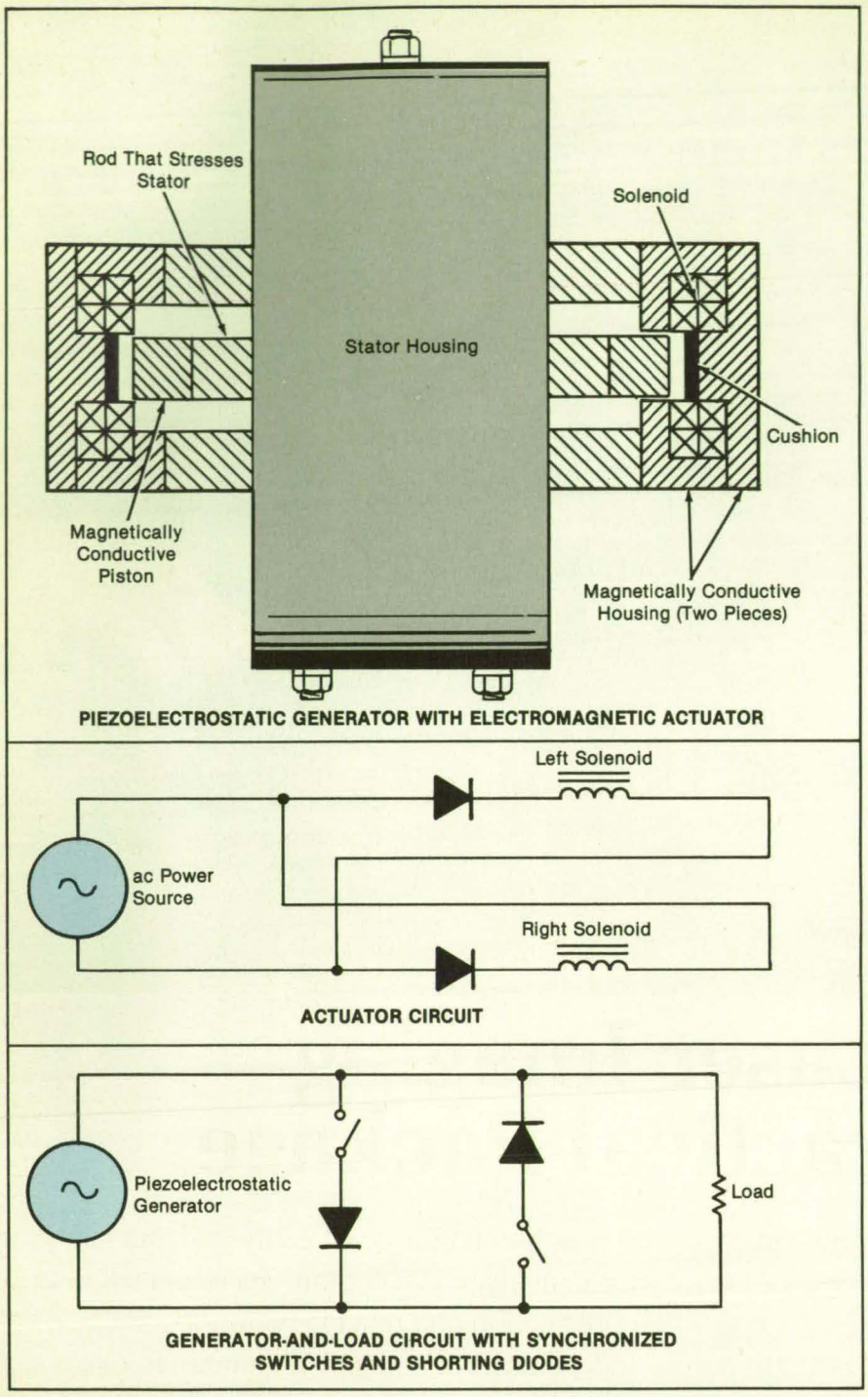

Figure 2. An **Electromagnetic Actuator** includes two opposing solenoidal electromagnets, which apply alternating axial stress to the multiple-element piezoelectrostatic stator shown in Figure 1. The electronic switches in the circuit shown at the bottom are synchronized with the applied force.

strips connected in series between two outer electrodes, insulated from the electrodes by two dielectric strips. The elements are mounted in cantilever configuration and connected in parallel to combine the piezoelectric currents generated in all of them.

An alternating axial force tending to bend the piezoceramic elements is applied to the inner tips of the elements; for example, by supplying a sinusoidal voltage through diodes to alternate solenoidal actuators as shown in Figure 2. By the piezoelectric effect, the bending stresses induce electric charges on the opposite faces of the elements.

While the bending force rises from zero to maximum during the first half of each half cycle, diodes and switches synchronized with the applied-force signal short-circuit the electrodes together to allow electric charges to flow between them and balance the charges on the piezoceramic elements. When the stator reaches maximum flexure, the maximum charge has been stored in the electrodes. The electrodes are then disconnected from each other, and then the stator is allowed to relax. By the piezoelectric effect, this causes a change in the charge on the faces of the elements, which in turn causes a high-voltage pulse as the electrodes discharge through the load.

The voltage achievable by short-circuiting during bending is greater than that achievable by sending current to the load during the entire cycle. This is because of the increase in electric permeability of the piezoceramic with an increase in stress. The net result is that the capacitance of the elements decreases during relaxation while some of the charge induced during bending is retained, so that the voltage due to the remaining charge in the elements is increased.

This work was done by Glen A. Robertson of **Marshall Space Flight Center**. *For further information, Circle 34 on the TSP Request Card.*

Inquiries concerning rights for the commercial use of this invention should be addressed to the Patent Counsel, Marshall Space Flight Center [see page 16]. Refer to MFS-28298

Books and Reports

These reports, studies, handbooks are available from NASA as Technical Support Packages (TSP's) when a Request Card number is cited; otherwise they are available from the National Technical Information Service.

SEU in an Advanced Bipolar Integrated Circuit

Vulnerability to SEU varies with size and applied current.

A report summarizes an investigation of single-event upsets (SEU) (changes in logic states caused by cosmic rays and the like) in a bipolar integrated-circuit set of flip-flops (memory cells). The device to be tested was made by the advanced digital bipolar silicon process of Honeywell, Inc. The device was a circuit chip containing 4 cells: a minimum-geometry cell (linear scale 1×) and 3 cells of linear scale 2×, 4×, and 10× (areal scales of 1×, 4×, 16×, and 100×, respectively). The emitter areas ranged from 2 square microns for the minimum geometry (IX) device to 200 square microns for the 10× device. This construction enabled the study of the effect of size on SEU behavior. In addition, each cell was externally biased so that the effect of bias current (or, equivalently, power) on SEU behavior could be studied.

In one series of tests, the device was irradiated with 250-MeV bromine ions. The resulting data show that these high-stopping-power ions result in the collection

of charge far in excess of the critical charge for SEU (Q_C). This is manifested by the large SEU cross sections in excess of the areas of the buried layers in the device. This behavior indicates that even ion tracks that hit in the substrate area surrounding the buried layer area can cause SEU by the diffusion of charge to the junctions of the substrate and buried layers.

As the cell current (I_{CELL}) was increased above 40 μA, the SEU cross sections of the 1 × and 2 × cells decreased, as expected, due to the increase in Q_C. However, the cross sections of the 4 × and 10 × cells increased for I_{CELL} above 80 μA on account of the saturation of the large transistors, which caused the response times to increase, thereby allowing ion-generated charge to be collected by diffusion for a longer time.

Another series of tests involved irradiation with 150-MeV iron ions. The most striking feature of the data from these tests was a dramatic decrease in the SEU cross section of the 10 × cell at increasing values of I_{CELL} above 65 μA. At I_{CELL} below 65 μA, the SEU cross section of the 10 × cell approached the area of the buried layer. This indicates that any ion track that intersects the junction of the buried layer and the substrate will cause SEU. As I_{CELL} is increased, ion tracks must inject charge into the base or the emitter as well as the substrate/buried-layer junctions to cause SEU. The SEU cross section continues to decrease to less than one-tenth the emitter area at I_{CELL} = 200 μA. In the 1×, 2×, and 4 × cells, the SEU cross sections decreased slightly with increasing I_{CELL}, their values converging on the areas of the buried layer for each device.

A third series of tests was conducted with 100-MeV oxygen ions. SEU was not observed in the 10 × cell. The other cells exhibited decreases in the sensitivity to SEU with increasing I_{CELL}. The SEU cross section of each device fell sharply with increasing I_{CELL} above 50, 100, and 150 μA in the 4×, 2×, and 1× cells, respectively.

The results of this study provide important information for the optimal design of devices fabricated using a buried-layer bipolar process that must operate in heavy-ion SEU environments. Designers can use this information to provide required levels of suppression of SEU in specific applications via combinations of size and/or cell-current (or power) scaling.

This work was done by John A. Zoutendyk and Elaine C. Secrest of Caltech and Dale F. Berndt of Honeywell, Inc., for **NASA's Jet Propulsion Laboratory**. *To obtain a copy of the report, "Increasing Resistance of Bipolar IC's to Radiation-Induced SEU's by Increasing Power," Circle 23 on the TSP Request Card.*
NPO-17553

Electronic Systems

Measuring Winds With Pulsed C-Band Radar

The objective is to provide quick forecasts of impending thunderstorms.

John F. Kennedy Space Center, Florida

Research has begun on the use of pulsed C-band radar in a multistatic configuration to measure winds in the absence of clouds. The ultimate objective of this effort is to develop the capability to use wind-measurement data to predict, as early and as accurately as possible, the formation of local thunderstorms — desirably, with lead times of several hours.

The proposed experimental system is based on the principle of multistatic radar: because a single radar can measure only the component of velocity along its line of sight by means of the longitudinal Doppler effect, multiple receivers will be tracked on the same point in the sky to measure the winds from different angles, thereby obtaining the complete wind vector at that point.

The proposed system (see figure) will include one radar station that both transmits and receives and one or more other stations that receive only. The advantage of the multistatic configuration is the greatly reduced effects of ground clutter on the receive-only stations. Each site will require a 5-MHz reference signal for coherent detection. This signal, modulated by the radar-pulse-triggering signal, will be sent from the transmitting/receiving station to the receiving (only) stations on a coaxial cable.

The raw data from each radar will be fed to a radar video processor, which computes radial velocities and can produce displays of velocities in five different intensities of blue and red, and reflectivities in 13 colors, in plan-position-indicator or range-height-indicator format. These plots can be obtained in real time or from data stored on tape. The velocity data from each such processor will be sent over a telephone line to a central computer, which will produce displays of windflows.

This work was done by Carl Lennon, Richard Wesenberg, Thomas O. Britt, Michael Brooks, Deloris Edwards, Chris Franklin, John Kiriazes, Brad Kitayama, and Jim Medina of **Kennedy Space Center**. *For further information, Circle 31 on the TSP Request Card.*

Inquiries concerning rights for the commercial use of this invention should be addressed to the Patent Counsel, Kennedy Space Center *[see page 16].* *Refer to KSC-11415*

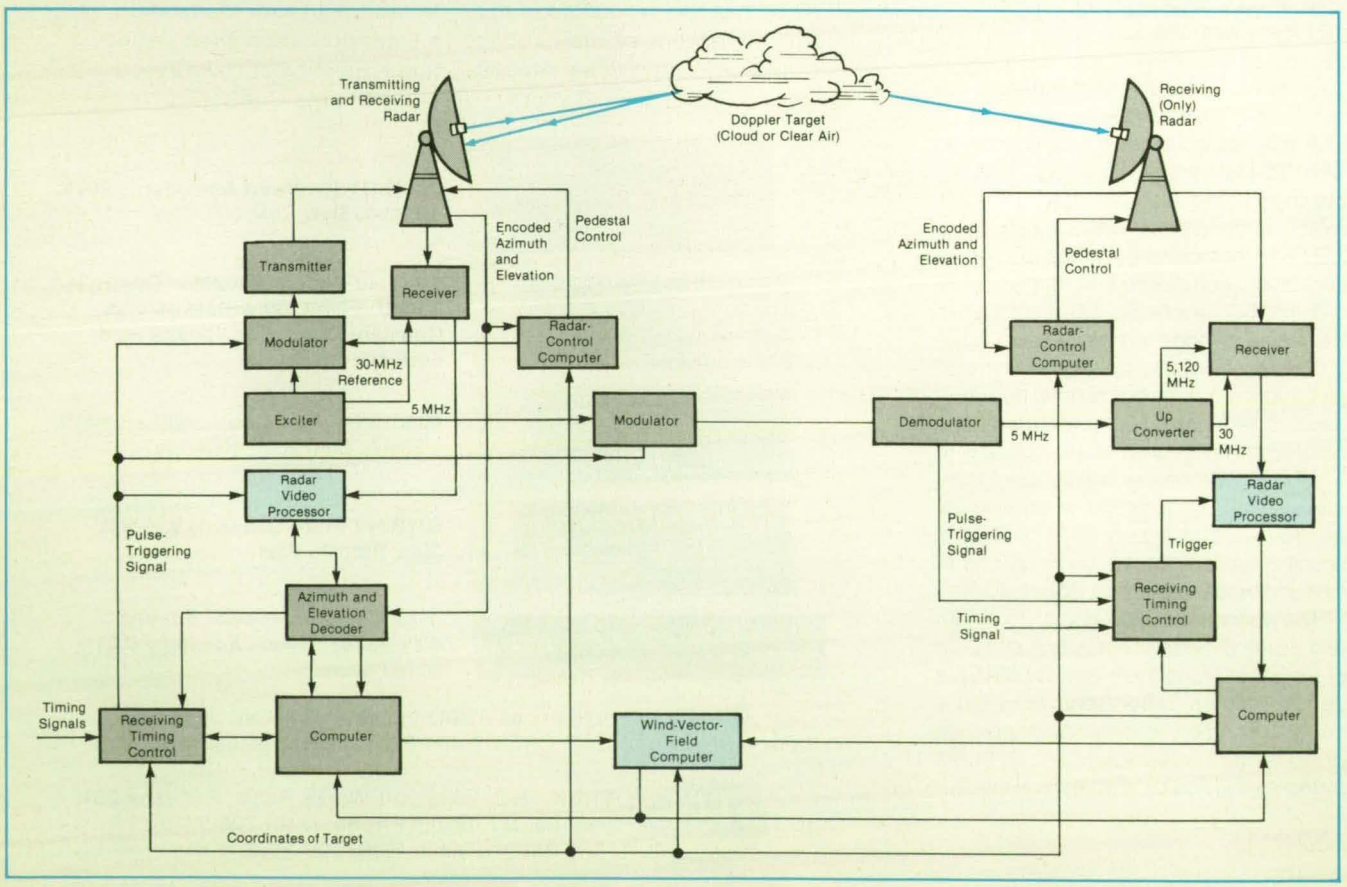

Simultaneous Measurements by Multiple Radars will be combined to produce wind-vector plots for the prediction of local thunderstorms.

THE SHAPE OF THE FUTURE

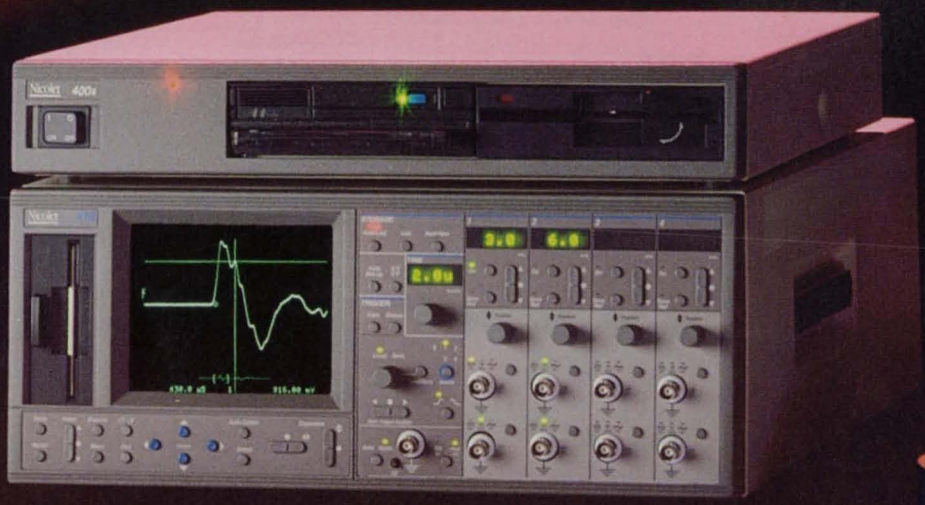

The new Nicolet 400 Series. Complete with 64K-256K expandable memory. Easy upgradability. Even removable hard drive.

Facts are facts.

Only one digital oscilloscope provides 64K-256K expandability. Software that upgrades your unit instantly. And a 44 Megabyte removable disk providing fast, easy data retrieval.

That's the new Nicolet 400 Series—a rare combination of power and speed, flexibility and convenience. It gives you all this *today* . . . so you'll be in better shape *tomorrow.*

Its expandable memory multiplies your ability to record transients over time. And along with on-board calculations, its 32-bit CPU provides waveform processing ten to 100 times faster than a PC.

The 400 takes a fresh look at data collection, too. Disk-downloadable sequences and programs help you transfer and archive data with new-found speed and accuracy. You can even cascade together four channels for memory as long as one MegaSample. And programs can be loaded with the simple touch of a button.

See how much Nicolet has done to improve your future. Send for a new 400 brochure now.

Nicolet Test Instruments Division

Nicolet

INSTRUMENTS OF DISCOVERY

5225-2 Verona Road, Madison, WI 53711, 608/273-5008 or 800/356-3090

Circle Reader Action No. 696

Real-Time Optimization of Receiver Bandwidth

Estimates of signal and noise spectra enhance the reception of weak signals.

NASA's Jet Propulsion Laboratory, Pasadena, California

A digital signal-processing subsystem continually seeks the optimum bandwidth for the digital carrier-tracking phase-locked loop (see figure) in a receiver of weak subcarrier-phase-modulated telemetry signals. The optimum bandwidth is defined here as the one that minimizes the steady-state root-mean-square (rms) phase error within the loop. It is typically wide enough to enable the receiver to track out phase jitter in the received carrier signal, yet narrow enough to limit the entry of thermal noise into the loop. Although the subsystem is intended specifically for the reception of signals from the *Pioneer 10* spacecraft, the principle of real-time optimization of bandwidth can be adapted to other situations to enhance the reception of weak signals that might otherwise be "buried" in noise.

The determination of the optimum bandwidth is based on the spectral densities of the additive receiver noise and of the components of the phase signal in the output of the phase detector in the phase-locked loop. Estimates of the spectrum are first obtained by applying fast Fourier transforms to the output of the phase detector. Given a knowledge of the transfer function of the closed phase-locked loop, the subsystem uses the data from the transforms to estimate the phase spectrum, the noise spectrum of the receiver, and the power of the received carrier signal. The optimum bandwidth is then calculated from these estimated components.

The success of this technique depends in part on the correctness of the mathematical model of the phase noise, because any real-time characterization of the phase can assist in reception. In the original application, the significant components of phase noise are generated by the transmitter, propagation of the signal (including the effects of motion, the Sun, and the atmosphere), and the voltage-controlled oscillator in the receiver. Analytic expressions for the optimum bandwidth have been derived for phase-noise spectral densities proportional to $f^{-\alpha}$ (where f = frequency), a model often quoted in the literature. For oscillator phase spectra at low frequencies, one can use $\alpha = 3$, while the effect of solar scintillation can be represented by $\alpha = 8/3$.

The value of the technique was demonstrated in the application to *Pioneer 10*. Loop bandwidths and minimum carrier-to-noise ratios for which tracking could be done were estimated for various operating conditions. It was found that the minimum signals that can be tracked are 5 to 15 dB below those that can be tracked by current receivers. This improvement is accomplished by the use of bandwidths of 0.1 to 1.0 Hz, in contrast with the 3-Hz bandwidth in current use.

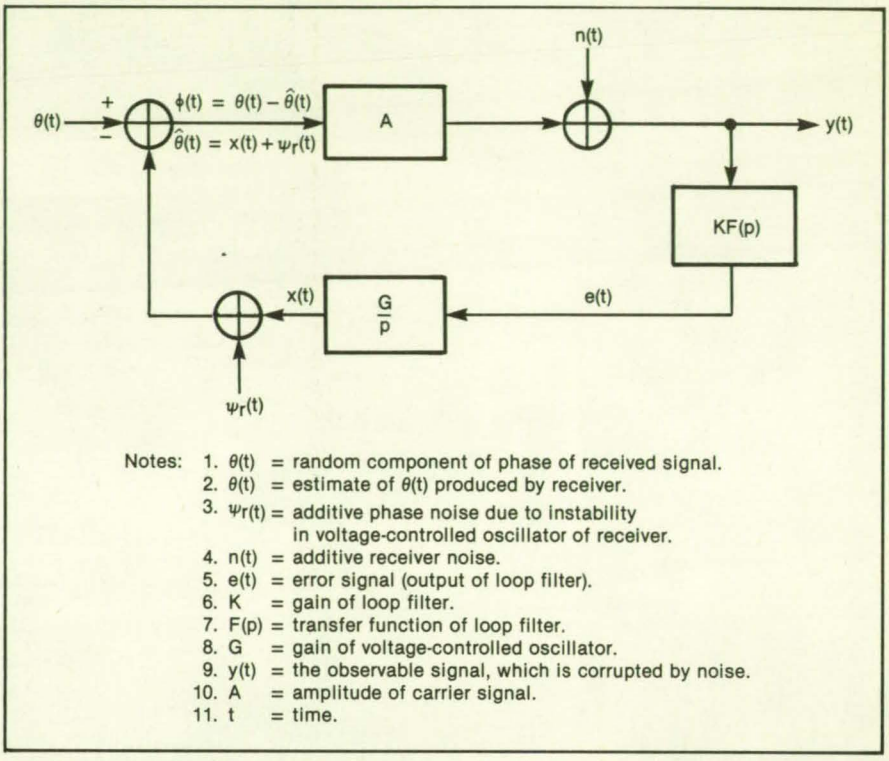

Notes:
1. θ(t) = random component of phase of received signal.
2. θ(t) = estimate of θ(t) produced by receiver.
3. ψr(t) = additive phase noise due to instability in voltage-controlled oscillator of receiver.
4. n(t) = additive receiver noise.
5. e(t) = error signal (output of loop filter).
6. K = gain of loop filter.
7. F(p) = transfer function of loop filter.
8. G = gain of voltage-controlled oscillator.
9. y(t) = the observable signal, which is corrupted by noise.
10. A = amplitude of carrier signal.
11. t = time.

The **Carrier-Tracking Phase-Locked Loop** is represented by a linear mathematical model at small rms phase errors. The loop continuously generates estimates $\hat{\theta}(t)$ of the received phase $\theta(t)$. The bandwidth (in effect, the scale of the complex-frequency variable p) can be optimized to minimize the rms phase error.

This work was done by V. A. Vilnrotter, W. J. Hurd, and D. H. Brown of Caltech for **NASA's Jet Propulsion Laboratory**. *For further information, Circle 40 on the TSP Request Card.*

NPO-17400

VLSI Universal Noiseless Coder

Features would include reliability, low weight and power, and small volume.

NASA's Jet Propulsion Laboratory, Pasadena, California

A proposed universal noiseless coder (UNC) would compress a stream of data signals for efficient transmission in a channel of limited bandwidth. The coder would be noiseless in the sense that the original data would be completely recoverable from the output code. The system would be built as a very-large-scale integrated (VLSI) circuit, which could compress data in real time at input rates as high as 24 Mb/s, and possibly faster, depending on the specific design. The VLSI approach would yield a small, lightweight system that would operate reliably and consume little power.

The conceptual UNC includes a block preprocessor and an adaptive variable-length coder (AVLC) (see figure). The block preprocessor reversibly reformats the input data stream by taking differences between successive data and relabeling the differences. The AVLC can execute any of eight optional code algorithms: namely, backup (in which it puts out the original subblock of n-bit-sampled data), fundamental sequence (in which each nonnegative integer m is converted to a string of m zeros followed by 1), and a combination of

TEAM WORK

THE COOPERATION OF 5 COUNTRIES HAS ASSURED EFFICIENCY ON THE GROUND AND RELIABILITY IN THE AIR: AIRBUS WAS DESIGNED AND EQUIPPED THROUGH THE COOPERATION AND PARTNERSHIP OF 4 EUROPEAN COUNTRIES AND THE U.S.A. THE ENGINES AND AVIONICS FOR EXAMPLE, ARE PARTLY DESIGNED AND BUILT IN COOPERATION WITH THE AMERICANS. AIRBUS ANSWERS THE PRECISE REQUIREMENTS OF AMERICAN, PAN AM, NORTHWEST, EASTERN, CONTINENTAL, AIR CANADA AND CANADIAN INTERNATIONAL, WHO FLY AND WILL FLY THEIR COLORS. THE QUALITY OF THE WORK AND THE ORIGINALITY OF THE CREATIVE EFFORT KEEPS US UP THERE — MEET THE TEAM.

aerospatiale

aerospatiale

AEROSPATIALE INC. 1101 15TH STREET N.W. WASHINGTON DC 20005
PHONE: 202 293 0650

PUBLICIS ZB-A1

fundamental sequence with k-bit sample splitting (in which each n-bit sample is split into a sample of $n-k$ most significant bits and a sample of k least significant bits) with $k = 1, 2, 3, 4, 5,$ or 6. The final coded output produced from each block of input data is a block that contains the compressed string of output bits, plus a 3-bit header that identifies the code algorithm, thereby enabling the decoder to reconstruct the original data.

The AVLC includes a code estimator, which chooses the code algorithm that performs best on the current block of input data. The selection is made on the basis of simple arithmetical operations on the sequence of input bits. The code estimator also provides an accurate estimate of the number of bits that the selected algorithm will use to code the current block of input data.

In addition to the subsystems and functions of the conceptual system as described above, the VLSI version would include the following:

- A sensor interface circuit to acquire the input data;
- A host-processor interface to exchange, with a host processor, data related to the control and status of operation — specifically, in regard to the mode of operation and the size of the data blocks;
- A UNC controller to control the compressor and coordinate with the host processor according to the control and status data;
- A ping-pong block buffer to buffer the current and the previous data blocks for the two-level pipelined operation of the UNC compressor;
- An output formatter to convert the compressed data into the desired output format; and
- A link interface to transmit the compressed data onto the output bus.

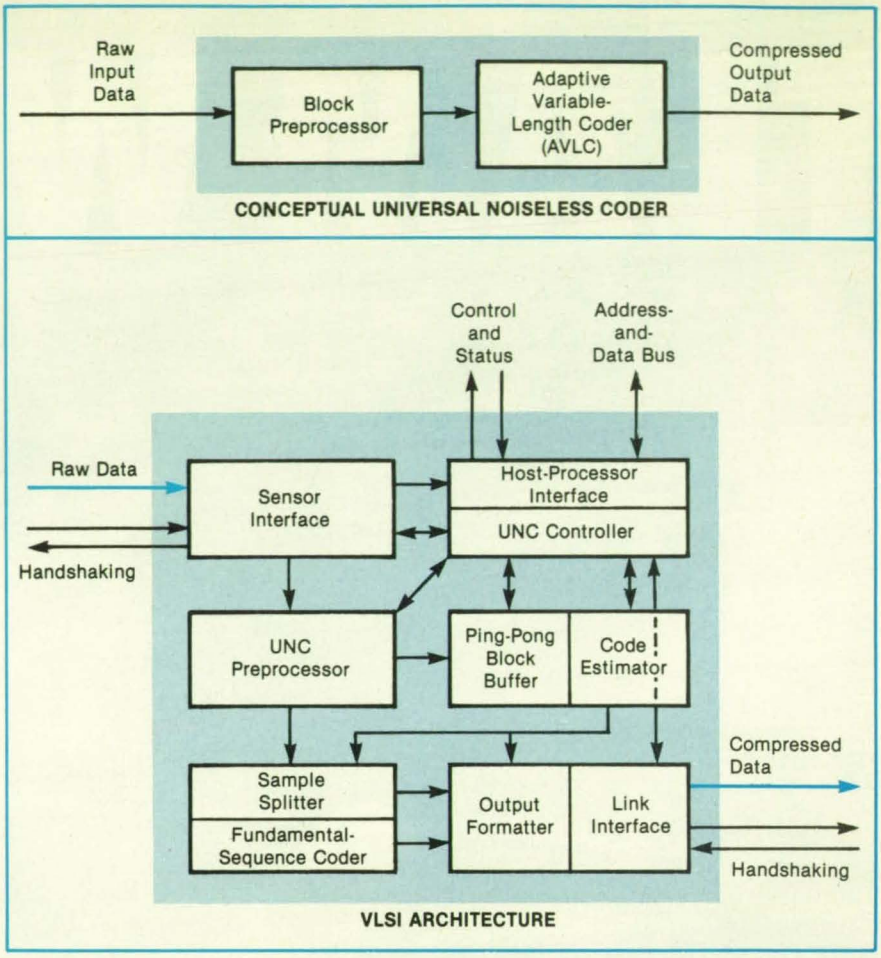

The **Universal Noiseless Coder** would be constructed as a single, compact, low-power VLSI circuit chip. The design of the coder would exploit the regularity, modularity, effective interconnections, flexibility, expendability, and concurrence that are principal features of VLSI architecture.

To promote efficiency, the design of the VLSI circuit chip would be made specific to the code algorithms. The entire UNC could be fabricated in a single chip, which would have a worst-case power dissipation less than 1 W.

This work was done by Robert F. Rice, Jun-Ji Lee, and Wai-Chi Fang of Caltech for **NASA's Jet Propulsion Laboratory**. *For further information, Circle 157 on the TSP Request Card.*
NPO-17469

Digital Video Measurements of Wing Deflections in a Wind Tunnel

Solid-state cameras and a computer-controlled image-acquisition system measure deformations of wind-tunnel models.

Langley Research Center, Hampton, Virginia

The dynamic pressure of the National Transonic Facility (NTF) is greater than three times that of other transonic wind tunnels and can cause wingtip deflections of several centimeters. A number of techniques have been suggested to measure these deflections. A photogrammetric approach was chosen because of its inherent rapid recording of data on the entire object field.

Video cameras were used instead of film cameras to acquire data because the cameras must be housed within the cryogenic, high-pressure plenum of the facility and are, therefore, inaccessible for the exchange of photographic film. The digital video model-deformation (VMD) system includes solid-state-array cameras and a digital image-acquisition system controlled by a personal computer. It is an improved version of an earlier VMD system that included high-resolution-tube cameras. The new system eliminates both the vibration-induced distortion associated with tube cameras and the manual processing of video hardcopy images necessary in the earlier version.

An AT-class personal computer controls two commercially available image-capture boards ganged to capture simultaneously two video images, each 752 picture elements wide and 480 picture elements high, in one-thirtieth of a second. The video images are digitized into 256 gray levels. The figure is a block diagram of the system.

The ability to interact conveniently with image files and processing algorithms is important in the developmental stage. The current system incorporates the flexibility

TEAM WORK

ARIANE PUTS SATELLITES INTO SPACE THAT SPEAK 27 LANGUAGES. AS INDUSTRIAL ARCHITECT AEROSPATIALE COOPERATES WITH 11 EUROPEAN COUNTRIES PROVIDING SPACE-AGE TECHNOLOGY AND MANAGEMENT SKILLS. WITH THE NUMBER OF SATELLITES LAUNCHED FOR AMERICAN COMPANIES, WE PROVE OUR CAPABILITY OF WORKING TOGETHER. AND AEROSPATIALE HAS BUILT MORE THAN 40 TECHNICALLY DIVERSIFIED SATELLITES, MANY OF THEM WITH AMERICAN PARTNERS. WORKING AND CREATING TOGETHER KEEPS US UP THERE. MEET THE TEAM.

aerospatiale

aerospatiale

AEROSPATIALE INC. 1101. 15TH STREET N.W. WASHINGTON DC 20005
PHONE: 202 293 0650

Circle Reader Action No. 661

of a popular operating system (DOS) and higher-level programming languages (e.g., C and BASIC) to facilitate the development of code. Commercially available software written in C enables a personal computer to digitize, process, display, and store video images. The video images, which are stored as DOS files, can be randomly read with code written by the user in either compiled BASIC or C for such operations as the computation of centroids. This technique, in addition to specifying the required algorithms, also details methods for calibrating both the solid-state sensors and the imaging lenses.

Tests were conducted at the NTF to establish the best-case accuracy of the digital VMD system. These tests were conducted without flow to avoid operational constraints and uncertainties in the effects of flows as well as to enable independent verification of measurements. The accuracy of the system was shown to be about 5 mils (0.13 mm) root mean square under best-case conditions over a test wing that had a semispan of 26.5 in. (67.3 cm). The accuracy of the system for the measurement of controlled single-point deflections is less than 2 mils (0.05 mm). Although this particular application was restricted to remote measurements of wing deflections in a wind tunnel, the calibration and software procedures would be generally useful to anyone attempting highly accurate remote measurements by use of charge-coupled-devices or charge-injection-device solid-state cameras.

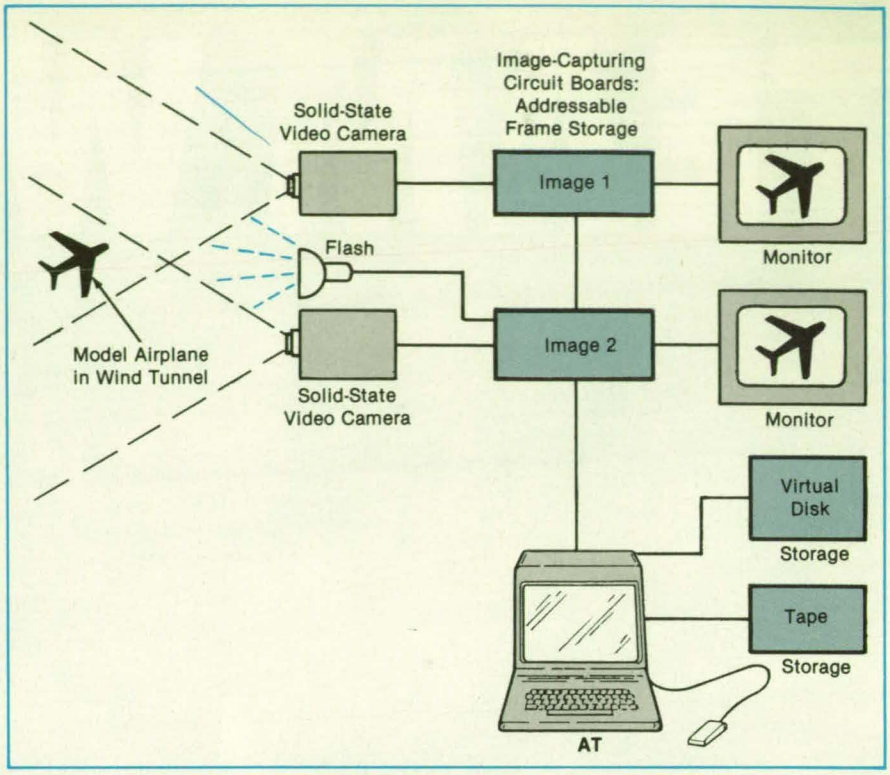

A Computer Controls Two Image-Capturing Boards used for triangulation measurements of deflection of the model.

This work was done by Alpheus W. Burner, Walter L. Snow, William K. Goad, and Brooks A. Childers of **Langley Research Center**. *For further information, Circle 109 on the TSP Request Card.*
LAR-13917

Books and Reports

These reports, studies, handbooks are available from NASA as Technical Support Packages (TSP's) when a Request Card number is cited; otherwise they are available from the National Technical Information Service.

Exciter for X-Band Transmitter and Receiver

Design and performance are described.

A report describes a developmental X-band exciter for the X-band uplink subsystem of the Deep Space Network. The X-band transmitter-exciting signal is expected to have a fractional frequency stability of 5.2×10^{-15} during a 1,000-second integration period. The exciter also generates coherent test signals for the S- and X-band Block III translator of the Deep Space Network, a Doppler-reference signal for the associated Doppler-extractor system, the first-local-oscillator signal for the associated receiver, and a reference signal for the associated ranging subsystem.

The main transmitter-exciting signal is generated by a heterodyne principle often used to stabilize output frequencies; a stable higher frequency is added to a less-stable lower frequency so that the resultant fractional stability is close to that of the more stable source. In this case, the higher-frequency input signal at 6,500 MHz is obtained by multiplying by 65 the frequency of a 100-MHz input reference signal from a hydrogen maser. The lower-frequency input signal at 690 MHz is obtained by multiplying by 16 the frequency of a portion of a 43.125-MHz signal from a synthesizer.

The two input signals are mixed and band-pass filtered to produce a signal at the transmitter-exciting frequency of 7,190 MHz. This signal is amplified, then fed through X-band command and ranging phase modulators and a radio-frequency relay to an output terminal.

Before multiplication, the portion of the 43.125-MHz signal used to generate the exciter output is passed through a voltage-controlled phase shifter, which is part of the overall-phase-control loop that reduces the variations in phase of the transmitted signal due to changes in temperature, voltages, and characteristics of components. The other portion of the raw 43.125-MHz input is multiplied directly and added to the 6,500-MHz signal to generate an unmodulated 7,190-MHz reference signal for use in the phase detector of the phase-control loop.

The coherent S- and X-band test signals and the local-oscillator, Doppler-reference, and ranging-subsystem-reference signals are generated from the inputs and outputs of the main exciter by various combinations of frequency multiplication, mixing, addition, and subtraction. Other engineering details described in the report include the physical configuration of the components and subsystems, stabilization of temperature, controlling and monitoring circuits, the distribution of the Doppler-reference signal, and the Doppler-signal-extracting system.

Tests of the prototype exciter show that the controlling and monitoring and internal phase-correcting loops perform according to the applicable design criteria. Measurements of the stability of the frequency and of the single-sideband noise spectral density of the transmitter-exciting signal are to be made subsequently.

This work was done by Carl E. Johns of Caltech for **NASA's Jet Propulsion Laboratory**. *To obtain a copy of the report, "Block III X-Band Receiver-Exciter," Circle 119 on the TSP Request Card.*
NPO-17261

MULTIBUS® II

RESTORES

A

GREAT

VIRTUE:

ARCHITECTURAL Disc

Multibus® II's Architectural Discipline is your design freedom. A solid Multibus II the clear choice for virtually

1 SIMPLE

Multibus II brings more than just power to your application. It brings simplicity that speeds development and eliminates risk. Without compromising performance or economy. ■ The spec itself (IEEE 1296) is clean, complete, disciplined. It defines a bus that is synchronous and highly deterministic. ■ Multibus II is supported by the Multibus II Systems Architecture (MSA)—an extensive *system-level* open standard. MSA implements advanced functions so you don't have to. And supports standard transport protocol to simplify complex systems. MSA even includes firmware for system configuration and self-test. ■ Choosing Multibus II can cut months off your development cycle. And zeros off your budget. ■

2 COST EFFECTIVE

Multibus II helps you reduce costs in all the places you'd expect. Plus quite a few you wouldn't. ■ Initially, Multibus II speeds development by increasing on-board functionality, and simplifying system integration. Which doesn't just reduce costs, it helps you recover them faster by getting to market sooner. ■ A range of bus interface silicon economically meets the needs of high-end multiprocessor systems, low-cost single-CPU applications, and everything in between. ■ Assembly, test and maintenance costs are reduced by features like jumperless board configuration, and built-in self test and diagnostics. For the life of your system. ■

3 FLEXIBLE

Architectural Discipline increases your choices. Of applications you can solve. And ways to solve them. ■ The Message Passing Coprocessor (MPC) and two new lower cost slave interface chips let you build systems ranging from high bandwidth to low-speed I/O. Economically. With full compatibility. ■ You have complete freedom of processors and software. 80x86s, 680x0s and 88000s. Running iRMX*, DOS, OS/2*, UNIX*, FlexOS* and VRTX*. In the same box. At the same time. ■ iSBX*, iLBX* II, MIX and OME allow vast memory expansion and custom I/O. ■ And, Multibus II's unused P2 connector opens a world of possibilities. Like AT Bus on P2 that's available now. And other buses on P2 that are planned. ■

ipline

specification, orderly design approach, and host of new products make any application requiring more than a PC.

4

INTEROPERABLE

Nowhere is the virtue of Architectural Discipline more apparent than in the superior interoperability of Multibus II. ■ *All* Multibus II boards from *all* manufacturers work together. Right out of the box. ■ Problematic issues like interrupt line assignments, dual-port memory allocations and slot dependence simply don't exist. ■ You can even mix message passing and shared memory communications methods. Or migrate from one to the other with ease. ■ This makes uniprocessor systems simpler to integrate, and multiprocessor systems a practical reality. And restores the original idea behind open bus architectures—"mix-and-match" computing. ■

5

RELIABLE

Multibus II's unique advanced features make your application more reliable and easier to maintain. ■ Like synchronous operation with full parity error detection/correction. Built-in self test and diagnostic capabilities. The freedom to plug any board into any slot. And the system's ability to automatically configure each board without jumpers or DIP switches. ■ And, naturally, Multibus II uses only DIN connectors for all backplane and I/O connections. ■ All these features are designed into the architecture itself, as well as all Multibus II boards, backplanes, chassis and other products. ■ Multibus II's Architectural Discipline means reliability you can depend on. ■

6

SCALABLE

Only Multibus II provides a virtually linear increase in performance as the number of boards grows. For scalable performance across your complete systems architecture. ■ Multibus II supports simple applications with low-cost "dumb" I/O boards, and shared memory communications. At the high end, Multibus II's cohesive structure for multiprocessing operates like a 40 Mb/sec. Local Area Network. With backplane protocols that can extend to Ethernet or fiber-based LANs. ■ Of all the buses available today, only Multibus II is capable of efficiently handling the full range of applications—from simple single-processor systems, to very complex multiple-CPU applications. Just about anywhere a PC is not enough. ■

Available

Today, Multibus II is supported by a wide range of products. Including important recent announcements that open new avenues of opportunity for engineering teams designing for the next decade, and beyond. ■ The Multibus Manufacturers Group (MMG) members who sponsored this ad invite you to send for their all-new 1990 *Multibus II Product Data Book*. It's full of information on their complete lines of Multibus II boards, systems, software and bus interface chips. And it's available free to qualified engineers and managers. ■ To request your copy just send your business card to the MMG. Or call our special toll free number today:

800 448 9602. (U.S. and Canada)

Discover a world of design freedom made possible by the Architectural Discipline of Multibus II. For large, complex applications. And small, simple ones. Just about anywhere a PC is not enough. ■

MULTIBUS MANUFACTURERS GROUP

P.O. Box 6208, Aloha, Oregon 97007 503·696·7155

CENTRAL DATA

800·482·0315 FAX 217·359·6904
Contact: Mark Decker
Family of high performance intelligent boards including single- and dual-channel SCSI host adapters, 80386 SBC, communications/terminal controller, and SBX motherboard.

CONCURRENT TECHNOLOGIES

217·356·7004 FAX 217·356·6238
Contact: Jerry Hoffman
Full line of high performance 386 and 186 CPU boards, analog and digital I/O, communications, Ethernet, Cheapernet, and 16-channel terminal controllers.

DIGITAL RESEARCH INC.

408·982·0700 FAX 408·982·0715
Contact: Director of OEM Sales
Full-featured systems software OEM products including 186, 286 and 386 FlexOS operating systems, Token Ring and TCP/IP network software, and new X/GEM graphics user interface.

HEURIKON CORP.

800·356·9602 FAX 608·831·4249
Contact: Jeremy Wright
Range of quality CPU boards and systems. The most recent introduction is a 68030-based SBC with on-card Ethernet.

INTEL

800·548·4725
Comprehensive Multibus II solutions: UNIX/iRMX based System 520, new i486 CPU, new 80386-based modular I/O, and new low cost MPI-based I/O.

MICRO INDUSTRIES

614·895·0404 FAX 614·882·6357
Contact: Susan Lawton
Complete line of Multibus I and II products for industrial control, office automation, telecommunications, military and aerospace.

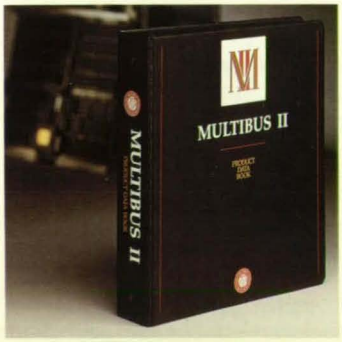

MICRO MEMORY INC.

818·998·0070 FAX 818·998·4459
Contact: Mosé Jadon
Full line of high density memory modules up to 128M bytes in a single card slot. Single and dual ports (iPSB/iLBX), Dynamic and non-volatile CMOS RAM memories.

MICROBAR SYSTEMS

408·720·9300 FAX 408·773·9475
Contact: Alex London
Reduces board development cycles to 12 weeks while meeting your application-specific requirements through our design library based on 80X86 or 680X0 processors.

PLX TECHNOLOGY, INC.

800·759·3753 FAX 415·960·0479
Contact: Gaylord Galiher
Low-cost, high drive current, bus interface specialists. Programmable and off-the-shelf interface chips for Multibus II and all other high performance buses.

SIEMENS AG

Advertising Dept., 333 State Bridge Road
Alpharetta, GA 30201
A complete range of CPU, memory and I/O cards, including local buses as OME, AMS, SMP, and AT, from the leading European board supplier for industrial automation.

THE WOLLONGONG GROUP

415·962·7200 FAX 415·969·5547
Contact: Douglas Ambort
TCP/IP and NFS protocol suites on Multibus computers running the UNIX System V Release 3.2 operating system supported on the 186/530 and 186/622A.

XYLOGICS, INC.

617·272·8140 FAX 617·273·5392
Contact: Dave Padley
Full line of very high performance, multichannel peripheral controllers under development, supporting such interfaces as ESDI, IPI and SCSI.

Legend:
- Boards
- Systems
- Software
- Bus Interface Silicon

Physical Sciences

Cryogenic Shutter Mechanism

A device minimizes heating by external and internal sources.

Goddard Space Flight Center, Greenbelt, Maryland

An electromagnetic shutter mechanism operates at ambient and cryogenic temperatures to shield an optical element, such as a mirror, filter, polarizer, beam splitter, or detector, from external light and radiation in a cryogenic Dewar that is equipped with a window for optical evaluation. The shutter can be rapidly opened and closed during the evaluation process, thus minimizing or eliminating thermal gradients in the optical element so that it can be tested accurately.

Unlike a purely mechanical shutter, the electromagnetic shutter can be installed without piercing the vacuum shell and thermal shrouds of the Dewar to install a linkage. Instead, the shutter utilizes existing electrical connections through the bottom of the Dewar and, therefore, minimizes vacuum leaks and cryogenic fluid losses. In addition, the shutter draws current only briefly, when it opens or closes, thus generating minimal internal heat.

The shutter consists of a circular copper paddle attached to a coil and magnet housing (see Figure 1). With the housing mounted directly on a cold plate in the Dewar housing and the paddle connected to the plate by a braided-copper thermal strap, the paddle is at nearly the same temperature as that of the optical element. When the mechanism torques the paddle to the open position, the optical element is exposed to radiation entering through the window. When the mechanism torques the paddle to the closed position, the radiation path to the test item is completely blocked.

The paddle is bolted to a shaft that extends through the housing (see Figure 2). Nylon bearings support the shaft. The bearings are split to accommodate thermally induced contractions when the assembly cools. The shaft supports a permanent magnet encircled by a coil mounted in the housing.

The force of gravity keeps the paddle in the closed position, resting on a mechanical stop. When current is passed through the coil, it creates a magnetic field that turns the magnet, shaft, and paddle almost 90° until the paddle strikes another mechanical stop. The paddle is then in the open position. At cryogenic temperatures, a current of 0.3 A at 8 V is required to produce movement.

When the shutter mechanism is at cryogenic temperature, it has enough mechanical resistance to stay in the open position with the current turned off, thereby generating no additional heat. When a reverse current is passed through the coil, the mechanism returns to the closed position.

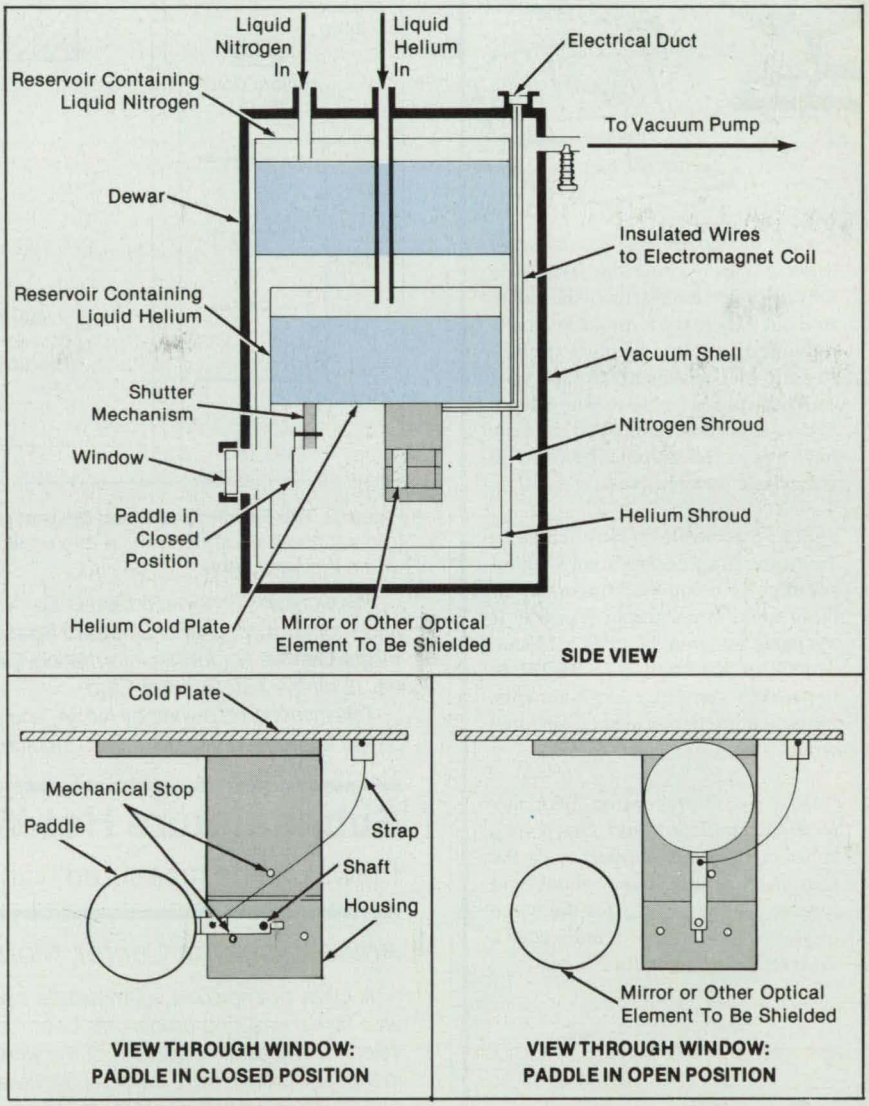

Figure 1. The **Shutter Mechanism** in the Dewar container alternately shields and exposes an optical element as a paddle is rotated between mechanical stops. The mechanism is mounted on the cold plate of the liquid-helium reservoir.

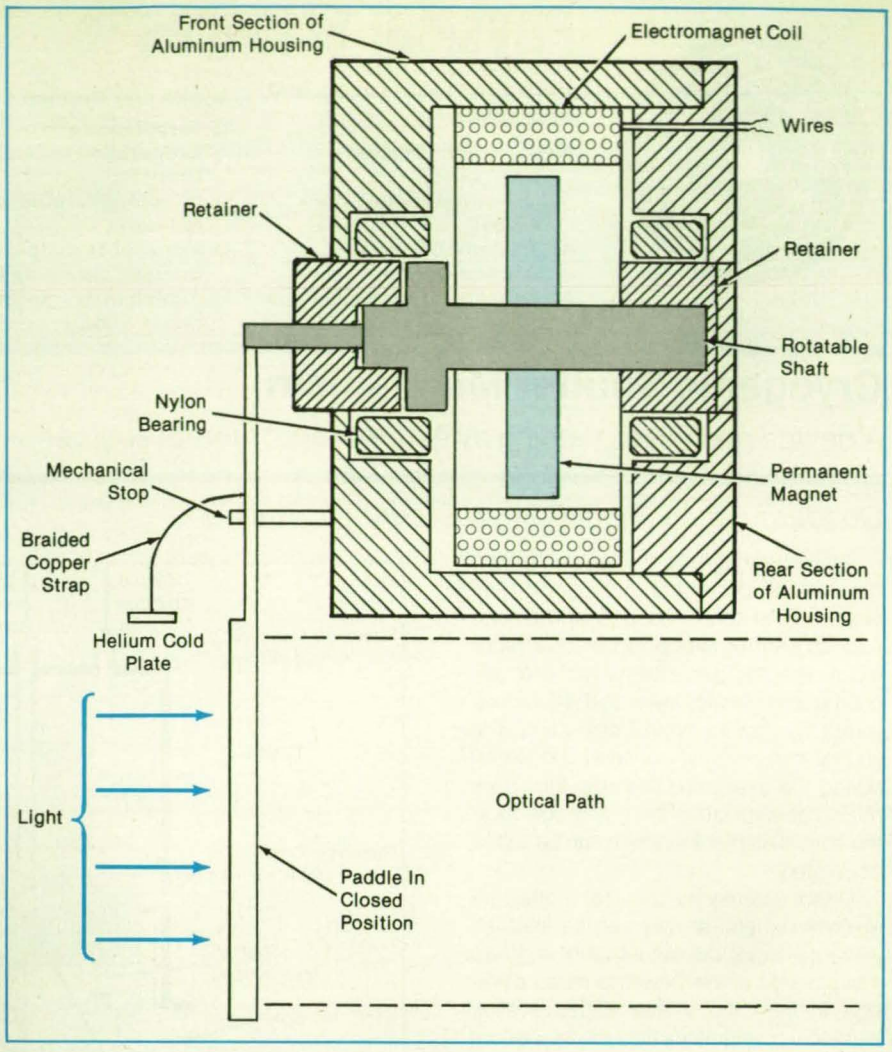

Figure 2. The **Paddle, Shaft, and Magnet** constitute an assembly that is rotated by the electromagnetic field of the coil. In this cross section, the paddle is shown in closed position, where it blocks light.

This work was done by Richard D. Barney and Thomas J. Magner of **Goddard Space Flight Center**. *For further information, Circle 15 on the TSP Request Card.*

This invention is owned by NASA, and a patent application has been filed. Inquiries concerning nonexclusive or exclusive license for its commercial development should be addressed to the Patent Counsel, Goddard Space Flight Center [see page 16]. Refer to GSC-13189

Subminiature Hot-Wire Probes

Flows can be measured with higher resolutions.

Ames Research Center, Moffett Field, California

A class of improved subminiature hot-wire flow-measuring probes has been developed. The sensing portions of the wires in the new probes have a typical diameter of 0.63 μm and lengths of 200 μm, as compared with those of the smallest conventional probes, which have typical diameters of 2 to 5 μm and lengths of 400 to 1,000 μm. The smaller sizes yield improved resolution in measurements of practical aerodynamic flows.

A probe can be made in a one-wire, two-perpendicular-wire, and three-perpendicular-wire version for measurements of one, two, or all three components of flow, respectively. Because it is so small, a probe must be oriented and positioned on a micromanipulator stage and viewed under a microscope during fabrication.

The shank of a probe includes a stainless-steel tube that surrounds an insulating ceramic cylinder, which has two, four, or six longitudinal holes for the electrical connections. Protruding from the holes at the tip of the probe are tapered nickel prongs that support the probe wire(s) (see figure).

Each probe wire is a piece of platinum/rhodium wire plated with silver. The

probe wire is cut to length, then fastened to the ends of the tapered nickel prongs with electrically conductive epoxy. The sensing length of the probe wire is defined by electrochemically etching the silver coat from the wire with a small laminar jet of nitric acid that is translated along the desired sensing length. The acid residue is then rinsed from the wire by a small jet of distilled water translated similarly along the wire. After construction, the probe is tested electrically and examined under the microscope to ensure that the length of the etched portion is consistent with the length expected on the basis of the measured electrical resistance.

Prototypes of the subminiature probes have been operated with commercial hot-wire circuitry, but some changes in the electronics and procedures were needed to reduce breakage and optimize frequency response. Calibration methods identical to those employed for conventional probes were found satisfactory for the subminiature probes. Drift was occasionally observed to be about twice that of conventional probes, resulting in slightly larger uncertainties in measurements of flows.

The subminiature probes were tested by using them to take measurements in a constant-pressure turbulent boundary layer. Measurements of mean statistical quantities, including Reynolds stresses, and spectra were obtained to evaluate the performances of the subminiature sensors compared with those of conventional probes. The results indicate that the new probes can give improved measurements of turbulence quantities near surfaces and that the anisotropies of flows strongly influence the relative errors caused by phenomena related to spatial resolution. Therefore, classical theories based on the assumption of isotropic turbulence cannot be expected to provide accurate estimates of spatial-resolution effects in cross-wire probes near walls.

This work was done by R. V. Westphal and F. R. Lemos of **Ames Research Center** *and P. M. Ligrani of the Naval Postgraduate School. Further information may be found in NASA TM-100052 [N88-22336], "Development of Subminiature Multi-Sensor Hot-Wire Probes."*

Copies may be purchased [prepayment required] from the National Technical Information Service, Springfield, Virginia 22161, Telephone No. (703) 487-4650. Rush orders may be placed for an extra fee by calling (800) 336-4700. ARC-12228

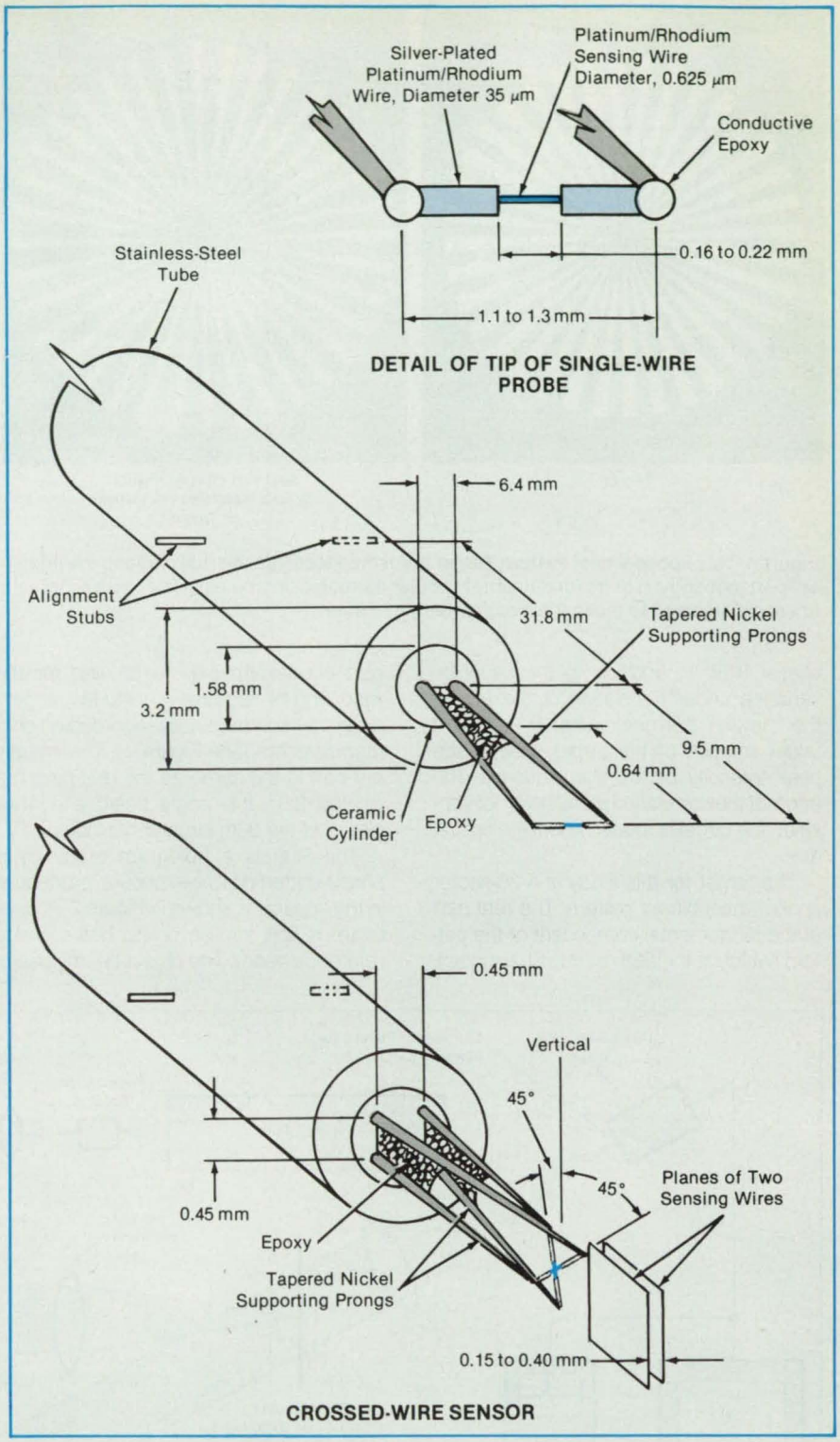

The Subminiature Probes can be made in one-wire and two-wire versions with typical configurations and dimensions like those shown here. (A three-wire version can also be constructed.) Note that the sensing wires in the crossed-wire version do not touch each other.

Making a Circular-Harmonic Filter

An optical image-correlating system is made rotationally invariant.

NASA's Jet Propulsion Laboratory, Pasadena, California

An experiment has shown that a circular-harmonic filter can be generated optically. Such a filter could be used in an optical image-recognition system that is based on the correlation between the target (the image to be recognized) and a matched

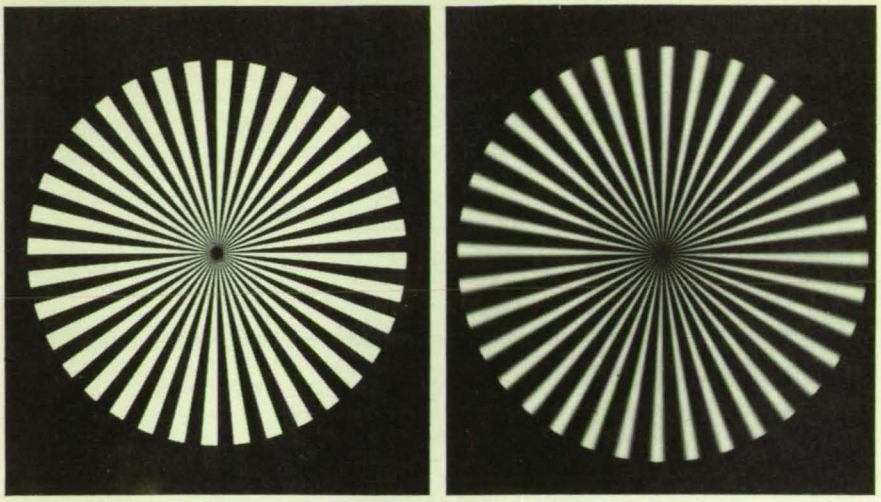

Target

Real Part of Fundamental Circular Harmonic Component of Target

Figure 1. This **Spoke-Wheel-Pattern Target** is decomposed into the real part and the imaginary part (not shown) of its fundamental circular-harmonic component. The real and imaginary parts are used to make the circular-harmonic filter.

spatial filter. In addition to the usual invariance under translation of the target, the circular harmonic filter is invariant under rotation of the target; that is, the peak intensity of the illumination at the origin of the correlation plane does not vary when the target is rotated about the optical axis.

The target for this study is a 36-sector spoke-wheel binary pattern. The real part of the fundamental component of the pattern (which is the 36th circular harmonic), plus a constant bias to provide for the recording of negative amplitudes, is generated by computer and recorded on photographic film (see Figure 1). The imaginary part is the same as the real part, but rotated 2.5°, this angle being a quarter period of the 36th circular harmonic.

The filter is a hologram made by a phase-shifted-double-exposure procedure in the apparatus shown in Figure 2. A laser beam is split into an object beam and a reference beam. The object beam passes through the target mounted on a rotation stage and is focused onto the holographic plate that is to become the filter. The reference beam is reflected from a mirror on a piezoelectric transducer through the holographic plate at an angle, where it interferes with the object beam to generate the hologram.

During the first exposure, the piezoelectric transducer is turned off, and the function recorded in the hologram is the Fourier transform of the real part of the circular-harmonic filter. During the second exposure, the piezoelectric transducer is turned on to shift the phase of the reference beam 90°, and the target is rotated 2.5° to record the Fourier transform of the imaginary part of the circular-harmonic filter.

To perform a correlation test, the reference beam is blocked by a shutter. The image to be correlated with the target is placed in the rotation stage. Correlation or the lack thereof is observed as a bright spot or the lack of a bright spot, respectively, at the center of the test image. In the experiment, the correlation was performed with the target itself. The brightness of the correlation spot was found to be invariant under both rotation and translation of the target, as expected.

This work was done by Yeou Yen Cheng of Caltech for **NASA's Jet Propulsion Laboratory**. *For further information, Circle 43 on the TSP Request Card.*
NPO-17263

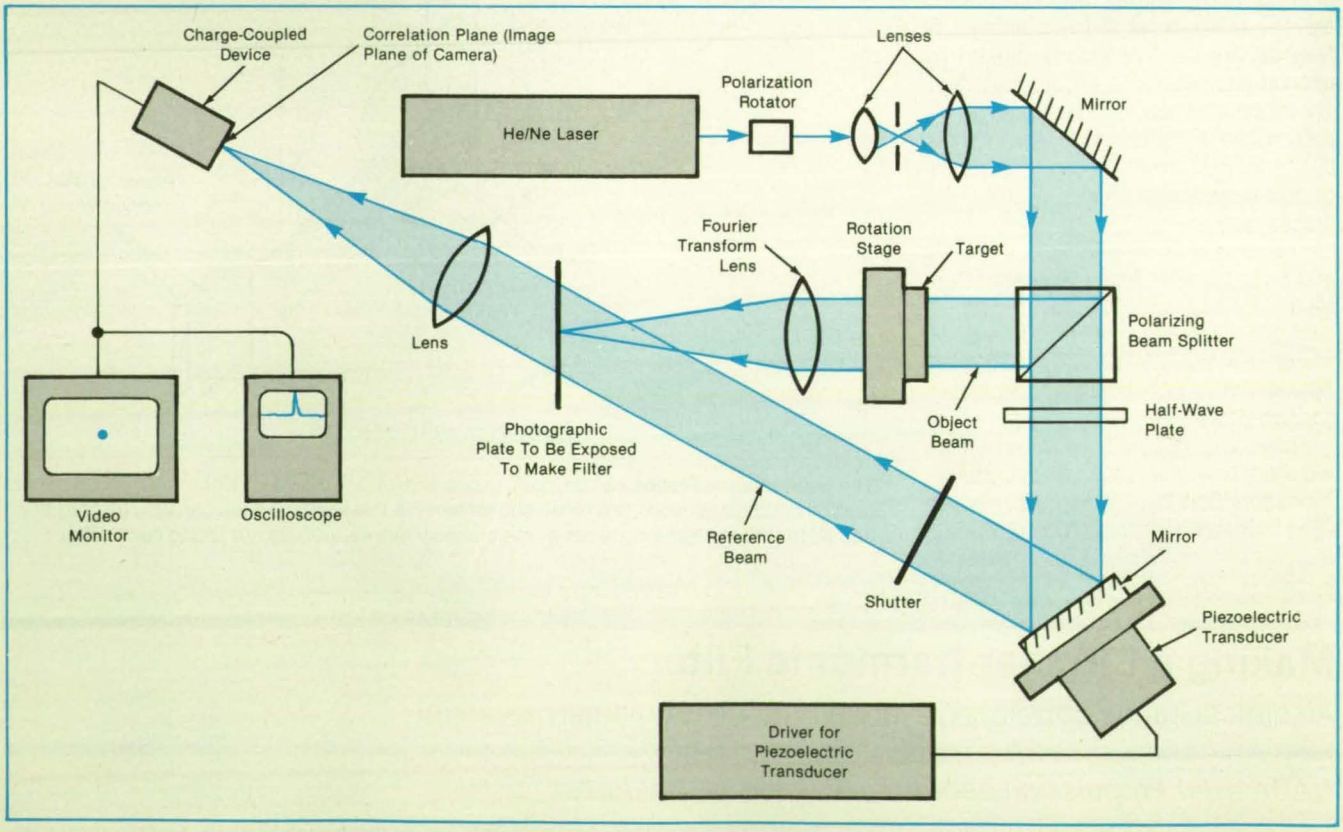

Figure 2. This **Holographic Apparatus** is used to make the circular-harmonic filter and to perform correlation tests.

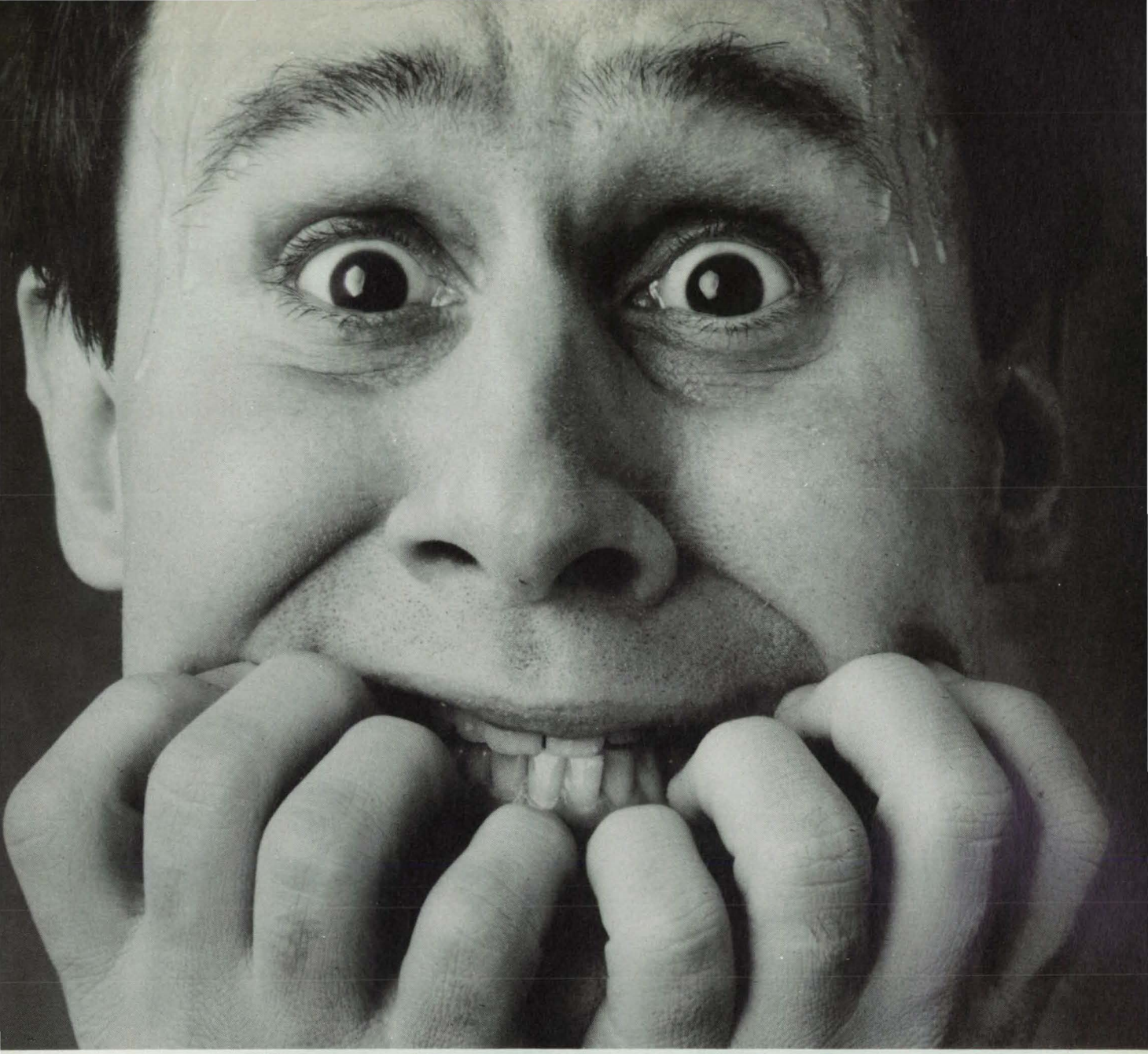

Sometimes overnight is absolutely, positively too late.

We're not knocking the other guys, but sometimes you need to get it there right away. The very same day. Today, not tomorrow.

With TWA's Next Flight Out® delivery service, you're in business.

Even as you read this, TWA planes are about to take off. We can make sure your small package is on the next flight out to any one of over 100 U.S. cities. And we'll deliver it door-to-door or airport-to-airport. Same day. Seven days a week.

We'll give you our money-back guarantee and Frequent Flight Bonus miles, too (exciting details when you call).

We also deliver next day to Europe and second day to the Middle East.

So for anything up to 70 pounds domestic and 50 pounds international, just call the 800 number. It's that easy. It's *not* that expensive. And most of all, it's fast —very, very fast.

1-800-638-7380

For information or immediate pick-up, ask for Agent 196.

Circle Reader Action No. 438

Protecting Fuel Cells From Drowning

Water in the fuel is extracted before it reaches the cells.

Lyndon B. Johnson Space Center, Houston, Texas

A water collector at the hydrogen inlet of a stack of fuel cells prevents moisture from "drowning" the cells; that is, condensing on them so that they can no longer function. The water collector includes an empty reservoir of the type normally used to hold electrolyte, a component that is used in considerable numbers in a fuel-cell powerplant.

The empty reservoir is placed next to a cooling plate (see figure). Water in the stream of hydrogen collects in the cooling plate. A wick carries the collected water to the reservoir. Because the reservoir is not part of any active cell, the water there does not degrade the performance of the stack.

The reservoir retains the water until it evaporates. The water does not pour out if the stack is tipped during handling.

This work was done by George T. Suljak and Nunziato J. Maio of United Technologies Corp. for **Johnson Space Center**. *For further information, Circle 35 on the TSP Request Card.*
MSC-21477

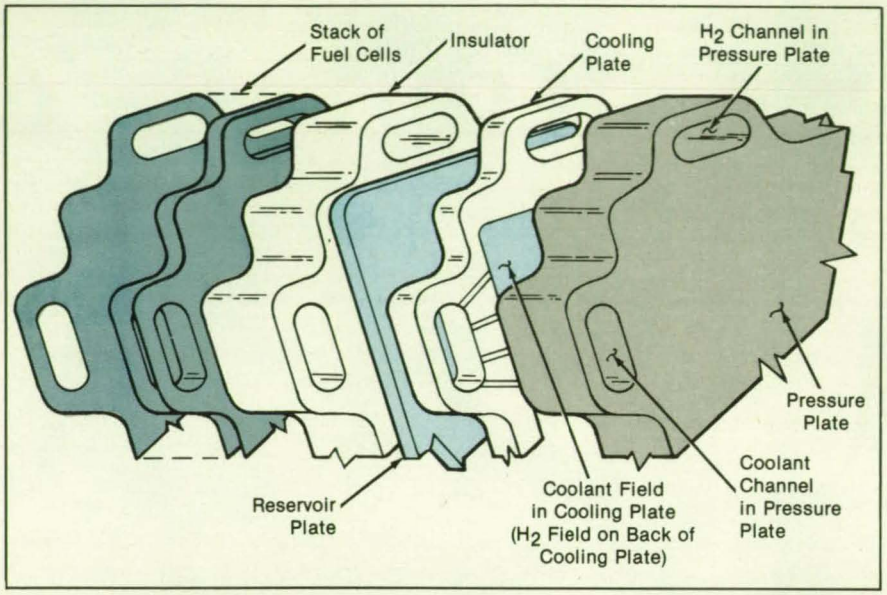

The **Stack of Fuel Cells** gets a supply of hydrogen from a manifold. The heat-exchanger plate and reservoir collect water from the flow of hydrogen. The water in the reservoir is evaporated with heat from the coolant heat-exchanger plate.

Books and Reports

These reports, studies, handbooks are available from NASA as Technical Support Packages (TSP's) when a Request Card number is cited; otherwise they are available from the National Technical Information Service.

Turbulence and Evaporation in Clusters of Drops

Turbulence speeds evaporation most effectively early in the process.

A report presents a theoretical model of the evaporation of a cluster of drops of a single-component liquid fuel in and of the processes of exchange between the cluster and the gas that surrounds it. This is a subscale (more precisely, a subgrid) model that describes the macroscopic behavior of the cluster. The cluster is smaller than the intervals of the stationary computational grid used to calculate the properties of the gas in the combustion chamber. The cluster is followed as it moves through the grid, and the cluster model is coupled with the model of the surrounding gas through the transfer of mass, molecular species, and heat across the boundary of the cluster.

For the purpose of the cluster model, the properties of the surrounding gas are assumed to be known. The drops are assumed to be spherical, of uniform size, and uniformly distributed throughout the cluster, which is assumed to be spherical. The cluster is immersed in and heated by the convectively-flowing, hot surrounding gas.

Each drop is considered to be surrounded by a sphere of influence of radius equal to half the distance between the centers of adjacent drops. The density of gas is not considered uniform inside each sphere of influence, but all drops of the cluster are assumed to behave identically. The pressure of the gases both within and without the cluster is assumed constant. As mass and energy are exchanged across the surface of the cluster, the cluster can expand or contract.

The formulation of the model has three components: (1) the description of the conservation of mass, molecular species, and enthalpy in the sphere of influence of each drop; (2) the description of the conservation of mass, molecular species, and enthalpy in the cluster volume; and (3) the description of convective effects by the use of differential equations that express the conservation of momentum for the gases and the drops. Two submodels of turbulence are considered: One describes the evaporation of the cluster in surroundings initially devoid of turbulence, and the turbulence builds up gradually with time; the other describes evaporation in surroundings where turbulence is present initially.

The results obtained from this analysis show that turbulence enhances evaporation and is a controlling factor in the evaporation of very dense clusters. For initial fuel/air mixtures of decreasing richness, both the history of the turbulence and the initial relative velocity between drops and gases can control evaporation. In this regime the evaporation time decreases with an initial increase in turbulence or relative velocity. As the initial fuel/air ratio decreases further and the initial number density of drops falls into the dilute regime, the history of turbulence and the initial relative velocity cease to control evaporation. The evaporation time decreases with the size of a dense cluster, but for a dilute cluster, size is not the controlling factor.

The practical implication of these findings is that the evaporation of fuel can be controlled more readily near the fuel injector than it can be farther along the combustor. To enhance evaporation, turbulence should be introduced into the air into

which the fuel is sprayed. This turbulence would break the clusters into smaller ones that evaporate faster and bring more hot gas from the surroundings into contact with the clusters.

This work was done by Josette Bellan and Kenneth G. Harstad of Caltech for **NASA's Jet Propulsion Laboratory**. *To obtain a copy of the report, "Turbulence Effects During Evaporation of Drops in Clusters," Circle 30 on the TSP Request Card.*

Inquiries concerning rights for the commercial use of this invention should be addressed to the Patent Counsel, NASA Resident Office-JPL [see page 16]. Refer to NPO-17323.

Effects of Turbulence on Ignition

The enhancement of evaporation by turbulence could be used to enhance ignition.

A report presents a theoretical study of the effects of turbulence on the ignition of drops of a single-component liquid fuel. This report is closely related to the one described in the preceding article, "Turbulence and Evaporation in Clusters of Drops" (NPO-17323). Although the use of turbulence to control ignition is well known to designers and experimenters, it has not previously been studied theoretically in the dense-spray regime.

The study uses a theoretical model for evaporation like the one of the preceding article and a model for ignition developed previously. The radial velocity, v_a, of gas at the surface of a sphere of influence is taken as an algebraic combination of the rate of evaporation and the speed, *da/dt*, with which the radius changes. The weighting factors of the algebraic combination are such that in a dilute spray, all new vapor coming from the drops is trapped in the cluster, whereas in a dense spray where evaporation is strong, maximum new vapor escapes to the ambient.

The rate of loss of mass from the cluster is taken as an algebraic combination of v_a and *da/dt*. It is assumed that mass, molecular species, and enthalpy are all transferred at rates proportional to that of the loss of mass. The transfers of heat, molecular species, and mass from the surroundings to the cluster are assumed to be of a turbulent nature and proportional to each other.

The fluxes of heat, mass, and molecular species into the cluster are assumed to be given by a correction to the solution for diffusion between the far field and the surface of the cluster, as in the report described in the preceding article. Thus, the convective correction contains the transfer due to turbulence. The two models of turbulence described in the preceding article — gradually increasing from zero and initially present at a high level — are used here to investigate the effects on evaporation and/or ignition.

Calculations were performed for a cluster of n-decane drops where the initial velocity of the gas is zero. The results show that turbulence promotes the evaporation necessary for ignition when the cluster is large, the temperature of the drops is low, or there is initially no fuel vapor in the gas phase. The mechanism of enhancement is increased transport between the surrounding gas and the cluster. However, the crucial control parameter is the initial ambient temperature of the gas phase because heat must be transported from the gas back to the cluster to support ignition.

This work was done by Josette Bellan and Kenneth G. Harstad of Caltech for **NASA's Jet Propulsion Laboratory**. *To obtain a copy of the report, "Ignition Enhancement for Dense Clusters of Drops Using Turbulence Effects," Circle 29 on the TSP Request Card.*
NPO-17335

Model of Turbulent Gas Eddies Containing Drops

This model applies to dense and dilute clusters of drops.

A report proposes the development of a mathematical model of a turbulent eddy of gas that contains drops of liquid fuel. This report is closely related to those described in the two preceding articles, "Turbulence and Evaporation in Clusters of Drops" (NPO-17323) and "Effects of Turbulence on Ignition" (NPO-17335). The goal is to initiate the development of a theory of the interactions of several eddies that contain drops during the evaporation, ignition, and combustion of liquid fuels injected into combustors.

As a first step, the subgrid model of a cluster of drops used in the preceding articles is introduced. Equations are written for the velocity of gas at the surface of the sphere of influence and for the loss of mass, molecular species, and heat from the cluster. As in the second of the preceding articles, transfers of mass, heat, and molecules from the surrounding gas to the cluster are modeled via a convective correction to a diffusive model, and the effects of turbulence are examined via the two submodels of turbulence.

The numerical results of the analysis are given as a plot of the nondimensionalized evaporation time versus the initial ratio of air mass to fuel mass. This plot and the conclusions with respect to the effects of turbulence on evaporation time are the same as those of the report described in the first of the two preceding articles.

This work was done by Josette Bellan of Caltech for **NASA's Jet Propulsion Laboratory**. *To obtain a copy of the report, "The Modeling of Drop-Containing Turbulent Eddies," Circle 160 on the TSP Request Card.*
NPO-17336

Aiming Instruments on the Space Station

An improved pointing system is needed to meet specifications.

A brief report discusses capabilities and requirements for the aiming of scientific instruments to be carried aboard the proposed Space Station. The report is the product of a study by a team of experts who were asked to address two issues: (1) whether the system then envisioned for pointing the instruments at celestial targets would offer sufficiently low jitter, high accuracy, and high stability to meet scientific requirements and (2) whether it would be able to do so even in the presence of the many vibrations and other disturbances on the Space Station.

The team assembled data on the pointing requirements and on the capabilities of various kinds of mounts, drives, gimbals, and other components of pointing systems. These data were analyzed by computer modeling of anticipated behaviors and by evaluation of the costs and feasibilities of the known equipment options. The team concluded that the system envisioned originally would not meet the requirements.

A tradeoff study then followed to determine the tentative architecture of a pointing system that could perform better. The salient conclusion of this study was the recommendation to develop a pointing-actuator system that includes a mechanical/fluid base isolator underneath a reactionless gimbal subsystem. This kind of system appears to offer the greatest promise of high performance, cost-effectiveness, and modularity for the job at hand.

This work was done by Jay M. Estus, Robert Laskin, and Yu-Hwan Lin of Caltech for **NASA's Jet Propulsion Laboratory**. *To obtain a copy of the report, "NASA Office of Space Science and Applications Study on Space Station Attached Payload Pointing," Circle 22 on the TSP Request Card.*
NPO-17518

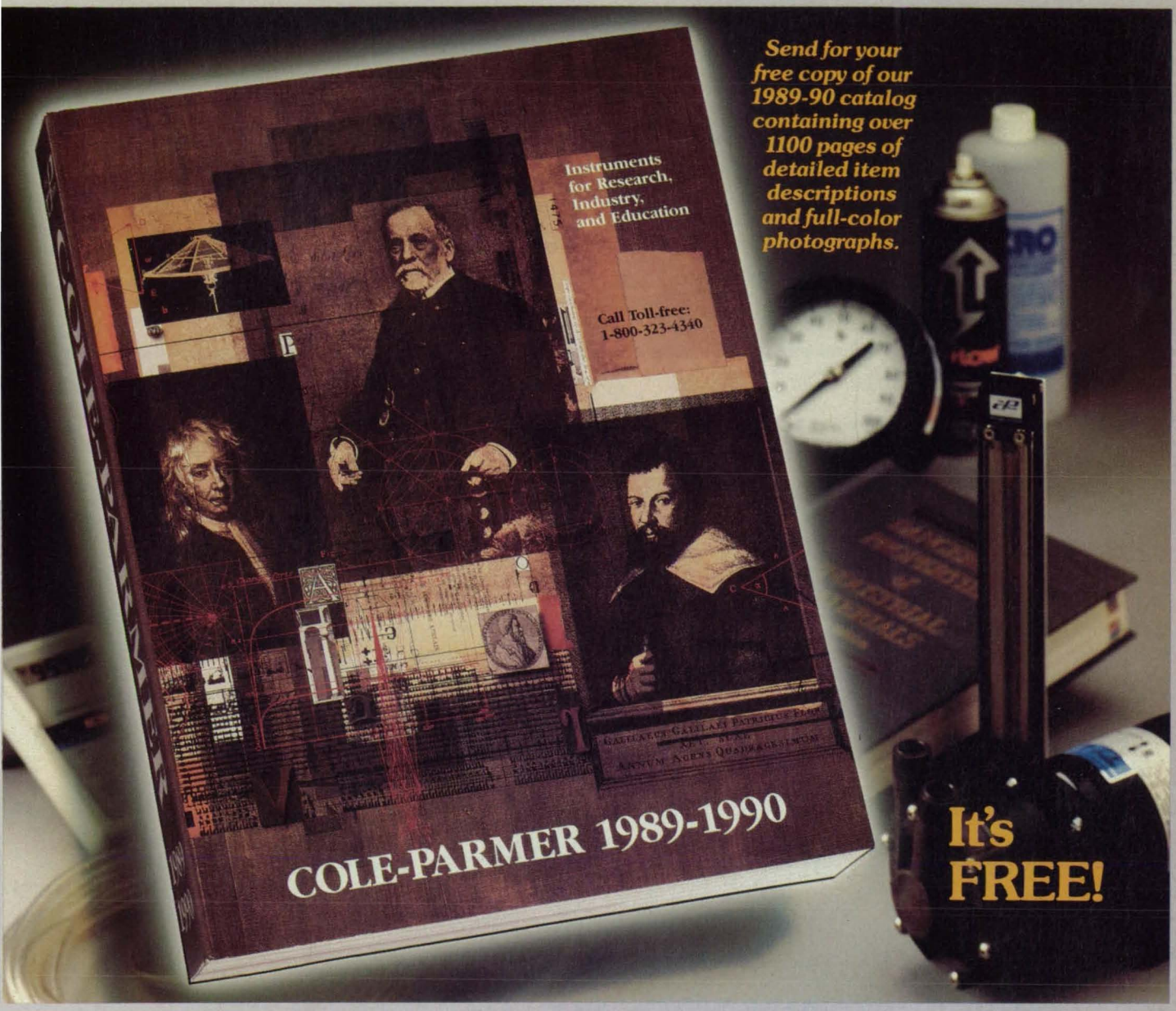

Cole-Parmer is...
industrial instruments *and more!*

Cole-Parmer offers a wide selection of instruments, transmitters, and supplies for use in today's industrial market— over 20,000 items.

And we go one step further with:

Skilled technical application support—Our network of technical and service specialists is available to assist you with your measurement and control applications.

Fast delivery—90% of all orders are shipped within 72 hours.

Responsive customer service—We're committed to your satisfaction.

Easy ordering—Our experienced sales staff stands ready to assist you with your product needs.

Our many product lines include:

• Books • Computer software • Conductivity • Data acquisition • Environmental testing equipment • Distributed process controllers • Temperature measurement and control • Flowmeters • Fluid handling equipment • Humidity measurement and control • Liquid level control • Mixers • Ovens and furnaces • pH measurement and control • Pressure monitors and controls • Pumps • Recorders • Tubing • Viscosity controls... and more.

Cole Parmer **Cole-Parmer Instrument Company** 7425 North Oak Park Avenue Chicago, Illinois 60648 1-800-323-4340

Circle Reader Action No. 638

Ozone/Ultraviolet-Photo-oxidation Reactor

Hydrazines are processed more thoroughly into harmless substances.

Lyndon B. Johnson Space Center, Houston, Texas

An experimental chemical-processing system destroys waste hydrazine in water by use of ozone in an ultraviolet-photo-oxidation reactor. The conventional process for the disposal of hydrazines is chlorination and oxidation by stirring with calcium hypochlorite in open tanks. This process emits partially oxidized compounds and chlorinated and cyclic hydrocarbons, some of which are more dangerous than the hydrazines. In contrast, the new process reduces the concentrations of hydra-

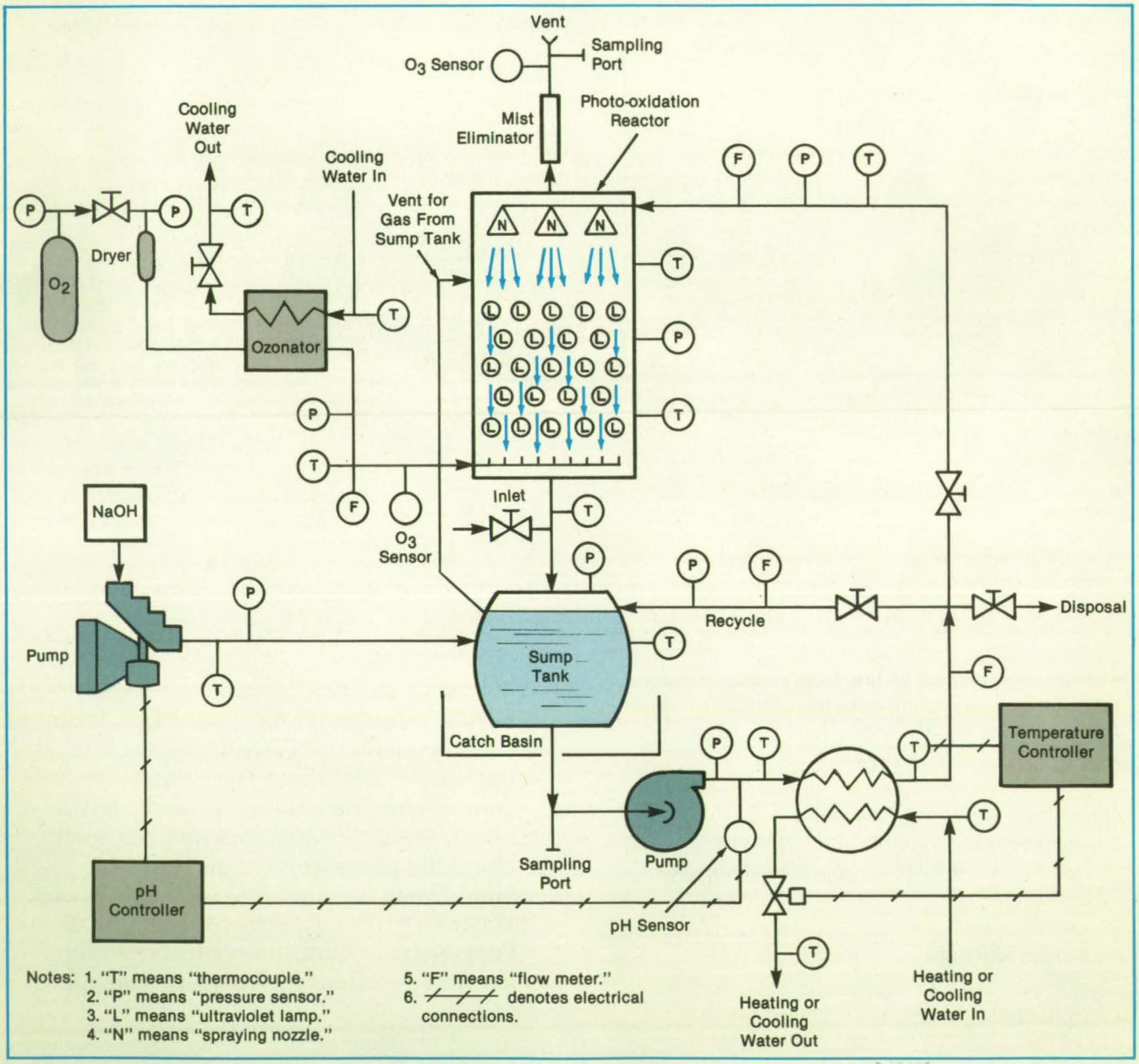

Liquid Is Sprayed in a reaction chamber past ultraviolet lamps, against a flow of oxygen and ozone. Hydrazines and intermediate decomposition products thereof are oxidized to harmless substances.

After centuries of practice, mankind perfects engineering calculations: MathCAD.

Announcing MathCAD 2.5: The Dawn of a New Age.

What the historians will call it, only time will tell.

Perhaps the Century of Speed, or the Era of Ease. But whatever the name, this is the age of MathCAD 2.5, the only math package that looks and works the way you think.

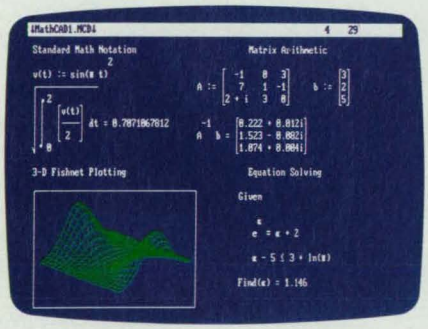

MathCAD 2.5 includes 3-D plotting, HPGL sketch import, and PostScript output.

MathCAD is far and away the best-selling math package in the world. Because it lets you perform engineering and scientific calculations in a way that's faster, more natural and less error-prone than the way you're doing them now—whether you're using a scratchpad, calculator, spreadsheet or program that you wrote yourself.

And now we've made the best even better. MathCAD 2.5 is a dramatically improved version that includes three-dimensional plotting, enhanced numerical analysis, and the ability to import HPGL files from most popular CAD programs, including AutoCAD.® And now you can print on PostScript® compatible printers.

And like before, MathCAD's live document interface™ lets you enter equations anywhere on the screen, add text to support your work, and graph the results. Then print your analysis in presentation-quality documents.

It has over 120 commonly used functions built right in, for handling equations and formulas, as well as exponentials, differentials, cubic splines, FFTs and matrices.

No matter what kind of math you do, MathCAD 2.5 has a solution for you. In fact, it's used by over 60,000 engineers and scientists, including electrical, industrial, and mechanical engineers, physicists, biologists, and economists.

But don't take our word for it; just ask the experts. PC Magazine recently described MathCAD as "everything you have ever dreamed of in a mathematical toolbox."

PC MAGAZINE EDITORS' CHOICE
March 14, 1989 issue.
Best of '88
Best of '87

And for Macintosh® users, we present MathCAD 2.0, rewritten to take full advantage of the Macintosh interface. Entering operators and Greek letters into equations is pure simplicity!

Look for MathCAD 2.5 at your local software dealer, or give us a call. For more information, a free demo disk, or upgrade information, dial 1-800-MATHCAD (in MA, 617-577-1017).

Available for IBM® compatibles and Macintosh computers.

TM and ® signify manufacturer's trademark or manufacturer's registered trademark respectively.

MathCAD®

MathSoft, Inc. One Kendall Square, Cambridge, MA 02139

22

U.K.: Adept Scientific 0462-480055; **France:** ISE CEGOS 1-46092768; **Germany:** Softline 07802-4036; **Japan:** CRC 03-665-9768. *PE*

Circle Reader Action No. 628

zines and intermediate decomposition products in the effluent liquid and gas to below the limit of detectability.

The batch of water containing hydrazines is circulated between a sump tank and the photo-oxidation reactor (see figure). The liquid is sprayed downward from 6 nozzles at the top of the reactor, past a bank of 23 mercury-vapor germicidal lamps that generate the ultraviolet light. A flow of oxygen containing ozone is introduced through sparging tubes at the bottom of the reactor, directed upward against the spray. The ultraviolet light excites the ozone molecules to a more reactive state. The top of the reactor is vented to the atmosphere through a stainless-steel-wire-mesh mist eliminator. The reactor chamber and many of the other components of the system are also made of stainless steel.

To generate the stream of oxygen containing ozone, oxygen from a tank is passed through a drier to eliminate contamination by moisture, then fed to a high-voltage discharge in a commercially available ozonator. The ozonator is cooled to a temperature of about 287 K (14 °C, slightly below room temperature) to increase the concentration of ozone from the manufacturer's stated figure of 2 weight percent to about 2.75 weight percent.

The effectiveness and speed of the process depend on the maintenance of the circulating liquid at the correct pH, which appears to determine the lower limit of oxidation by ozone. A pH sensor and controller maintain the pH of the basic hydrazine solution within ±0.5 of the optimum value, which lies between 9 (for low concentrations of chlorine-oxidizable species) and 11 (for high concentrations).

The temperature of the circulating liquid is sensed and controlled because it strongly affects the process in two competing ways: higher temperature increases the rate of reaction but also hastens the dissolution and decomposition of the ozone. Which of these effects predominates depends on the concentration of the solution to be processed. The results of some experiments suggest that a higher temperature (~314 K) should be used initially because the net effect is to speed the reaction at a high concentration of chlorine-oxidizable species. Once the concentration is reduced to 2.5 ppm, a lower temperature (~286 K) favors faster and more-complete chemical reactions.

This work was done by Ari Ben Swartz and Richard E. Agthe of Lockheed Engineering & Management Services Co. for **Johnson Space Center**. *For further information, Circle 47 on the TSP Request Card.*
MSC-21488

Books and Reports

These reports, studies, handbooks are available from NASA as Technical Support Packages (TSP's) when a Request Card number is cited; otherwise they are available from the National Technical Information Service.

Pourable Foam Insulation

A study identifies commercial materials for demanding applications.

A report describes a search for polyisocyanurate/polyurethane foam insulation with superior characteristics. The search was prompted by difficulties with the proprietary insulation used on the external fuel tank of the Space Shuttle and by the desire to find a formulation of nonproprietary ingredients for which chemical information is generally available.

A typical current formulation consists of part A, containing isocyante functionalities; and part B, containing one or more polyol(s) and various additives. The report discusses the chemistry of current formulations. Tests of these formulations, of individual ingredients, and of alternative new formulations are described.

The search revealed commercially available formulations that exhibit increased thermal stability at temperatures up to 600 °C, can be poured readily before curing, present a good appearance after curing, and remain securely bonded to aluminum at cryogenic temperatures. Besides thermal stability, pourability, appearance, and cryogenic bond strength, candidate formulations had to be curable at room temperature and to lose all tackiness — inside and out — within 3 hours after mixing. Of the total of 42 different formulations investigated, 10 were found to meet these requirements. On the basis of its overall performance, one of these formulations was selected as a standard for experiments to determine the effects of additives. Fire retardants, foaming agents, and catalysts were thus evaluated.

This work was done by James A. Harvey, John M. Butler, and Richard P. Chartoff of the University of Dayton for **Marshall Space Flight Center**. *To obtain a copy of the report, "Development of Polyisocyanate Pour Foam Formulation for Space Shuttle External Tank Thermal Protection System," Circle 92 on the TSP Request Card.*
MFS-27217

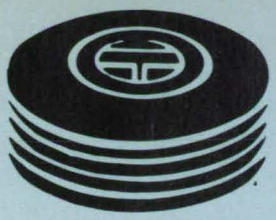

Computer Programs

COSMIC: Transferring NASA Software

COSMIC, NASA's Computer Software Management and Information Center, distributes software developed with NASA funding to industry, other government agencies and academia.

COSMIC's inventory is updated regularly; new programs are reported in *Tech Briefs*. For additional information on any of the programs described here, circle the appropriate TSP number.

If you don't find a program in this issue that meets your needs, call COSMIC directly for a free review of programs in your area of interest. You can also purchase the 1988 *COSMIC Software Catalog*, containing descriptions and ordering information for available software.

COSMIC is part of NASA's Technology Utilization Network.

COSMIC® — *John A. Gibson, Director,* (404) 542-3265
The University of Georgia, 382 East Broad Street, Athens, Georgia 30602

Computer Programs

These programs may be obtained at a very reasonable cost from COSMIC, a facility sponsored by NASA to make computer programs available to the public. For information on program price, size, and availability, circle the reference number on the TSP and COSMIC Request Card in this issue.

Physical Sciences

Tracing Rays in a Solar Power System

The optical behavior of an offset paraboloidal collector and receiver is computed.

OFFSET is a ray-tracing computer code for analysis of the optics of a solar collector. The code models the distributions of solar flux within the receiver cavity, produced by reflections from the collector. The code was developed to model mathematically the offset solar collector of the solar dynamic electric power system that is being developed for Space Station Freedom. This solar dynamic system includes a receiver offset from the axis of a paraboloidal collector, which reflects solar energy into the cylindrical cavity of the receiver. The solar energy heats a gas that drives a turbogenerator that produces electric power.

The collector consists of 19 hexagonal panels. Each panel contains 24 triangular, reflective facets. The offset-paraboloidal-collector configuration is determined by an input file of coordinates of the corners of the facets. Other configurations could be chosen by changing this file, but modifications to the FORTRAN code would be required to simulate collectors that have other than 19 groups of 24 triangular facets.

Unique features of this code include the following:

1. Equations were developed to select sources of rays on the Sun pseudo-randomly. These sources appear evenly distributed, and their relative strengths show solar-limb darkening.
2. Cone-optic techniques are used to add surface specular errors to the sources to determine the apparent sources of the reflected sunlight.
3. The contours of the reflective surfaces of the facets can be chosen to be spherical, ideal paraboloidal, or toroidal.
4. Gaussian distributions of radial and tangential components of surface-slope errors are added to the perpendiculars to the surface at the 10 nodal points on each facet.
5. Color contour plots of the distribution of flux incident on the receiver can be generated by PATRAN processing of the output of the computer code.

The code has been used to develop a revised collector-facet concept of four groups of toroidally contoured (instead of spherically contoured) facets. The four groups have different facet curvatures, but the facets within each group are identical and interchangeable. The code is being used to develop methods for tailoring the distribution of flux incident on the receiver. These methods include offsetting the aperture of the receiver from the axis of the receiver and selecting aiming points for alignment of each of the facets.

The OFFSET program was developed for the IBM 370 (VM) and is written in FORTRAN 77 (100 percent). Color contour plots require PATRAN (PDA Engineering, Costa Mesa, CA). OFFSET was developed in 1987 and 1988.

This program was written by Kent Jefferies of **Lewis Research Center** *and Chris Gallo of W. L. Tanksley and Associates. For further information, Circle 116 on the TSP Request Card.*
LEW-14778

Simulating Scenes in Outer Space

Scientifically accurate simulations are generated quickly.

The Multimission Interactive Picture Planner, MIP, is a computer program for scientifically accurate and fast, three-dimensional animation of scenes in deep space. MIP is also versatile, reasonably comprehensive, and portable, and runs on microcomputers. New techniques were developed to perform rapidly the calculations and transformations necessary to animate scenes in scientifically accurate three-dimensional space. At the same time, portability is maintained, inasmuch as the transformations and clipping have been written in FORTRAN 77 code. MIP was primarily designed to handle Voyager, Galileo, and the Space Telescope. It can, however, be adapted to handle other missions.

The simulated scene includes a rotating body (usually a planet), any natural satellites, a spacecraft, the Sun, stars, descriptive labeling, and field-of-view boxes. The central body and natural satellites are triaxial wire-frame representations with terminators, limbs, and landmarks. Hidden lines are removed for the central body and natural satellites, but not for the scene as a whole, so that bodies can be seen behind one another. The program has considerable flexibility in its step time, observer position, viewed object, field of view, and the like. Most parameters can be changed from the keyboard while the simulation is running.

When MIP is executed, it asks the user for a control file, which should be prepared before execution. The control file identifies which mission MIP should simulate, the star-catalog files, the ephemerides files to be used, the central body, landmarks, and other constants. The control file also describes the fields of view. Control files are included to simulate the Voyager 1 encounter with Jupiter and the passage of the Giotto spacecraft by Halley's comet. Data are included for Voyager 1 and 2 (all six planetary encounters) and Giotto.

MIP comes in IBM PC or compatible format, including a working example. It requires 512K of random-access memory, a CGA or compatible graphics adapter, and DOS 2.0 or higher. However, the program is primarily designed to be ported and configured on a wide variety of computers. Users must supply their own graphics primitives to clear the screen, change the color, and connect two-dimensional points with straight lines. Also, the users must tie in the graphics primitives along with their ephemeris readers. MIP does everything else, including clipping. MIP was developed in 1988.

This program was written by John D. Callahan of Caltech for **NASA's Jet Propulsion Laboratory**. *For further information, Circle 113 on the TSP Request Card.*
NPO-17246

Gaussian-Beam Laser-Resonator Program

Radii of laser beams are calculated as functions of position.

In designing a laser cavity, the engineer is frequently concerned with more than the stability of the resonator. Other considerations include the sizes of the beam at various optical surfaces within the resonator and the performance of intraresonator line-narrowing or other optical elements. Laser resonators obey the laws of Gaussian beam propagation, not geometric optics. The Gaussian Beam Laser Resonator Program models laser resonators by use of Gaussian-beam-propagation techniques. It can be used to determine the radii of beams as functions of position in laser resonators.

The algorithm used in the Gaussian Beam Resonator Program has three major components. First, the ray-transfer matrix for the laser resonator must be calculated. Next, the initial parameters of the beam are calculated. These parameters are the stability of the beam, the radius and location of the waist of the beam in the input element of the resonator, and the curvature of the wavefront and radius of the beam at the input surface of the first element of the resonator. Finally the propagation of the beam through the optical elements is computed.

The optical elements that can be modeled are parallel plates, lenses, mirrors, dummy surfaces, and gradient-index (GRIN) lenses. A gradient-index lens is a good approximation of a laser rod operating under a thermal load. The optical system may contain up to 50 elements. In addition to the internal beam elements, the optical system may contain elements external to the resonator.

The Gaussian Beam Resonator program was written in Microsoft FORTRAN (Version 4.01). It was developed for the IBM PS/2 80-071 microcomputer and has been implemented on an IBM PC compatible under MS DOS 3.21. The program was developed in 1988 and requires approximately 95K bytes to operate.

This program was written by Patricia L. Cross, Clayton H. Bair, and Norman Barnes of **Langley Research Center**. *For further information, Circle 17 on the TSP Request Card.*
LAR-14080

ATAM — Automated Trade Assessment Modeling

Figures of merit are generated for comparisons of proposed Space-Station data-management systems.

The Automated Trade Assessment Modeling program, ATAM, is one of the software tools designed to assess candidate architectures for the data-management system of the proposed Space Station. It is designed to discriminate among the candidates that have equally acceptable performance and reliability characteristics. It utilizes a data base, defined by the user, that contains information (cost, weight, volume, crew time, subsystem grouping, etc.) on a candidate architecture.

ATAM assesses such trade factors of a system as weight, power consumption, and life-cycle cost. It produces detailed parameter assessments as well as a single figure of merit for the candidate architecture. This information is then stored for comparison with the figure of merit assessed for other candidate architectures.

ATAM was written for an IBM PC X/AT or compatible computer. It requires 400K of random-access memory, a hard disk, a printer with 132 columns, and DOS 3.1 or higher. ATAM was developed in 1986.

This program was written by Antonio Vallone, Mei-Zong Wu, and Keith Hogie of Computer Sciences Corp. for **Langley Research Center**. *For further information, Circle 102 on the TSP Request Card.*
LAR-13999

Nonlinear Curve-Fitting Program

A nonlinear optimization algorithm helps in finding the best-fit curve.

A common method for fitting data is a least-squares fit. In the least-squares method, a fitting function specified by the user is introduced in such a way as to minimize the sum of the squares of distances between the data points and the fitting curve. The Nonlinear Curve Fitting Program, NLINEAR, is an interactive curve-fitting routine based on a description of the quadratic expansion of the χ^2 statistic.

NLINEAR utilizes a nonlinear optimization algorithm that calculates the best statistically weighted values of the parameters of the fitting function and the χ^2 that is to be minimized. The inputs to the program are the mathematical form of the fitting function and the initial values of the parameters to be estimated. This approach provides the user with such statistical information as goodness of fit and estimated values of parameters that produce the highest degree of correlation between the experimental data and the mathematical model.

In the mathematical formulation of the algorithm, the Taylor expansion of χ^2 is first introduced, and justifications for retaining only the first term are presented. From the expansion, a set of n simultaneous linear equations are derived and are solved by matrix algebra. To achieve convergence, the algorithm requires meaningful initial estimates for the parameters of the fitting function.

NLINEAR is written in FORTRAN 77 for execution on a CDC Cyber 750 computer under NOS 2.3. It has a central-memory requirement of 5K 60-bit words. Optionally, graphical output of the fitting function can be plotted. Tektronix PLOT-10 routines are required for graphics. NLINEAR was developed in 1987.

This program was written by Joel L. Everhart of **Langley Research Center** *and Forooz F. Badavi of PRC Kentron, Inc. For further information, Circle 101 on the TSP Request Card.*
LAR-13934

Mechanics

Gland With Cantilever Seal

A tube is sealed by deformation.

Marshall Space Flight Center, Alabama

A single-piece gland forms a tight seal on a probe or tube that contains liquid or gas at high pressure. The gland and probe align themselves as they are assembled by a simple torquing procedure. They can be disconnected easily and reused at the same site. They can be made from any of a wide variety of materials so that they are compatible with the application.

Conventional pressure fittings for probes consist of two to four pieces and require more-complicated assembly procedures. Often they include soft sealing parts that cannot be reused. Often too they demand custom engineering to ensure compatibility with the particular operating environment.

The gland is placed on the tube or probe. In one version (see figure), a metal boss seal is added below the gland. The gland is then threaded into a hole in the housing to which the tube or probe is to be sealed. The cantilever action of the upper end of the gland deforms the wall of the tube or probe, thereby sealing the wall to the gland around the circumference. At the same time, the gland compresses the boss (in one version) or mates with a conical sealing surface of its lower end (in another version), thereby sealing the base of the gland. The lower pressure inside the gland enhances the deformation and pressure seals.

The wall of the tube or probe must be thick enough to accommodate the deformation without rupturing. The maximum deformation is designed in coordination with the seating and deformation of the boss or conical seal.

This work was done by Patrick B. Melton of United Technologies Corp. for **Marshall Space Flight Center**. *No further documentation is available.*

Inquiries concerning rights for the commercial use of this invention should be addressed to the Patent Counsel, Marshall Space Flight Center [see page 16]. Refer to MFS-28328

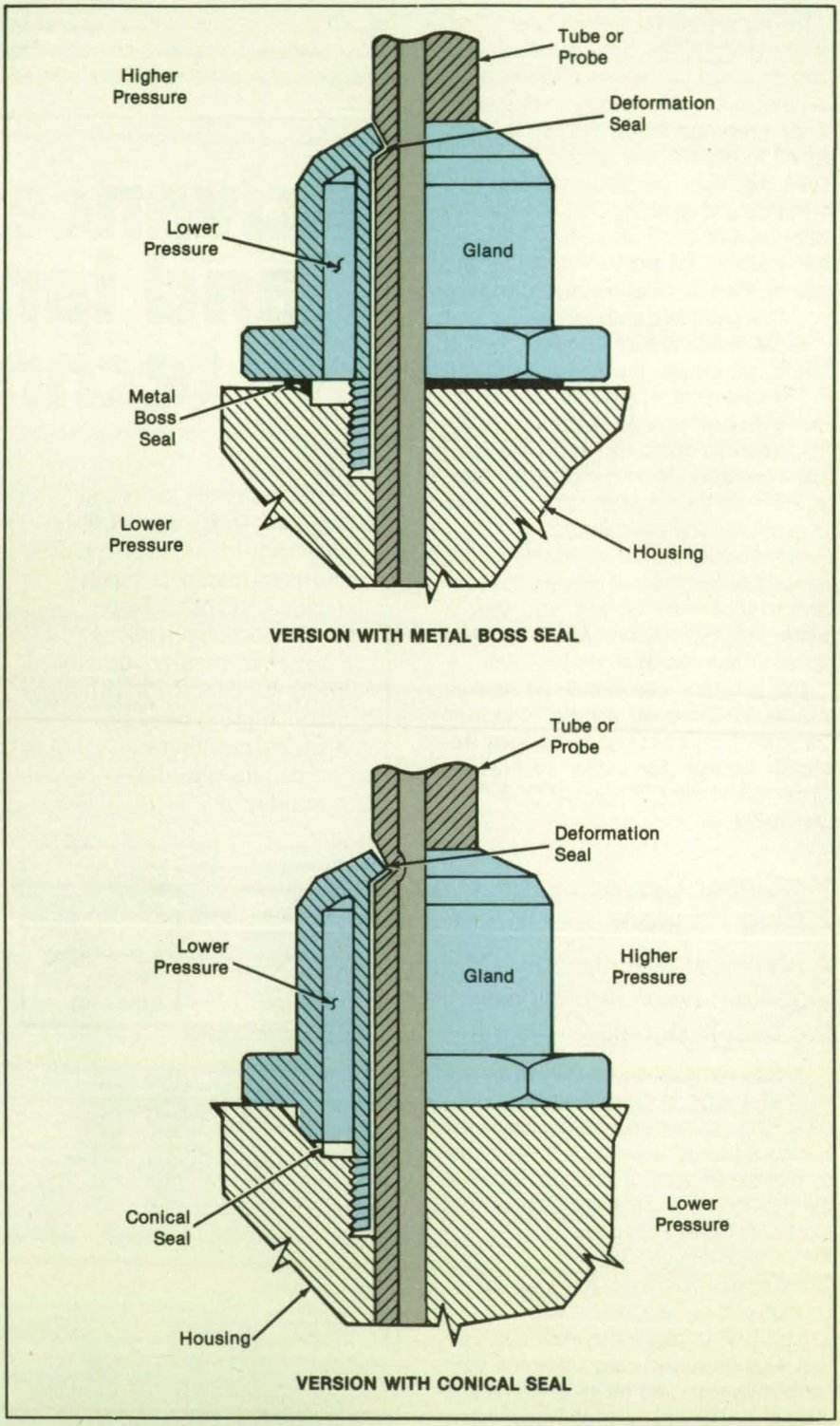

The Cantilever Ring at the Top of the Gland bites into the wall of the tube or probe, sealing it. The deformation is exaggerated in this partial cutaway view.

Mechanical Device Traces Parabolas

Continuous curves are generated and points located with ease.

Lyndon B. Johnson Space Center, Houston, Texas

A mechanical device simplifies the generation of parabolas of various focal lengths. The device is simple in design and easy to use because it is based on the fundamental geometric construction of the parabola. Likely applications of the device include the design of paraboloidal antennas, approximating catenaries on drawings of powerlines or long-wire antennas, and general tracing of parabolas on drawings.

The device (see figure) includes a radius track (dimension *r*) and a perpendicular focal-point track that lies along the axis (dimension *z*) of the parabola. A depth track, also aligned along the *z* direction, is joined to the radius track by a pair of back-to-back linear bearings. These bearings allow the depth track to slide along its own length or to move along the radius track, while constraining the depth and radius tracks perpendicular to each other.

A nonrotating pulley is clamped at the desired position along the focal-point track. The center of this pulley defines the focal point. A cable clamped to this pulley extends to and around a movable pulley of equal diameter on the $-z$ end of the depth track and terminates at a cable clamp on the back-to-back linear bearings on the *r* axis. The vertex of the parabola is chosen to lie at the desired focal distance, *f*, along the *z* axis below the focal point. (Alternatively, the vertex could be chosen first and the focal point located at a distance *f* along the *z* axis above the vertex.)

After the focal point and vertex are chosen, the depth track is moved near the focal-point axis and adjusted until the center of the movable pulley lies at the vertex. While the depth track remains in this position, the cable is unclamped at one end, tightened to remove slack, and then reclamped.

Thereafter, pulling downward and rightward on the depth track while keeping the cable in tension causes the center of the pulley at its end to move along the locus of points for each of which the sum of the distance to the focal point and the distance to the radius track is the total length of the clamped cable less the length of cable wrapped on the two pulleys. By definition, this locus is the parabola

$$z = (r^2/4f) - a$$

where *a* is the distance from the *r* axis to the vertex. It is not necessary to correct for the wrap of the cable on the pulleys because the total length of wrap about both pulleys remains constant as the curve is traced.

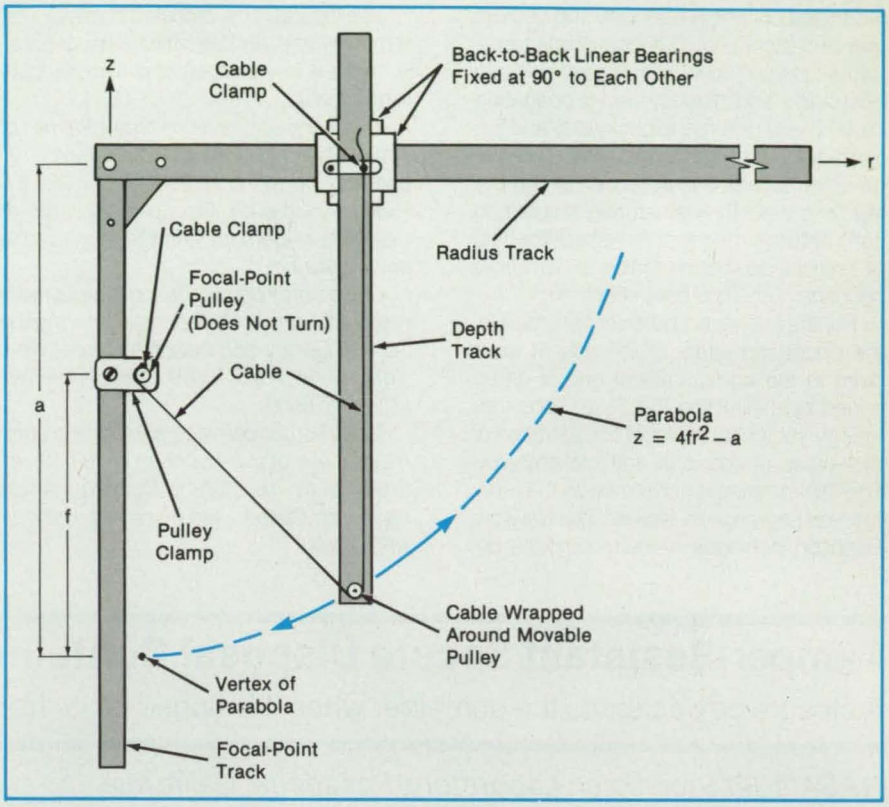

The **Parabola-Tracing Device** is based on the fundamental geometrical construction of the parabola. The constancy of the critical total distance is enforced by maintaining the cable in tension.

This work was done by Terry A. Soper of Lockheed Engineering and Management Services Co. for **Johnson Space Center**. *For further information, Circle 165 on the TSP Request Card.*
MSC-21421

Algorithm for Hypersonic Flow in Chemical Equilibrium

An improved shock-capturing scheme is mathematically stable.

Ames Research Center, Moffett Field, California

An implicit, finite-difference, shock-capturing algorithm calculates inviscid, hypersonic flows in chemical equilibrium. The algorithm is an intermediate product of continuing efforts to understand flows of air and other gases about blunt bodies where ideal-gas conditions do not apply. The shock-capturing scheme was chosen over a shock-fitting scheme because shock-fitting schemes tend to be less flexible and computationally more expensive. Although it is more difficult to make into a computer program, the implicit formulation was chosen because it overcomes the limitation on mathematical stability encountered in explicit formulations.

For the dynamical portion of the problem, the Euler equations are written in conservation-law form in a Cartesian coordinate system (x, y) for two-dimensional or axisymmetric flow. These equations are reformulated in terms of a generalized, equispaced coordinate system (ξ, η) that can be related via a Jacobian transformation to a curvilinear coordinate system that conforms to the body in the flow field. An equation of state is derived to relate the total energy density to the pressure and the kinetic-energy density. The temperature, pressure, and density are related via the

thermally perfect equation of state.

The part of the algorithm devoted to the foregoing equations is similar in its basic form to the approximate-factorization algorithm of Beam and Warming. The differences that correspond to the spatial derivatives are calculated via a flux-splitting technique, in which matrices and vectors that express the various coordinate transformations and flow variables are split into upstream- and downstream-propagating parts. These give rise to backward- and forward-difference approximations. The major advantage of this approach is that the resulting algorithm is naturally stable and can capture strong shocks without the help of artificial-dissipation terms to damp out spurious numerical oscillations.

For the chemical portion of the problem, the equilibrium state of the gas at each point in the computational grid is determined by minimizing the local Gibbs free energy, subject to the local conservation of molecules, atoms, ions, and total enthalpy. The minimization is performed by the technique of Lagrange multipliers. The Newton-Raphson technique is used to find the updated values of these multipliers and of the temperature and the number densities of the species.

The algorithm was tested with a Mach-20 flow of air over a hemisphere at free-stream conditions of pressure corresponding to an altitude of 20 km and a temperature of 216.7 K (see figure). The calculated pressures, temperatures, and densities were generally within a few percent of previously published results.

This work was done by Grant Palmer of **Ames Reseach Center**. *Further information may be found in AIAA Paper No. 87-1580, "An Implicit Flux-Split Algorithm to Calculate Hypersonic Flowfields in Chemical Equilibrium."*

Copies may be purchased [prepayment required] from AIAA Technical Information Service Library, 555 West 57th Street, New York, New York 10019, Telephone No. (212) 247-6500.

Inquiries concerning rights for the commercial use of this invention should be addressed to the Patent Counsel, Ames Research Center [see page 16]. Refer to ARC-12140.

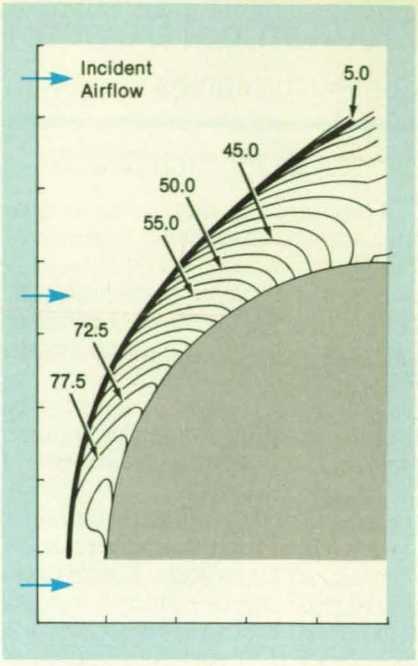

Normalized Temperatures as computed by the algorithm for the flow around a hemisphere are plotted on isothermal lines in half of a meridional plane.

Tamper-Resistant Secure Disposal Container

A closure device shuts the container when it is tipped on its front, back, or sides.

NASA's Jet Propulsion Laboratory, Pasadena, California

A closure device for secure waste containers prevents classified papers and other proprietary articles from being withdrawn when the container is turned on its side. In an earlier version of this device, a secure container has interdigitating combs hanging at its opening. If the container is turned upside down in an attempt to shake out its contents, the combs flop downward and mesh over the opening, preventing the contents from falling out. However, if this type of container is laid sideways, it could be vulnerable to tampering by a pair of tongs.

The new closure has a pendulum that swings a comb into its closed position when the container is turned on its side. The pendulum is suspended with its axis of rotation perpendicular to the axes of the combs (see figure). The pendulum extends through a D-shaped cam ring, that is attached to the upper comb with standoff struts.

When the container is tilted sideways, the pendulum swings along the arc side of the D-shaped ring. In so doing, it forces the cam ring aside, thereby moving the upper comb toward the closed position.

If the container is tilted forward or backward so that the combs close, the pendulum does not interfere with the comb movement. The width of the D ring accommodates the closing motion of the upper comb without engaging the pendulum on the flat side.

Like the combs, the pendulum shank and the cam ring can be made of inexpensive, heavy-gauge wire. The pendulum should be quite heavy so that it can overcome pivot friction and other restraining forces. Spring catches can be added to the combs so that if they are actuated and close the container opening, they lock in place to prevent further tampering.

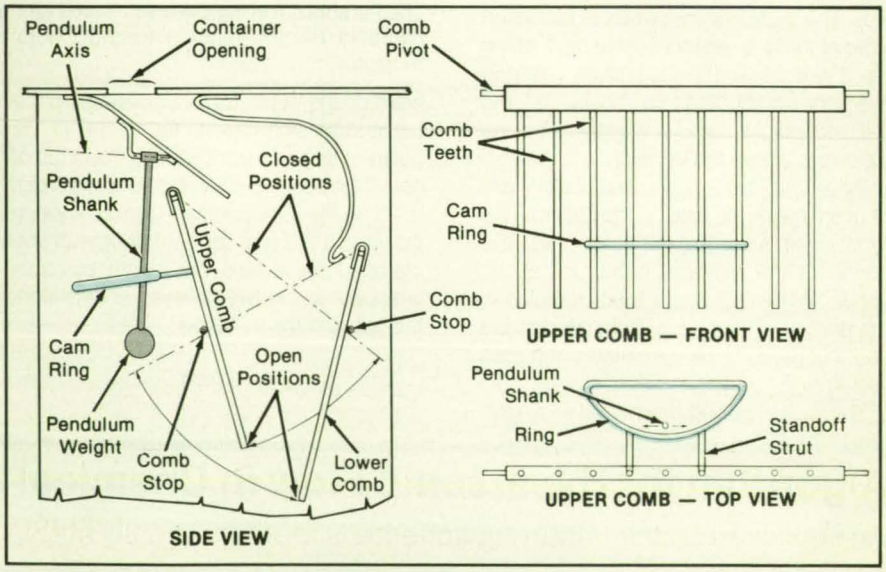

The **Sideward Movement of the Container** swings the pendulum, which drives the upper comb toward the container opening. Forward or backward movement of the container actuates both the upper and lower combs in the conventional manner but does not involve the pendulum.

This work was done by Earl R. Collins, Jr., of Caltech for **NASA's Jet Propulsion Laboratory**. *For further information, Circle 128 on the TSP Request Card. NPO-16639*

Books and Reports

These reports, studies, handbooks are available from NASA as Technical Support Packages (TSP's) when a Request Card number is cited; otherwise they are available from the National Technical Information Service.

Bearing-Bypass Loading on Bolted Composite Joints

An unexpected interaction between the effects of bypass and bearing loads is reported.

Joints of composite materials have often been designed by use of simple procedures developed for parts made of metals. In most such cases, the design strains in the affected structures have been limited by considerations of tolerance to damage, and at low levels of strain in the structures, the joints have been adequate. However, as tougher composites come into use, design strains will rise, and requirements on the joining of structures will become more stringent.

Analytical procedures for the design of joints should be based on a sound understanding of the responses of composite materials under loading conditions similar to those in multi-fastener joints. Within multi-fastener joints, fastener holes may be subjected to both bearing loads and loads that bypass the holes. The ratios of the bearing loads to the bypass loads depend on the stiffnesses and configurations of the joints.

As a joint is loaded, this bearing-bypass ratio at each fastener remains nearly constant until damage begins to develop. In general, different bearing-bypass ratios produce various failure modes and a different strength for each fastener hole. Accordingly, a combined experimental and analytical study described in a NASA technical memorandum was conducted to investigate the effects of simultaneous bearing and bypass loading on a graphite/epoxy laminate.

Tests were conducted with a test machine that enables the bearing-bypass load ratio to be controlled while a single-fastener coupon is loaded to failure in either tension or compression. Each test coupon consisted of 16-ply quasi-isotropic graphite/epoxy laminate with a centrally located 6.35-mm bolt that had a clearance fit. The center of the specimen was bolted between two bearing-reaction plates that were attached to the load frame via two load cells.

The ends of the specimen were then gripped and loaded independently by upper and lower servocontrol systems. Any difference between these two end loads produced a bearing load at the central bolt hole. This bearing load was measured by the load cells under the bearing-reaction plates. The end loads were synchronized by a common input signal. As a result, a constant bearing-bypass ratio was maintained throughout each test.

Damage-onset and ultimate strengths were determined for each test case. The computed local stresses were used with appropriate failure criteria to analyze the observed failure modes and strengths. An unexpected interaction of the effects of the bypass and bearing loads was found for the onset of compression-reacted bearing damage. This interaction was caused by a decrease in the bolt-hole contact arc and a corresponding increase in the severity of the bearing loads. The amount of bolt-hole contact had a significant effect on local stresses and thus on the calculated damage-onset strengths.

An offset-compression mode of failure of the laminate was identified under compression bearing-bypass loading. This mode of failure appears to be unique to compression bearing-bypass loading and, therefore, cannot be predicted from simple tests. Therefore, there may be a need to combine predictions of laminate bearing-bypass strengths with selected bearing-bypass testing to account for the offset-compression failure mode.

These results are important in the emerging technology of composites for use in a wide range of applications. These include applications in aircraft, boats, and automobiles, in which bolted connections to composites will be increasingly important.

This work was done by John H. Crews of **Langley Research Center** *and Rajiv-Vikas A. Naik of PRC/Kentron. Further information may be found in NASA TM-89153 [N87-25437], "Bearing-Bypass Loading on Bolted Composite Joints."*

Copies may be purchased [prepayment required] from the National Technical Information Service, Springfield, Virginia 22161, Telephone No. (703) 487-4650. Rush orders may be placed for an extra fee by calling (800) 336-4700.
LAR-14106

Mathematical Models of Turbulence in Transonic Flow

Predictions of several models are compared with measurements of a well-documented flow.

A report reviews the performances of a variety of mathematical models of turbulence in transonic flow. The predictions of these models are compared with measurements of the flow in a wind tunnel along

the outside of a cylinder that has an axisymmetric bump of circular-arc cross section in a meridional plane. This review is part of a continuing effort to calibrate and verify computer codes for the prediction of transonic flows about airfoils.

The bumpy-cylinder experiment was chosen as the standard of comparison for two reasons: (1) the aerodynamic effect of the bump is similar to that of the upper surface of an airfoil, and (2) the experiment is well documented and free of both uncertainties in the angle of attack and interference from the walls of the wind tunnel. The measurements included surface pressures, mean velocities, and Reynolds stresses.

The flow about the cylinder was computed by a series of computer codes that accommodate the various turbulence models under test. The codes used an explicit second-order, predictor/corrector finite-difference algorithm modified by an efficient implicit algorithm. The computational mesh had variable spacing in the radial and axial directions. The upstream boundary conditions were uniform free-stream conditions, with the total pressure and temperature held constant and the static properties found from relationships based on the method of characteristics. Downstream, the boundary conditions were the setting of all axial gradients to zero. In all cases, the surface boundary conditions were zero velocity and nearly adiabatic wall temperature. Uniform free-stream conditions were applied at the far radial boundary.

The models tested are summarized as follows:

- The Cebeci-and-Smith turbulence model divides the boundary layer into inner and outer sublayers. In the inner sublayer, the eddy viscosity is expressed algebraically with a length scale that is the distance from the surface and with a velocity scale that is the shear velocity. In the outer sublayer, these scales are the displacement thickness and the velocity at the edge of the boundary layer.
- The model of Johnson and King also divides the boundary layer into two sublayers wherein the eddy viscosities are expressed algebraically. In the inner sublayer, the velocity scale in this model depends on the maximum shear stress within the boundary layer. This stress is found from the solution of an ordinary differential equation that represents the rate of the development of the maximum shear stress with distance along the surface. Compared to the Cebeci-and-Smith model, the Johnson-and-King model contains two additional coefficients.
- The model of Jones and Launder is an example of models that employ two additional partial differential field equations to evaluate the velocity and length scales of the turbulence, thereby allowing for the rate processes in the development in the local state of the scales of turbulence. In this model, the dependent variable in the first equation is the kinetic energy of turbulence, whereas that in the second equation is the rate of dissipation of the kinetic energy of turbulence.
- The model of Wilcox and Rubesin is similar to that of Jones and Launder in that two turbulence field equations also are employed to yield turbulence scale quantities on which to base the eddy viscosity. In this model, the variable used to develop the length scale is the rate of dissipation divided by the kinetic energy.
- Two models developed by Coakley are modified versions of the Jones-and-Launder and Wilcox-and-Rubesin models, designed to ease numerical difficulties encountered with them.

The Johnson-and-King model proved superior in predicting the transonic flow over the bumpy cylinder. However, as the authors are careful to indicate, it is generally accepted that there is no unique way of mathematically modeling turbulence in transonic flow fields, and some field-equation models with wall-function boundary conditions can be competitive with the Johnson-and-King model.

This work was done by Morris W. Rubesin and John R. Viegas of **Ames Research Center**. *To obtain a copy of the report, "Turbulence and Modeling in Transonic Flow," Circle 117 on the TSP Request Card.*
ARC-12292

Analysis of Straight and Wavy Annular Seals

Rotordynamic coefficients are derived.

A report presents an analysis of incompressible flow in an annular turbopump seal with a straight or radially/axially wavy (azimuthally symmetrical) surface facing the shaft. The purpose of the analysis is to quantify the effects of the waviness on the rotordynamic coefficients of the seal.

The basic equations of incompressible flow in the seal are derived by use of a control-volume model. The flow is assumed to be completely turbulent in the axial and circumferential directions with no separation and is modeled by Hirs' equations of turbulent lubrication. Linearized zeroth- and first-order perturbation equations are developed for small motion about a centered position by an expansion in the eccentricity ratio.

The zeroth-order continuity and momentum equations are solved exactly, yielding the axial and circumferential velocity components and the pressure distribution. The first-order equations are reduced to three ordinary complex differential equations in

the axial coordinate. The equations are integrated to satisfy the boundary conditions and yield the perturbation pressure distribution. This resultant pressure distribution is integrated along and around the seal to yield the force developed by the seal and the corresponding dynamic coefficients.

A comparison of the rotordynamic coefficients for wavy smooth, wavy rough, straight smooth, and straight rough seals shows the following:

- A wavy seal produces less direct stiffness than does the corresponding straight seal.
- A wavy seal produces more direct damping than does the corresponding straight seal.
- A wavy seal produces more cross-coupled stiffness than does the corresponding straight seal.
- The whirl frequency is approximately the same in both of the smooth seal configurations. However, the whirl-frequency ratio of the wavy rough seal is considerably less than that of the straight rough seal.

This work was done by Joseph K. Scharrer of Rockwell International Corp. for ***Marshall Space Flight Center****. To obtain a copy of the report, "The SSME HPFTP Wavy Interstage Seal: Part I — Seal Analysis," Circle 32 on the TSP Request Card.*

Inquiries concerning rights for the commercial use of this invention should be addressed to the Patent Counsel, Marshall Space Flight Center [see page 16].Refer to MFS-29584

Numerical Simulation of Turbine Rotor/ Stator Interaction

Unsteady effects in flows are studied.

A report describes the numerical simulation of time-varying flows around multiple rotor and stator airfoils in a turbine. Studies like this one can be helpful in improving the performance obtainable from various turbine designs and in studying unsteady effects — for example, unsteady loads on the airfoils.

The study is conducted with the help of a new computer program that can simulate the flow in a turbine stage configured with unequal numbers of rotor and stator airfoils. The program is based on the thin-layer Navier-Stokes equations of unsteady, two-dimensional flow. The region of interest is discretized with patched and overlaid grids that move relative to each other to simulate the motion of the rotor airfoils with respect to the stator airfoils. The program integrates the Navier-Stokes equations via an upwind finite-difference scheme that is spatially accurate to third order, temporally accurate to second order, and set in an iterative implicit framework.

The computer code was used to simulate subsonic flow past a turbine stage for which considerable experimental data have been collected. Numerical results are obtained for a one-rotor/one-stator configuration and for a four-rotor/three-stator configuration. The four-rotor/three-stator case had a pitch ratio much closer to that of the experimental case.

Numerical results presented include time-averaged pressures on the surfaces of the airfoils, the amplitudes and phases of the fluctuations in those pressures, and instantaneous pressure contours. The time-averaged surface pressures for the two configurations are almost identical and agree well with the experimental data. The surface-pressure amplitudes and phases calculated for the four-rotor/three-stator configuration are found to agree much better with the experimental data than do the data calculated for the one-rotor/one-stator configuration.

This work was done by Man Mohan Rai of ***Ames Research Center*** *and Nateri K. Madavan of Sterling Federal Systems. To obtain a copy of the report, "Multi-Airfoil Navier-Stokes Simulations of Turbine Rotor-Stator Interaction," Circle 118 on the TSP Request Card.*
ARC-12293

R-Curve Instability Calculations of Crack Growth

In some cases, calculations can be done on pocket calculators.

A report discusses the use of the instability method of calculation and R-curve mathematical models to analyze the growth of cracks in fracture-mechanics specimens. In the case of a single material and structure, such an analysis is sometimes simple enough to be done on a pocket calculator. Where a microcomputer or larger computer is available, a comprehensive program can include libraries of driving-force equations for various configurations and R-curve mathematical models for different materials.

The R-curve is a phenomenological description of the monotonic fracture process. It is a plot of the resistance of a specimen to the growth of a crack versus the extension of the crack. For analysis in the region in which instability is expected (or in any other region of interest), any of a variety of mathematical models can be fitted to the data on the R-curve by nonlinear regression analysis. Representative models include polynomials, power laws, exponentials, inverted hyperbolas, arc tangents, and hyperbolic tangents.

In the instability method, one requires that both the magnitudes and the slopes of the crack-driving-force curve and the resistance curve of the specimen be equal at the point of instability. The author describes instability calculations that incorporate R-curve models of elastic behavior and others that incorporate R-curve models of elastoplastic behavior. These R-curve models are fitted to plots of experimental data on crack-growth resistance versus crack extension in aluminum and steel specimens.

The author concludes that the instability method is simple and effective and that the model equations studied are all viable in the sense that at least one of them should fit almost any applicable set of crack-growth data. The empirical coefficients of the models are estimated easily from plots of the raw data. In combination, the method and models constitute powerful mathematical tools for the analysis of fractures.

This work was done by Thomas W. Orange of **Lewis Research Center**. *Further information may be found in NASA TM-100935 [N88-23278], "Method and Models for R-Curve Instability Calculations."*

Copies may be purchased [prepayment required] from the National Technical Information Service, Springfield, Virginia 22161, Telephone No. (703) 487-4650. Rush orders may be placed for an extra fee by calling (800) 336-4700.
LEW-14841

Using NASTRAN To Analyze Vibrations of Rotor Blades

Nonlinear and linear analyses are combined.

A report gives information on the use of the NASTRAN computer program in the finite-element analysis of rotating flexible blades like those in compressors and on turboprop engines. The program predicts steady-state components of deflections and stresses under centrifugal forces, generates data for plots of natural frequency versus rotational speed, and provides vibration-mode data for calculations of flutter. NASTRAN is well suited to such analyses because it can compute steady-state displacements by geometrically nonlinear analysis and can use the results for normal-modes analysis.

The report describes the use of NASTRAN solution sequence 64 for geometrical nonlinear analysis and solution sequence 63 for the determination of the frequencies and vibrational-mode shapes. It includes a sample problem with NASTRAN input data. It emphasizes key factors in the analysis of rotating blades, such as the setting angle and centrifugal softening effects.

Solution sequence 64 performs a large-displacement analysis on a rotating blade, computes the displacements and stresses caused by rotation, and stores the final stiffness and mass matrices of the blade in a data base. The large-displacement analysis is necessary because the blades are flexible and deflect considerably.

Solution sequence 63 computes the modal parameters from the final mass and stiffness matrices. The matrices corresponding to the deformed blade must be used so that centrifugal stiffening and other effects of rotation are included in the modal analysis.

The combined analyses of solution sequences 64 and 63 reduce computer time and the number of output listings, in comparison with those of separate analyses. In general, central-processing-unit time can be cut in half.

This work was done by Charles Lawrence, Robert A. Aiello, and Michael A. Ernst of **Lewis Research Center** *and Oliver G. McGee of Ohio State University. Further information may be found in NASA TM-89861 [N87-21375], "A NASTRAN Primer for the Analysis of Rotating Flexible Blades."*

Copies may be purchased [prepayment required] from the National Technical Information Service, Springfield, Virginia 22161, Telephone No. (703) 487-4650. Rush orders may be placed for an extra fee by calling (800) 336-4700.
LEW-14799

THERE'S A NEW STANDARD IN REAL-TIME COMPUTING FOR MEASUREMENT AND CONTROL

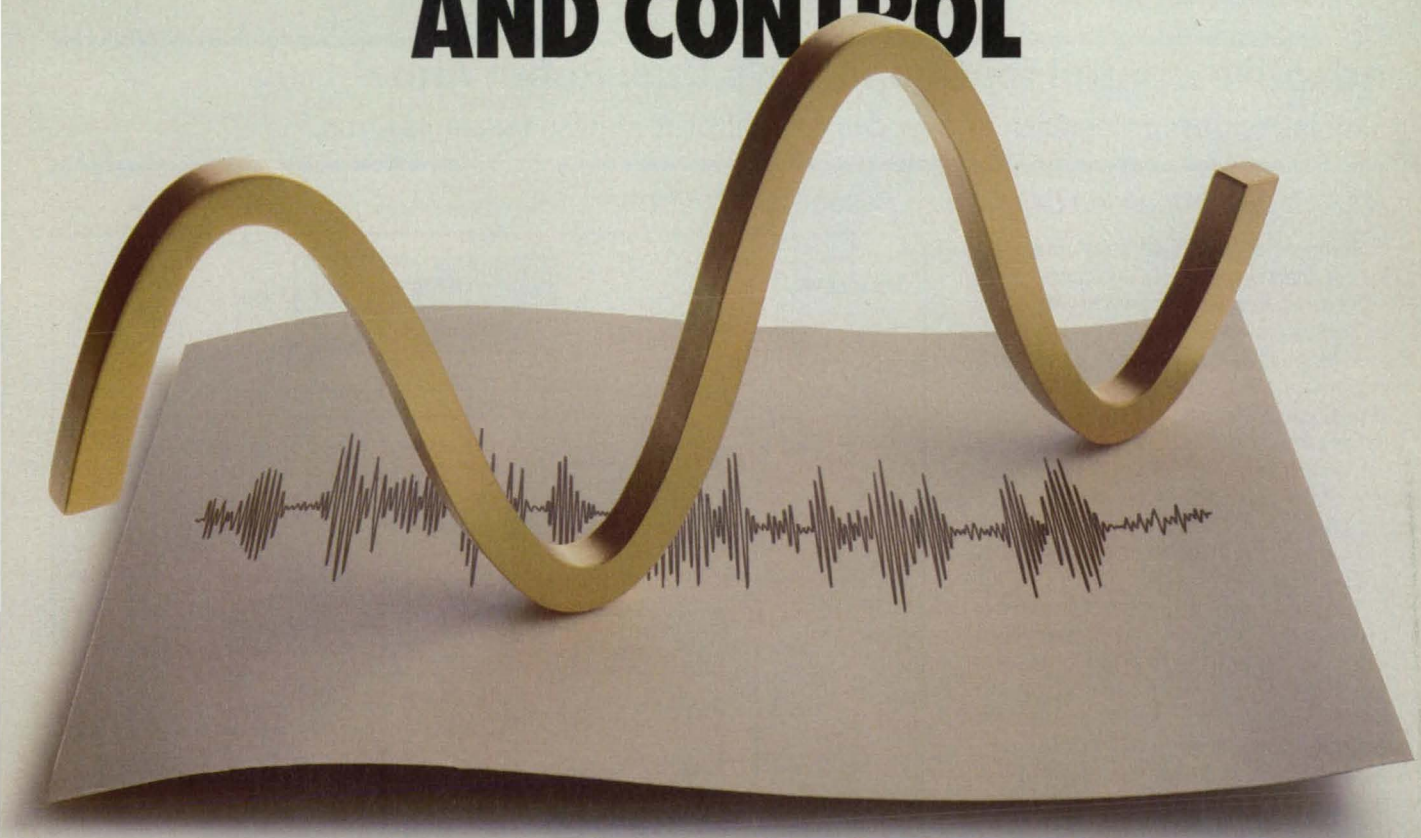

Find the 24-karat solution for your measurement and control applications at Concurrent Computer Corporation, the world leader in real-time computing.

Cost-effective real-time computing power coupled with standards like VMEbus,™ X Window system,™ DECnet,™ and a real-time enhanced UNIX® operating system are just a few of the solid-gold competitive advantages you get from Concurrent. With Concurrent you can shorten your software development cycle, lower your support costs, and get your new projects up and running faster. And our gilt-edged product line, ranging in price from $10,000 to more than $1 million, is backed by a world wide support organization.

Go for the gold! For your real-time information starter kit for measurement and control applications, send in the coupon today or call **1-800-631-2154** toll-free. Concurrent Computer Corporation—the company that sets the standards for real-time computing.

Send to Concurrent Computer Corp., Dept. MC-2, 106 Apple Street, Tinton Falls, NJ 07724

☐ Send me my information starter kit for measurement & control applications

☐ Send me information on the Concurrent real-time UNIX operating system

Name _____

Title _____

Company _____

Address _____

City _____ ST _____ Zip _____

Phone _____

My application is _____

Concurrent Computer Corporation

VMEbus™ is a trademark of Motorola Corporation. X Window system™ is a trademark of MIT. DECnet™ is a trademark of Digital Equipment Corporation. UNIX® is a trademark of AT&T.

Circle Reader Action No. 581

Adaptive Control for Cooperative Dual Robot Arms

Simple control strategies are derived from control strategies for single arms.

NASA's Jet Propulsion Laboratory, Pasadena, California

Three strategies have been proposed for the adaptive control of two cooperative robot arms. In comparison with other digital control systems that have been considered for multiple robot arms, controllers to implement these strategies would have simple structures and would be computationally fast enough for operation at high sampling rates. Dual-arm control strategies of the new type have yielded promising results in numerical simulations, and the general approach can be extended to greater numbers of arms.

The control architecture is based on the trilevel hierarchical control of two robot arms (see figure). The high level plans the task to be performed and decomposes the task into appropriate subtasks for the right and left arms. In the intermediate level, each subtask is transformed into a sequence of synchronous desired trajectories of end-effector motions and applied forces. The low level is concerned with the execution of the desired trajectories and employs feedback from the current status of the arms. In this hierarchy, the low level "achieves" the desired motion and operates in "millisecond" time scale, the intermediate level "determines" the motion desired for the subtask in "second" time scale, and the high level "plans" the subtask sequences in "minute" time scale.

Single-arm control strategies developed previously are applied at the low level of the hierarchy. In each dual-arm strategy, a suitable task-related coordinate frame of reference is chosen for both arms, and the desired motions and applied forces for each arm are expressed in this frame. Then each arm moves as though it were carrying out the commanded motion by itself in this frame. The adaptive controllers ensure that the controlled variables track the desired reference commands and reject the unwanted disturbances caused by interaction forces and torques exerted by each arm on the other arm through the load.

In the position/position control strategy, the adaptive controllers ensure that the end-effector positions of both arms track desired trajectories in Cartesian space despite unknown time-varying interaction forces exerted through the load. In the position/hybrid control strategy, the adaptive controller of one arm controls end-effector motions in the free directions and applied forces in the constraint directions, while the adaptive controller of the other arm ensures that the end effector tracks desired position trajectories. In the hybrid/hybrid control strategy, the adaptive controllers ensure that both end effectors track reference position trajectories while simultaneously exerting desired forces on the load.

In the generalization to N cooperative arms ($N > 2$), an important feature of this approach is that the overall control system is reduced to N decentralized independent single-arm controllers. Available techniques for single-arm control can be utilized directly in multiple-arm environments. The control schemes require no communication among individual controllers — an appealing feature in terms of both computation and reliability. The new control strategies do not require the knowledge of such load parameters as mass and stiffness or such dynamic parameters of the robot as the masses and inertias of links. Therefore, these strategies can cope with uncertainties or variations in the parameters. Furthermore, the complex dynamic models of the arms are not used in generating the control actions.

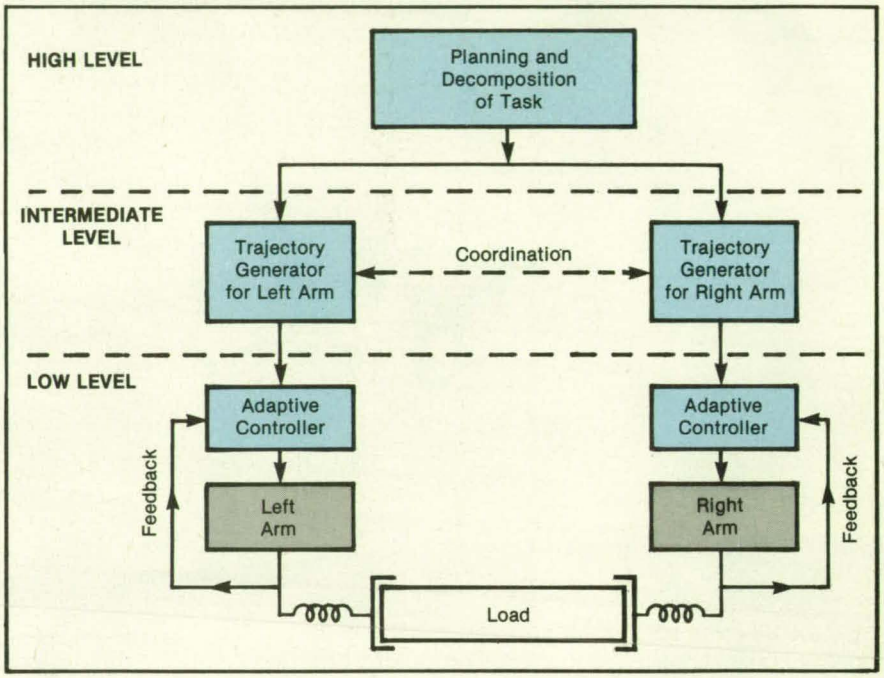

The **New Dual-Arm Control Strategies** are implemented at the low level of the control hierarchy. Each arm is operated independently under a single-arm control scheme that treats forces and torques transmitted through the load as though they were disturbances.

This work was done by Homayoun Seraji of Caltech for **NASA's Jet Propulsion Laboratory**. *For further information, Circle 27 on the TSP Request Card.*

Inquiries concerning rights for the commercial use of this invention should be addressed to the Patent Counsel, NASA Resident Office-JPL [see page 16]. Refer to NPO-17368

Fabrication Technology

Making Reliable Large-Diameter O-Rings

Vacuum curing yields joint-free, voidless elastomer seals.

Marshall Space Flight Center, Alabama

A method for manufacturing large-diameter O-rings produces them in single pieces, without bonded joints. The method also reduces the probability that trapped gases will form flaws. The O-rings thus produced, which may have diameters of as much as 144 in. (3.66 m), are reliable and of high quality.

Two O-rings are made simultaneously. An O-ring preform — a length of uncured elastomer — is placed in each of the two doughnut-shaped grooves in the lower half of a mold (see figure). The ends of each preform overlap by about 0.04 in. (1 mm) in a 20° skive joint. The thickness of the preform exceeds the final thickness by about 0.01 in. (0.25 mm).

The upper half of the mold is set in place on the lower half so that the grooves in the two halves become aligned, forming internal mold cavities. A vacuum is drawn in the mold through an internal manifold in the upper half, drawing the lower half firmly into the upper. O-rings on the circumference of the lower half seal the mold against the atmosphere. The vacuum makes a press unnecessary and draws off gases that could create voids in the elastomer. Hot oil is circulated through cavities in the upper and lower halves to provide heat to cure the elastomer rings.

The edges of the preform grooves protrude slightly more than do the edges of the adjacent grooves. This ensures that the preform grooves mate first when the top and bottom halves are joined and gives a clean, blemish-free surface to the O-ring. Excess elastomer extrudes past these edges and collects in the vacuum cavities for later removal. During curing, the abutting surfaces at the skive joints fuse to form seamless, joint-free rings.

This work was done by Glade L. Larsen and Albert R. Harvey of Morton Thiokol, Inc., for **Marshall Space Flight Center**. *For further information, Circle 145 on the TSP Request Card.*

Inquiries concerning rights for the commercial use of this invention should be addressed to the Patent Counsel, Marshall Space Flight Center [see page 16]. Refer to MFS-28371

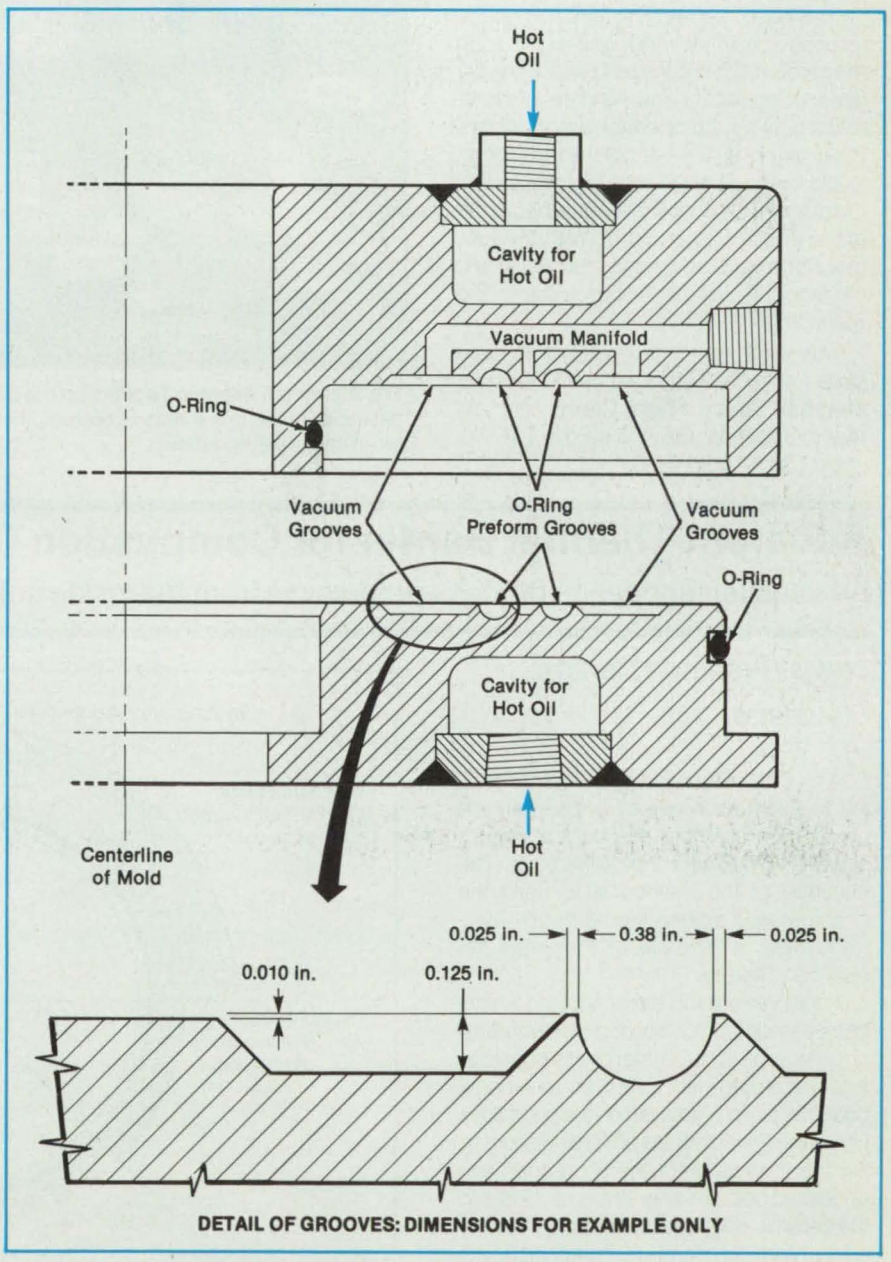

Nesting Upper and Lower Halves of the mold hold elastomer rings for curing. Oil flowing through upper and lower cavities heats the elastomer to cure it.

Aligning Plasma-Arc Welding Oscillations

A simple, easy-to-use tool improves weld quality.

Marshall Space Flight Center, Alabama

A tool aids in the alignment of the oscillator probe on a variable-polarity plasma-arc welding torch. The probe magnetically pulls the arc from side to side as it moves along the joint. The tensile strength of the joint depends on the alignment of the weld bead and, therefore, on the alignment of the probe.

Previously, the welding-machine operator used a protractor and hand level to align the probe with the center of the plasma orifice, but significant misalignment often remained. Now, the operator simply installs the new tool on the front of the torch body, levels it with a built-in bubble glass, inserts the probe in a slot on the tool, and locks the probe in place (see figure). With the new tool, the procedure is faster and easier and the resulting alignment more accurate and repeatable.

This work was done by Jeff Norris and Mike Fairley of Martin Marietta Corp. for **Marshall Space Flight Center**. *For further information, Circle 8 on the TSP Request Card. MFS-28303*

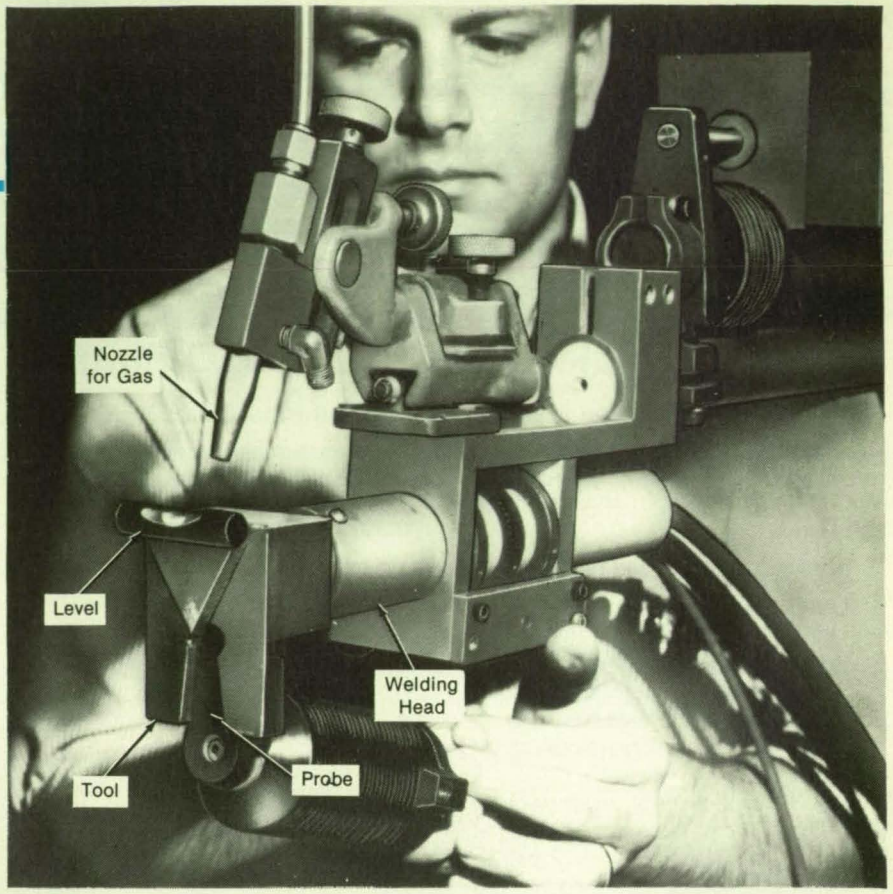

The **Aluminum Aligning Tool** fits on the body of a plasma-arc welding torch. It receives the oscillator probe in a slot at its bottom, thereby positioning the probe directly under the center of the plasma orifice.

Adherent Thermal Barrier for Combustion Chamber

An unusual fabrication process progresses from the inside outward.

Lewis Research Center, Cleveland, Ohio

A method of applying a heat-barrier coating to the interior wall of a rocket-engine combustion chamber produces a smooth coating with exceptional adherence. The essence of the method is to build the chamber wall around the barrier by electroforming, a reversal of the usual sequence of events.

In the previous method of applying a heat-barrier coating, a bond coat of nickel/chromium was applied to the interior of a chamber that was already fabricated, and a zirconia coat was plasma-sprayed on the bond coat. However, the substrate often oxidized during the application of the bond coat, and undesired compressive stress remained in the ceramic coat after the chamber returned to room temperature. In addition, the coating had a rough surface that increased the transfer of heat to the wall.

In the improved method, fabrication begins with the machining of an aluminum

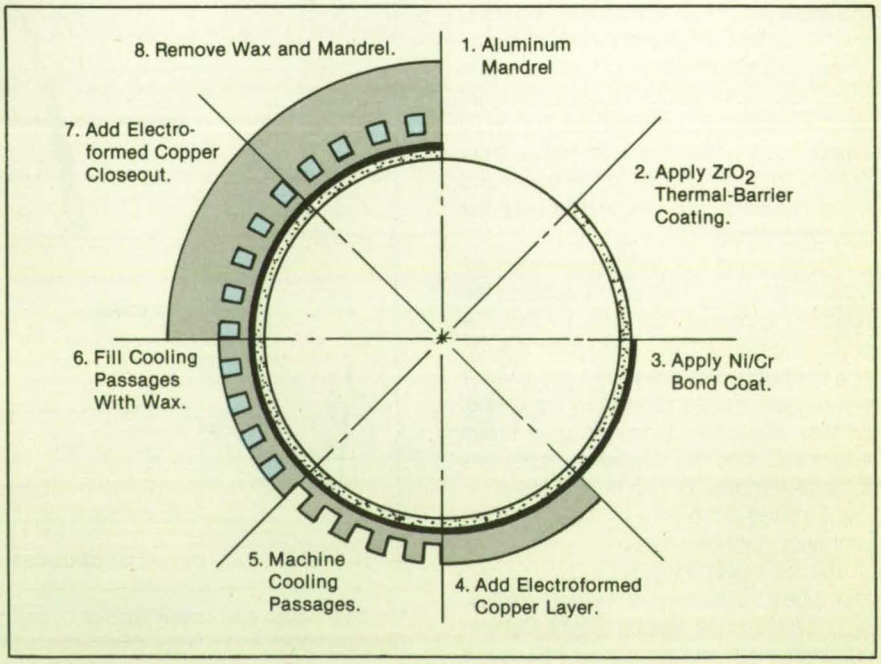

Sectors of a Cross Section show how a cylindrical chamber is built. Starting with an aluminum mandrel, layers are added from the inside out.

mandrel to the requisite cylindrical shape (see figure). The heat-barrier coating — yttria-stabilized zirconia — is plasma-sprayed on the mandrel to a thickness of 0.076 mm. A nickel/chromium layer about 0.025 mm thick is sprayed on the zirconia; this layer serves as an electrically conductive bond coat for electroplating. The assembly is then rotated continuously in a copper sulfate bath while copper is plated onto the bond coat.

Longitudinal grooves are machined into the copper layer. The grooves are filled with wax, and the assembly is returned to the plating bath, where a final layer of copper is plated overall, transforming the grooves into channels for the coolant. Finally, the wax is removed by melting, and the aluminum mandrel is etched away.

Heat-barrier coatings made by the new method were evaluated on a small rocket thrust chamber. The rocket engine was repeatedly started, run, and shut down with liquid oxygen and gaseous hydrogen as propellants and liquid hydrogen as the coolant. The testing was stopped after 1,450 cycles. The results of the tests were compared with those for an identical chamber without the heat-barrier coating.

The zirconia coat delaminated in some places in the region of low heat flux. However, the zirconia adhered well inasmuch as the delamination did not extend down to the bond coat. The coolant passages of the coated chamber retained their original sizes and shapes, and there was no apparent damage to the inner wall. In contrast, in the uncoated chamber, a crack developed in one of the coolant passages after 393 cycles, and the inner wall was deformed and thinned at the coolant passages.

The thin zirconia coating reduced the maximum operating temperature of the copper wall of the chamber from 844 to 334 K. At the lower temperature, the copper liner is stronger and undergoes less strain and thus has less tendency to distort and crack.

This work was done by Richard J. Quentmeyer of **Lewis Research Center**. *Further information may be found in NASA TM-100933 [N88-24690], "Thrust Chamber Thermal Barrier Coating Techniques."*

Copies may be purchased [prepayment required] from the National Technical Information Service, Springfield, Virginia 22161, Telephone No. (703) 487-4650. Rush orders may be placed for an extra fee by calling (800) 336-4700.
LEW-14840

Caldron for High-Temperature Alloys

Metals are melted by induction.

Lewis Research Center, Cleveland, Ohio

An induction-heated caldron melts high-temperature alloys. The use of the caldron prevents the sort of contamination of melts that occurs during arc melting in ceramic crucibles. The caldron can liquefy 200 grams of the solid metal components of an

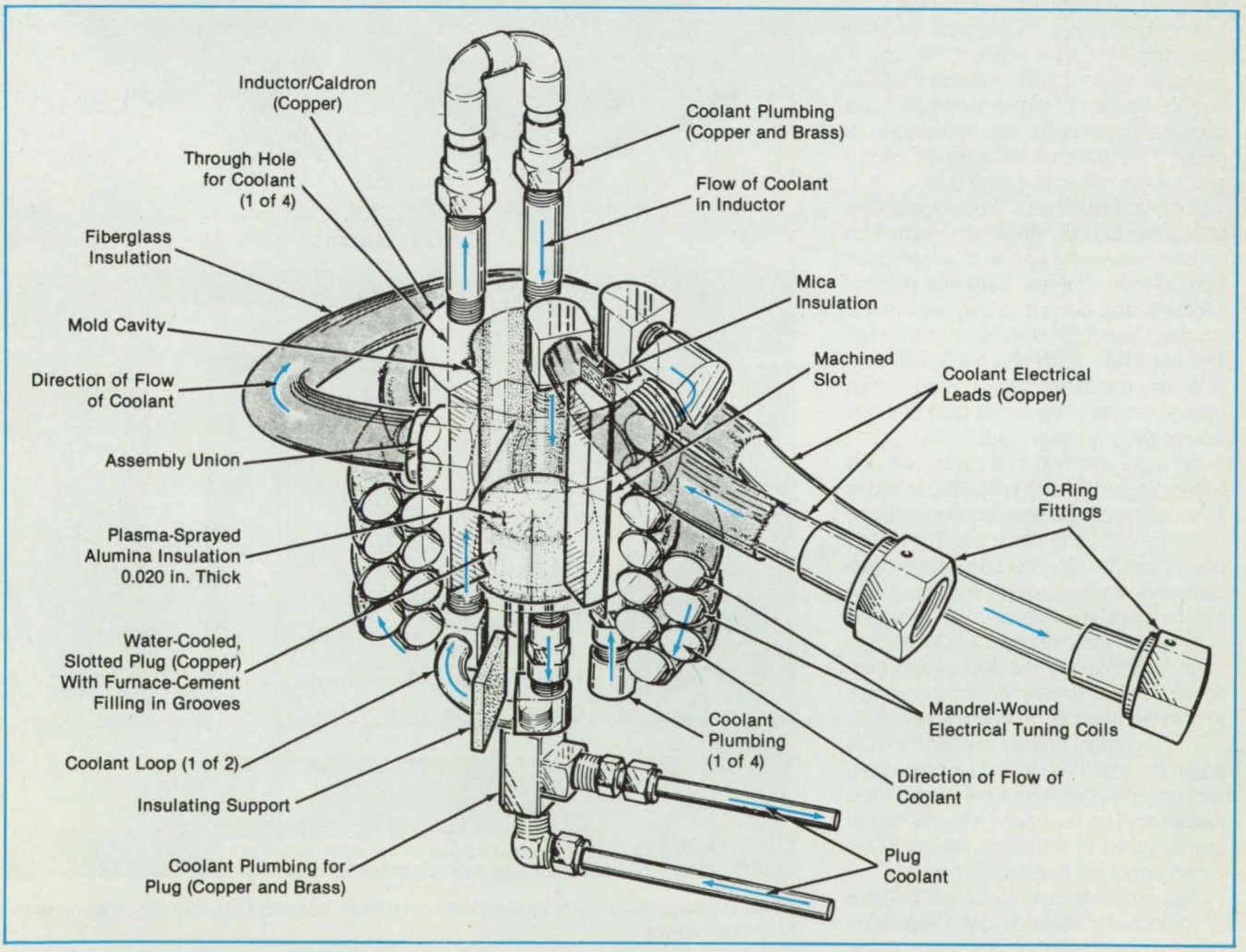

A **Plugged Sleeve** constitutes the main body of the caldron. Coolant flows through the sleeve to prevent it from melting. The mandrel-wound induction coils can be adjusted to tune the source of power.

alloy like niobium aluminum and make the alloy homogeneous in less than 3 minutes. It can also serve as a mold for casting alloys into such shapes as bars.

The caldron includes a thick copper sleeve, insulated on its inside with a layer of plasma-sprayed alumina. The bottom of the caldron is a tapered copper plug, also coated with alumina. Cooling water circulates in the channels in the thick sleeve. The combination of cooling and alumina insulation confines high temperatures to the interior of the caldron. Water-cooled, fiberglass-insulated induction coils surround the caldron (see figure). Copper tubes carry both coolant and radio-frequency energy to the coils.

The tapered surface of the plug contains vertical grooves filled with refractory cement. When the plug is inserted in the sleeve, the grooves let electromagnetic flux penetrate the melt. Coolant also flows through the plug. The plug can be removed for maintenance or for cleaning the caldron. If needed, a second plug can be inserted at the top of the sleeve so that the melt environment can be pressurized.

For loading and melting, the caldron is in the vertical position shown in the figure. After the alloy is melted and homogenized, the caldron can be rotated to a horizontal position to pour the melt out or to allow the melt to fill a molding cavity in the sleeve. Electrical power to the coils is then turned off, and the melt cools and solidifies in the cavity. A sound, pore-free casting results.

This work was done by Henry J. Geringer of **Lewis Research Center**. *For further information, Circle 72 on the TSP Request Card.*
LEW-14790

Jig Aligns Shadow Mask on CCD

Alignment can be viewed through a microscope.

NASA's Jet Propulsion Laboratory, Pasadena, California

An alignment jig positions a shadow mask on a charge-coupled device (CCD) so that a metal film can be deposited on it precisely. The jig allows the CCD package to be inserted and removed without disturbing the alignment of the mask. The jig holds the CCD package securely and isolates it electrostatically while providing electrical contact to each of its pins.

The jig fits on a microscope stage. It transmits light from the microscope illuminator at the bottom, through the CCD and the mask, so that a technician can align the mask under the microscope to obtain a translational accuracy of $\pm 5\ \mu m$ and a rotational accuracy of 0.15°.

A carrier holds the CCD package and its pins (see figure). Alignment pins and screws secure the carrier to a baseplate from below. Screws, Belleville (spring) washers, and clamps loosely secure the shadow mask to the baseplate from above. The baseplate holds the mask 0.005 in. (0.13 mm) above the glass membrane that constitutes the cover of the CCD and that will receive the metal coat.

An alignment ring that mates with the baseplate-and-carrier assembly includes three spring-loaded pins opposed by three micrometers to align the mask. The technician places the alignment ring on the baseplate-and-carrier assembly and adjusts the micrometers while viewing the mask and CCD under the microscope. Once alignment is achieved, the technician then tightens the restraining screws and clamps to hold the mask firmly in position.

The alignment ring is removed from the assembly, and the assembly is placed in a vacuum chamber where the metal film is deposited. The baseplate and the carrier are designed to withstand the harsh environment of the deposition chamber.

This work was done by Carlos V. Matus of Caltech for **NASA's Jet Propulsion Laboratory**. *For further information, Circle 10 on the TSP Request Card.*
NPO-17672

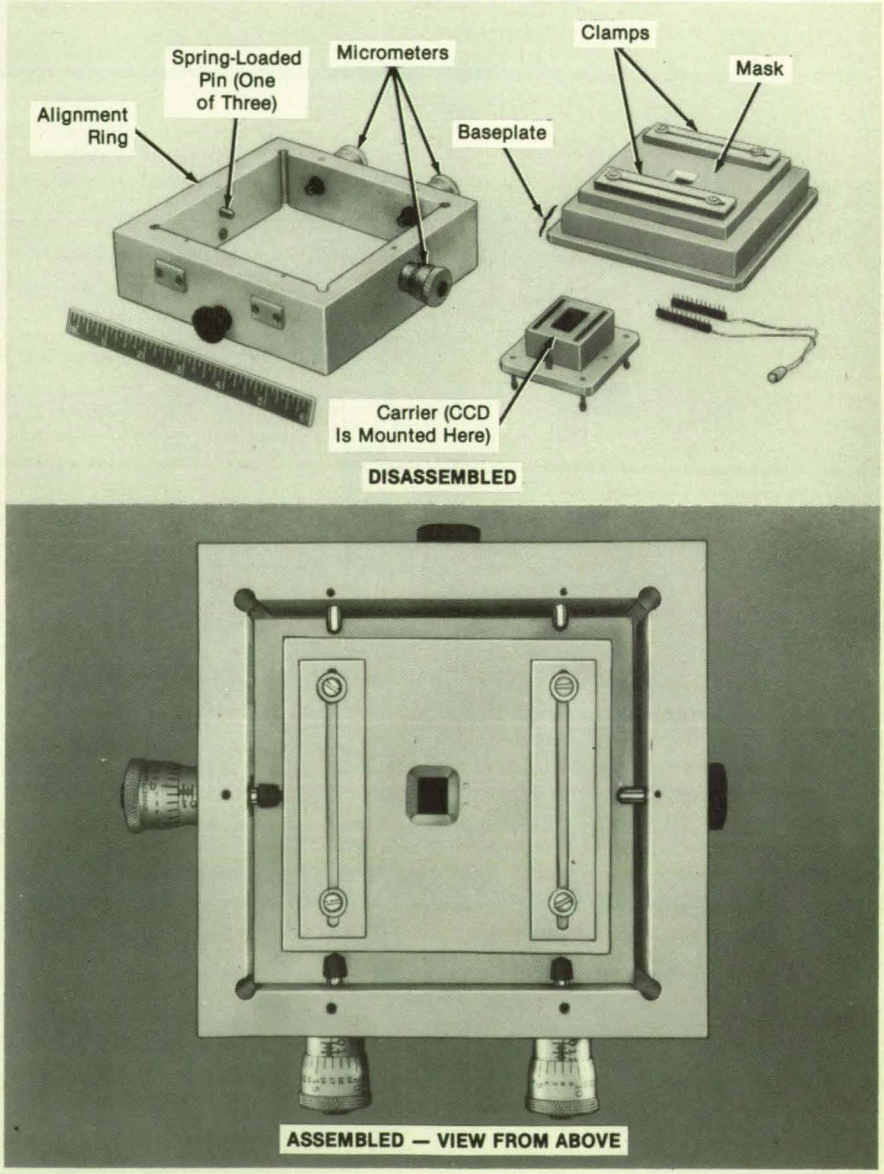

When the **Alignment Jig Is Assembled** with a CCD, it is used to move the mask under micrometer control.

da Vinci's ideas took centuries to perfect. He didn't have Design™/East

Free Show Admission With This Ad.

Staying on top of the latest technology and the newest products can reduce your product development time.

Attending the Design Engineering Show & Conference™/East, the East Coast's only comprehensive OEM Show, you'll meet over 250 vendors. See over a mile of product displays. Find the systems and components you need to reduce product costs. Shorten design cycles. And add technical innovation to your design. All in one place.

Save $25! Bring this ad to the Show for FREE Show admission. *For further information on the Show or concurrent Conference call 1-800-255-7798, (in CT, call 203-964-0000) today!*

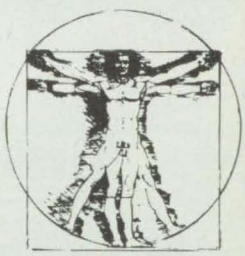

Design Engineering Show & Conference™/East

October 11-13, 1989
Jacob Javits Convention Center
New York, New York

SW

Mathematics and Information Sciences

Books and Reports

These reports, studies, handbooks are available from NASA as Technical Support Packages (TSP's) when a Request Card number is cited; otherwise they are available from the National Technical Information Service.

Further Results on Finite-State Codes

New codes are generated and analyzed.

A report discusses the application of a general construction for finite-state (FS) codes to known block codes. Decoding algorithms and the results of simulations are also discussed briefly.

The basic idea consists in choosing an (n,k_1) block code C_1 of minimum distance d_1 and then decomposing C_1 into the disjoint union of cosets generated by an (n,k_2) subcode C_2 of C_1 of minimum distance d_2. By properly assigning these cosets to the edges of a 2^m-state completely connected graph, it is possible to construct an (n,k,m) FS code, with $k = m + k_2$ and free distance $d_{free} \geq \min(d_2, 2d_1)$.

First, the general construction is applied to the (24,12) Golay code. It is shown that this code has a (24,5) subcode of minimum distance 12 and a (24,2) subcode of minimum distance 16. From these are constructed a (24,11,6) FS code of $d_{free} = 12$ and a (24,11,9) FS code of $d_{free} = 16$, respectively. These new codes are optimal in the sense that they have the largest possible free distances, as predicted by the Plotkin bound on FS codes.

Next, the general construction is applied to the (16,8) Nordstrom-Robinson code. It is shown that this code can be partitioned into 64 subsets, from which a (16,7,5) FS code can be constructed. This code has $d_{free} = 10$, which meets the Plotkin bound.

A computer simulation was performed to analyze the performances of these codes in a soft, maximum-likelihood decoder based on the Viterbi algorithm. The simulated decoder performs two basic steps: (1) Each received word (24 or 16 symbols) is compared to the code words in each coset (128 or 64), and the closest code word in each coset is stored together with its distance. (2) At each state, the decoder further selects the closest code word among those chosen in step 1, for the cosets assigned to branches reaching that state. The results are presented as plots of the bit-error probability versus the ratio of bit energy to noise energy. The plots compare the (24,11,6) FS code of $d_{free} = 12$ and the (16,7,5) FS code of $d_{free} = 10$ with the (2,1,6) Voyager convolutional code.

This work was done by F. Pollara, K. M. Cheung, and R. J. McEliece of Caltech for **NASA's Jet Propulsion Laboratory**. *To obtain a copy of the report, "Further Results on Finite-State Codes," Circle 57 on the TSP Request Card. NPO-17513*

Factorization of Positive Definite, Banded Hermitian Matrices

Speedup factors and efficiencies in parallel processing are evaluated.

A report discusses the application of the Cholesky factorization algorithm to positive definite, banded Hermitian matrices. One of the major purposes of this and related studies is to maximize the speedup and efficiency in a system of concurrent-data-processing elements.

The problem is basically to find an appropriate batching-and-scheduling stratagem to solve a given matrix problem N times as fast when N processing elements are used as when only one processing element is used. The actual speedup factor, g, is generally less than N, and the efficiency, e, of a concurrent-processing system is defined by $e = g/N$. The important intrinsic properties of a concurrent-processing system relevant to the speedup and efficiency include the modes of operation (systolic versus asystolic); the setups (such as the extent of seriality and parallelism between input, execution, and output); and architectures (hypercube, tree, bus, a combination of these, and the like).

The authors begin by extending the Cholesky factorization algorithm to cover uniformly-partitioned, banded, positive definite matrices of rank n that may be real symmetric or Hermitian. Then two stratagems are given for the use of this algorithm in a concurrent-processing system in which N is less than it would have to be to enable the factorization of the matrix in as few serial steps as possible and where uniformly high efficiency is expected from all processing elements.

The cost of processing is measured in terms of the number of operations. Equations are derived for the efficiencies of the two stratagems, and these are specialized for an N-node hypercube system of partition size $S = 1 + Int.[(b-1)/2N]$, where b = the half bandwidth of the matrix, the task is completed in n/s serial steps, and the ratio of the cost of interelement transmission of data to the cost of computing is assumed to be constant. The efficiencies of both stratagems are found to be close to 100 percent for $\mu \lesssim 0.1$ and $N \gtrsim 10$. In general, efficiencies increase with increasing s and decreasing μ.

This work was done by Moktar A. Salama of Caltech and Senol Utku and Robert Melosh of Duke University for **NASA's Jet Propulsion Laboratory**. *To obtain a copy of the report, "Concurrent Cholesky Factorization of Positive Definite Banded Hermitian Matrices," Circle 127 on the TSP Request Card.*
NPO-17130

Effect of Noise in the Ideal State Reconstructor

More measurements yield a better estimate.

A report discusses the effects of measurement noise on a system that includes a linear, time-invariant plant of measurable inputs and known parameters and a deterministic digital control subsystem governed by an algorithm called the "ideal state reconstructor." This algorithm is so named because in the absence of noise, it exactly reconstructs the vector that represents the state of the plant, even without knowledge of the initial state. The ideal state reconstructor adds no new states or eigenvalues to the system; it affects the measurement equation only.

The discussion begins with a review of the ideal state reconstructor. This is followed by an analysis of the behavior of the ideal state reconstructor in the presence of measurement noise. An equation for the error introduced by noise into the estimate of the state vector is derived and used to obtain a general expression for the state-estimation-error covariance matrix.

The analysis is applied to an example — a double-integrator plant with measurement noise and a special form of the ideal state reconstructor. The performance index J of the ideal state estimator is chosen to be the trace of the covariance matrix. The number of measurements N used in estimating the state vector during the state-estimate sampling period T is treated as a parameter to be varied to examine the effect on J. The result of this calculation is a plot on which J decreases with N; that is, the more the measurements, the better the estimate, on a statistical basis. Intuitively, one would expect this to be true in general. If it is, then the ideal state reconstructor is ideally suited for systems in which measurements become available more frequently than the states have to be estimated and the control-law equations have to be solved.

This work was done by Michael E. Polites of **Marshall Space Flight Center**. *Further information may be found in NASA TP-2881 [N89-13994], "The Estimation Error Covariance Matrix for the Ideal State Reconstructor With Measurement Noise."*

Copies may be purchased [prepayment required] from the National Technical Information Service, Springfield, Virginia 22161, Telephone No. (703) 487-4650. Rush orders may be placed for an extra fee by calling (800) 336-4700.

Inquiries concerning rights for the commercial use of this invention should be addressed to the Patent Counsel, Marshall Space Flight Center [see page 16]. Refer to MFS-28382

Controlled-Turbulence Bioreactors

Two versions provide conditions for growth and long life of cells.

Lyndon B. Johnson Space Center, Houston, Texas

Two versions of a bioreactor vessel provide steady supplies of oxygen and nutrients with little turbulence. They suspend cells in the environment they need for sustenance and growth, while inflicting less damage from agitation and bubbling than do propeller-stirred reactors. The gentle environments in the new reactors are well suited to delicate mammalian cells.

One of these reactors has kept human kidney cells alive for as long as 11 days. In this reactor, cells grow on carrier beads suspended in a liquid culture medium that fills a cylindrical housing (see Figure 1). A spinning filter is located on the axis. A set of rotating vanes stirs the liquid. The rotation of the filter and the flow of liquid keep the carrier beads in suspension, and the currents set up by the slowly moving vanes are gentle.

Oxygen- and nutrient-rich liquid enters the housing through valves on the outer cylindrical wall, passing through radial gaps between the filter, blade assembly, and end caps. Depleted liquid leaves through the spinning filter. A heating element wound on the outside wall of the vessel keeps the reactor at the desired temperature.

Several valves in the wall of the vessel provide for the venting of trapped air bubbles (which would cause unnecessary turbulence), draining the vessel, extracting samples, and adding cells. The valves seal flush with the interior wall to eliminate dead space and form a smooth surface, minimizing growth of unwanted bacteria.

Another version of the reactor creates even less turbulence. It does not include blades and supplies oxygen by diffusion through permeable tubing (see Figure 2). This version cultures mammalian cells to a density of 1.4×10^6 cells/cm^3 for as long as 15 days. The vessel, also a horizontal cylinder with end caps, is rotated by a motor. The speed is adjusted so that the rotating liquid medium suspends the cell-laden beads uniformly.

This work was done by David A. Wolf of **Johnson Space Center**, *Ray Schwartz of Technology, Inc., and Tinh Trinh of Krug International. For further information, Circle 36 on the TSP Request Card.*

This invention is owned by NASA, and a patent application has been filed. Inquiries concerning nonexclusive or exclusive license for its commercial development should be addressed to the Patent Counsel, Johnson Space Center [see page 16]. Refer to MSC-21293/21294

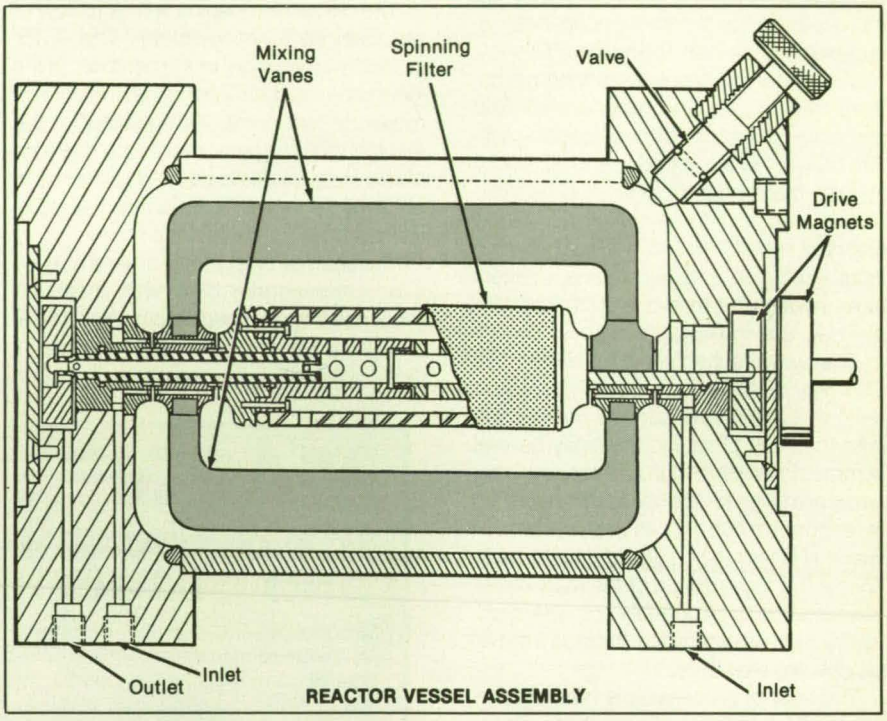

Figure 1. **Rotating Vanes** — inside the vessel but outside the filter — gently circulate the nutrient medium. The vessel is stationary; a magnetic clutch drives the filter cylinder and the vanes.

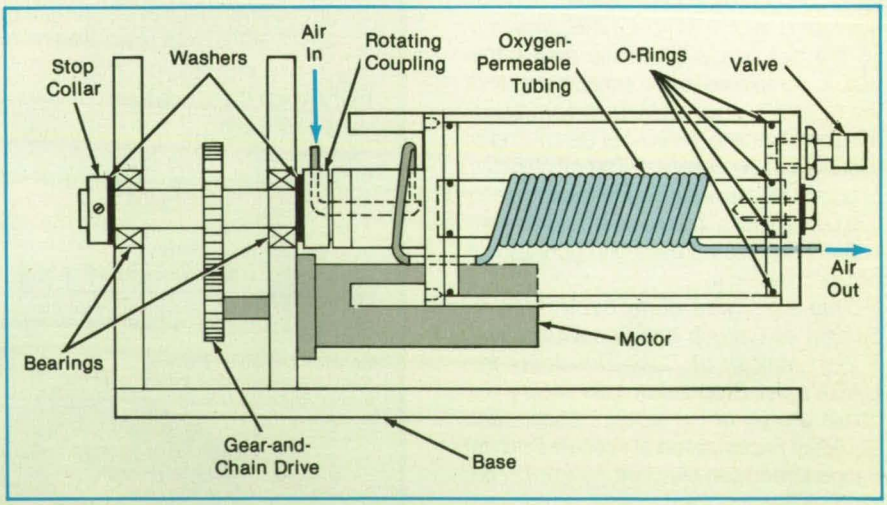

Figure 2. **Oxygen-Permeable Tubing** is wrapped around a rod extending along the central axis. A small external pump feeds oxygen to the tubing through a rotary coupling, and the oxygen diffuses into the liquid medium.

New on the Market

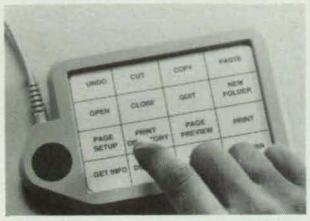

The UnMouse, a 3'' x 4-1/2'' **touch-sensitive glass tablet** that replaces a mouse is now available from MicroTouch Systems Inc, Wilmington, MA. The UnMouse features a built-in keypad for executing macro commands and a stylus that enables users to draw figures, annotate documents, enter signatures, or trace images into the system. Priced at $235, the UnMouse works with Apple Macintosh II and Macintosh SE computers.
Circle Reader Action Number 786.

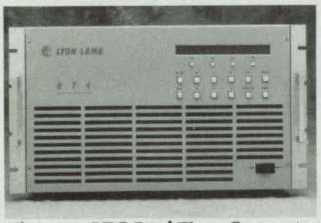

The new RTC **Real Time Converter** from Lyon Lamb Video Animation Systems Inc., Burbank CA, digitally converts up to three independent high-resolution sources of any scanning frequency in the 23 to 75 kHz range. Standard outputs include broadcast-quality NTSC and PAL composite video, component video, Y + C, and low-resolution RGB with sync. NASA used the RTC during Voyager's flyby of Neptune to convert graphic images of the planet into NTSC standard video for live broadcast.
Circle Reader Action Number 778.

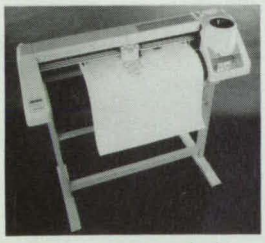

The ZETA 600, a new **drafting pen plotter** designed for use at individual workstations has been introduced by Bruning, Martinez, CA. Priced at $4395, the D-size, eight-pen unit can plot at 35.4 inches per second (ips) diagonally or 25.2 ips on axis, with acceleration up to 4.2 g. The ZETA 600 offers resolution of 0.0002 inches, accuracy of 0.1%, and repeatability of 0.004 inches. Digital servo motor and built-in smoothing function ensure precisely formed circles, arcs, and characters.
Circle Reader Action Number 782.

Automated Images, Woburn, MA, has developed PC-based **graphics application software** for electrical wiring, cabling, and harnessing designers who use AutoCAD. Called IDEEL-MicroEDS, the package tracks and displays connectivity in real time and generates customized manufacturing reports including verified runlists and bill of materials. Through IDEEL- MicroEDS, product information can be shared among IDEEL databases and AutoCAD, as well as other mechanical design, process planning, MRP, project management, and quality control systems.
Circle Reader Action Number 788.

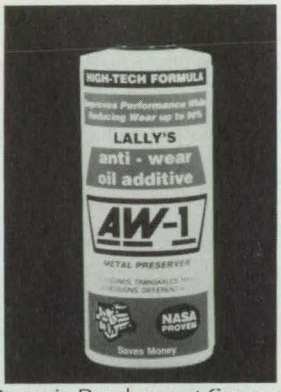

Dynamic Development Company, El Toro, CA, has introduced AW-1, an **oil additive that reduces engine wear up to 90%** while improving horsepower and torque performance. Developed by former NASA scientist Eugene F. Lally, AW-1 can be added to the lube oil in gasoline and diesel engines, transaxles, manual transmissions, differentials, and gear boxes. A 6-ounce container, selling for $14.95, serves as one application for any auto, truck, or boat engine, and will provide protection for 6000 miles. AW-1 is also offered in quart, gallon, and drum sizes for industrial applications.
Circle Reader Action Number 780.

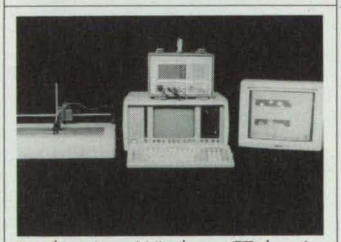

Amdata Inc, Windsor, CT, has introduced IntraSpect™ /ET20, a PC-based **eddy current data acquisition, imaging, and analysis system**. The portable unit provides automated inspection capability and generates high-resolution color-coded images, impedance plane maps, and strip charts showing inspection results. The I/ET20 was developed primarily for inspecting aging aircraft.
Circle Reader Action Number 784.

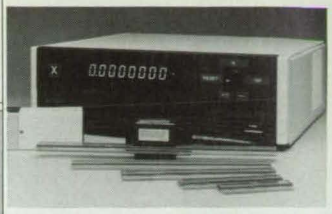

A family of **laser-based systems for submicron measurements** in precision machining and quality control operations has been introduced by Sony Magnescale America Inc., Orange, CA. Sony Laserscale products use holographic techniques to measure linear motion of a positioning device or probe with a resolution to .01 micron. To achieve the precision measurements, an ultra-fine array of lines are photolithographically deposited on a glass scale to create a three-dimensional grid. As a split beam of light passes through the moving glass, it detects the phase shift of the grid as motion of a hologram. The holographic effect provides a highly reliable signal, even with variations in the wavelength of the light source, since the beams are constant in relation to one another.
Circle Reader Action Number 772.

The Visualization Workbench, a new **imaging software system** from Paragon Imaging Inc., Lowell, MA, integrates image processing, graphics, a visual programming language, and an innovative personal programming system. It enables application developers and researchers to quickly analyze imaging problems and develop application programs. The system is based upon industry standards — X-Windows, C, UNIX, and Postscript — and is available on DEC and SUN workstations.
Circle Reader Action Number 766.

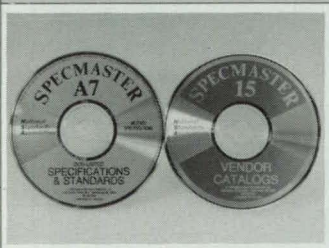

The full set of 50,000+ **Department of Defense listed military and federal specifications and standards** including handbooks, QPLs, DIDs, and CIDs, as well as thousands of vendor catalogs, are now available on a CD-ROM system called Specmaster. These files establish procedures, set standards, and provide specifications for nearly everything used by the US government — from weaponry and communications devices to electronics and medical equipment. A product of National Standards Association Inc., Gaithersburg, MD, Specmaster requires an IBM or compatible computer with DOS 3.1 or later.
Circle Reader Action Number 768.

Zymet Inc., East Hanover, NJ, has introduced a heat-curing **epoxy adhesive** specially formulated to bond fiber optic components. Designated F-701, the epoxy can operate continuously over 200°C and has a glass transition temperature of 125° to 135°C. Cure time ranges from five minutes at 120°C to one minute at 200°C. It has an initial mixed viscosity of 2000 cps and a pot life of four to eight hours.
Circle Reader Action Number 770.

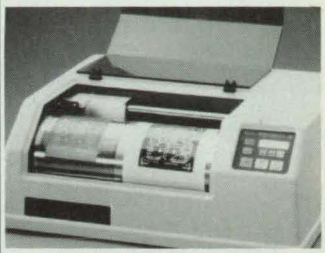

Girard Electronics, Hudson, WI, has developed the PROTOFLEX-III, a non-chemical system for **generating prototype circuits** directly from CAD schematics or artwork. Using optical-mechanical technology, the PF-III scans circuit artwork and then machines a prototype from copper/polyimide sheeting. Artwork can consist of any clear positive or negative image, including graph paper, photocopies, or even circuit designs cut from a trade journal. The PF-III handles materials 7'' x 15'' and machines flexible circuits in 60 minutes or less, depending on board size, with resolving power down to .012 inches in lines and spaces.
Circle Reader Action Number 776.

The new Fabricost™ **computer-aided cost estimating system** from Manufacturers Technologies Inc., West Springfield, MA, enables rapid and accurate cost estimating of complex sheet metal and fabrication jobs. In addition to detailed cost reports, users can create process plans, part routings, bill of materials reports, and shop load reports. The Fabricost database is programmed with information on more than 140 machines and departments, DOD labor standards, and a library of precalculated time elements. The menu-driven, PC-based system — which includes data on a variety of welding, cutting, shearing, and bending operations — is easily edited so that users can change existing values or add information on new machines.
Circle Reader Action Number 774.

New on the Market

A new **paging product** that combines a numeric display pager with the features of a digital wrist watch is available from Motorola Inc., Schaumburg, IL. The pager features separate controls for timekeeping and pager functions, a non-volatile memory that stores messages even when the pager is turned off, and a message timestamping function that displays the time a message is received on the LCD screen. It weighs less than two ounces and provides over 40 days of continuous operation on one battery.
Circle Reader Action Number 798.

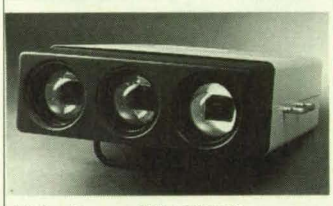

VideoBeam GRAPHICS, a new large-screen **computer graphics projector** from AmPro Corp., Woburn, MA, displays high-resolution images generated by virtually any computer or video source. The projector has 1200 lines of resolution and autoscan capability over a 14 to 72 kHz horizontal bandwidth. Applications include customer presentations, process control displays, medical imaging, large-scale simulation, training systems, and interactive CAD/CAM design reviews.
Circle Reader Action Number 796.

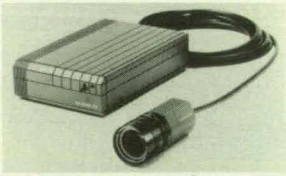

The 6700 Series **monochrome CCD camera** from Cohu Inc., San Diego, CA, features a lightweight remote imager measuring 1.5 inches in diameter and 2.1 inches in length. The camera offers high sensitivity up to 0.0125 lux, resolution of 525 horizontal TV lines, an electronic shutter for stop action, and a 100% blemish-free image sensor that eliminates dead pixels. The remote head is suited for machine vision, non-contact inspection, image processing, microscopy, robotics, and security/surveillance applications.
Circle Reader Action Number 792.

Resources Planning Associates Inc., Ithaca, NY, has introduced version 3.0 of CAPLIB, a **computer-aided planning library.** CAPLIB provides over 250 programming tools for building custom software that can utilize a broad range of complex spatial and temporal data, incorporate mathematical models, and integrate color graphics presentation capabilities. Version 3.0 offers an expanded set of cartographic data exchange utility programs, support of desktop publishing formats, provision of an icon generator, and new window routines. CAPLIB is available for both PC (DOS) or VAX (VMS) environments.
Circle Reader Action Number 790.

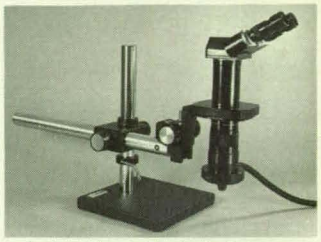

Infinity Photo-Optical Company, Boulder, CO, has developed a **continuously-focusable microscope** ideal for on-line inspection and imaging. At any working distance, the correct depth-of-field, magnification, and resolution are set by simply focusing the instrument. It has a continuous 1:45 magnification ratio, and focuses from infinity down to 6mm. The microscope has a primary magnification of 0.2 × at 150mm and 9 × at 6mm.
Circle Reader Action Number 800.

Boeshield T-9®, a new **penetrating lubricant** that protects metals against rust and corrosion, has been introduced by PMS Products Inc., Stuart, FL. Originally developed by the Boeing Company for use on aircraft components, Boeshield T-9 dries to a clean waxy film that will lubricate and protect any metal for months. It will also loosen rusted parts, and is safe for use on most paints, plastics and vinyls. A 12 ounce aerosol can sells for $7.95.
Circle Reader Action Number 794.

New Literature

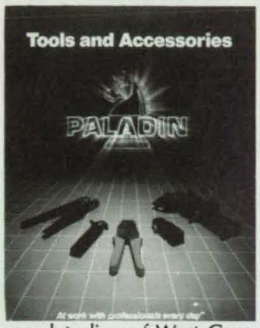

A complete line of West German-made **tools and accessories** is detailed in a four-color catalog from the Paladin Corp., Newbury Park, CA. Ergonomic screwdrivers, wire strippers and cutters, heat guns, telephone tools and kits, crimping tools, and production aid devices are described, as well as insulated safety and power transmission tools. The catalog contains product shots, application photos, and diagrams that explain the features and advantages of each product.
Circle Reader Action Number 740.

A new **silicone materials selection guide** from the Dow Corning Corp., Midland, MI, features over 150 products for the high-tech marketplace. The free booklet lists applications, product features needed for each application, and the matching silicone material. Application areas covered include conformal coatings, semiconductor molding compounds, organosilicon chemicals, and primers, as well as encapsulating, sealing, lubricating, laminating, and fire-resistant materials. General information on silicones and their processing characteristics is also provided.
Circle Reader Action Number 708.

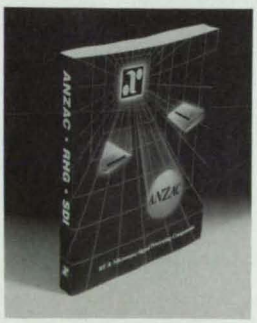

More than 500 **radio frequency (RF) and microwave signal processing components** are described in a new catalog from the Adams-Russell Components Group, Burlington, MA. The publication features state-of-the-art GaAs MMICs, logarithmic amplifiers, RF and microwave control devices, mixers, and hermetic surface devices, and includes application notes and design/selection guides.
Circle Reader Action Number 702.

Sprague Electric Company, Mansfield, MA, has published a catalog of standard **thick-film networks** available in molded and conformally coated or SIP and DIP packages. These networks are used in computer, telecommunications, military, and aerospace applications. The 52-page catalog includes test procedures, standard ratings data, and circuit diagrams.
Circle Reader Action Number 742.

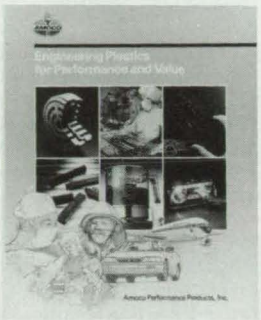

A new 20-page brochure from Amoco Performance Products Inc., Ridgefield, CT, illustrates the company's line of **engineering thermoplastics** including Udel® polysulfone, the Mindel® resin family, Radel® polyarylsulfone, Ardel® polyarylate, Torlon® polyamide-imide, Kadel® polyketone, and Xydar® liquid crystal polymers. Typical applications, properties, and comparative performance data are included.
Circle Reader Action Number 704.

Instrument Specialties Co. Inc., Delaware Water Gap, PA, has issued a new brochure on its **radio-frequency and electromagnetic interference testing capabilities.** Offered free of charge, the brochure covers the company's Certified Testing program to determine compliance with commercial and military EMC specifications. This includes RF, ESD, and EMP tests over the 20 Hz to 18 GHz frequency range with minimum radiated susceptibility levels of 200 V/m. Also covered are computer-controlled evaluations of shielded enclosures; cabinets and other facilities for magnetic and electric fields and plane wave attenuation; and EMP performance of shielded cables, connectors, RF gaskets, and other materials.
Circle Reader Action Number 706.

New Literature

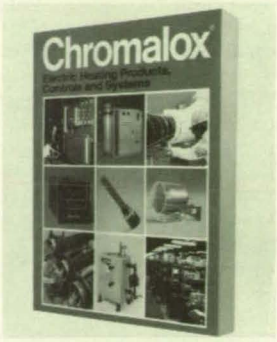

Over 8000 **industrial electric heaters, controls, and systems** are spotlighted in a free 600-page catalog from Chromalox Industrial Heating Products, Pittsburgh, PA. Product categories include process heaters, heat transfer systems, boilers, steam generators, heater components, appliance and other OEM heaters, space heaters, thermostats, monitors, and alarms.
Circle Reader Action Number 734.

Newport Corp., Fountain Valley, CA, has published a 496-page **precision laser and optics catalog** featuring over a hundred new products, including CAD Assistant™, a drawing library for optical experiment layout, and Projects in Optics, a self-paced course containing a study guide and the necessary equipment to complete ten projects. Stainless steel translation stages, vibration isolated workstations, precision rails, cylinder optic mounts, and a diode-pumped YAG ring laser are described as well. Tutorials and application notes supplement the product descriptions.
Circle Reader Action Number 730.

A new **optical encoder specifying guide** from the Industrial Encoder Division of BEI's Motion Systems Company, Goleta, CA, contains specifications for industrial position sensors, as well as various encoder options, such as count multiplications. Application areas for these products include robotics, process control, factory automation, and biomedicine.
Circle Reader Action Number 732.

The CAD Rating Guide from DSR Publishing Inc., Scarborough, ME, evaluates 103 **CAD software products** and systems. The guide compares software by price, compatibility, platform, and application, and lists user comments about each package. It also features a 30-page glossary of CAD terms.
Circle Reader Action Number 738.

A 12-page brochure on advanced **digital data communications links** is offered by Aydin Vector, Newtown, PA. Selected data link systems include computer to computer, programmable command and control, simplex burst-mode, simplex digital transmission, secure data, and secure voice. The systems are used in unmanned reconnaissance vehicles, drones, aircraft, weapons, land vehicles, and ships. Typical systems qualify for use in severe environments and provide multi-channel capability, with output up to 40 watts (100 W optional).
Circle Reader Action Number 736.

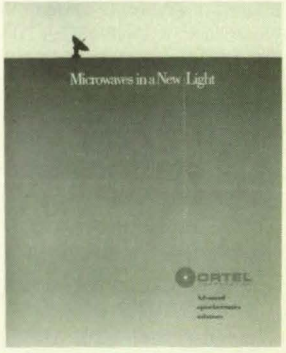

Ortel Corp., Alhambra, CA, is offering a brochure describing **laser fiber optic products** for radio frequency and microwave transmission. The publication outlines typical microwave applications for Ortel links, including satellites, delay lines, shipboard EW systems, phased array radars, remote antenna links, nanosecond measurements, test equipment, and antenna ranges. Diagrams and charts summarize typical link performance levels and the advantages of analog fiber optic links.
Circle Reader Action Number 728.

New Literature

Two new **epoxy prepreg systems** designed for use on high-performance military and commercial aircraft structures are described in literature from US Polymeric Inc., Santa Ana, CA. Offering a performance range of 180° to 350°F, the prepreg systems are suited for application where impact resistance and damage tolerance are needed. The brochures contain data on resin properties, prepreg properties on intermediate and standard modulus carbon fibers, cure cycles, and layup diagrams.
Circle Reader Action Number 716.

A new **desktop manufacturing system** jointly developed by DeSoto Inc. (Des Plaines, IL) and Laser Fare Ltd. (Smithfield, RI) enables rapid production of three-dimensional models or prototypes. As described in a free four-color brochure, the invention incorporates state-of-the-art optical fabrication technology; computer-generated design data is transmitted to a laser, which cures light-sensitive liquid polymer to form a solid model. The system can create a model in three days to two weeks, depending on part complexity, with accuracy of up to .005".
Circle Reader Action Number 726.

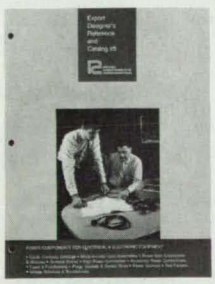

The Export Designer's Reference Guide published by Panel Components Corp., Santa Rosa, CA, features information on international electrical requirements, test and standards agencies, and regulations. The introduction illustrates how to design and manufacture electronic components for export markets, while each product section — international cords, cordsets, plugs, sockets, and connectors — outlines relevant international safety issues and regulations.
Circle Reader Action Number 718.

The MLC-XT™ **industrial computer** is described in a free brochure from Micro Linear Controls Inc., Racine, WI. A full computer and solid state disk drive on a compact 6.4" x 4.2" board, the MLC-XT combines the flexibility of 100% PC compatibility with the reliability of an industrial controller. It accomodates powerful programming languages such as BASIC, Fortran, and C, and features an integrated watchdog timer that monitors hardware and software behavior.
Circle Reader Action Number 712.

A new report spotlights **graphite fiber products** manufactured by Hercules Aerospace Company, Magna, UT. Endowed with high strength and stiffness, thermal stability, and resistance to corrosion and fatigue, the fibers have found widespread application in the aerospace, industrial, automotive, and recreational markets. Products featured include continuous and chopped fibers, woven fabrics, resin systems, prepregs, and 3D woven preforms.
Circle Reader Action Number 714.

Design and Manufacturing Corp., Cleveland, OH, is offering free literature on their **electro-thermal actuators.** The patented devices are designed to provide uniform thrust to a rolling diaphragm piston through rapid vaporization of a controlled working fluid inside a sealed chamber. Employed in automotive, aviation, heating, and other industries, the actuators require no external controls or lubrication and are electrically and mechanically silent.
Circle Reader Action Number 720.

The **local area network(LAN)** connectivity products market is expected to grow from the present level of $210 million to nearly $2.7 billion by 1993, according to a new report released by Market Intelligence Research Company, Mountain View, CA. Emerging trends include the collapse of market segments, an increase in software-based products, faster link speeds, and loss of distinction between wide area and local area networks. The report features an industry review, profiles of key competitors, and an extensive list of manufacturers.
Circle Reader Action Number 710.

Subject Index

NASA Tech Briefs, ISSN 0145-319X, USPS 750-070, copyright © 1989 in U.S., is published monthly by Associated Business Publications Co., Ltd. 41 E. 42nd St., New York, NY 10017-5391. The copyrighted information does not include the individual Tech Briefs which are supplied by NASA. Editorial, sales, production and circulation offices at 41 E. 42nd Street, New York, NY 10017-5391. Subscriptions for non-qualified subscribers in the U.S., Panama Canal Zone, and Puerto Rico, $75.00 for 1 year; $125.00 for 2 years; $200 for 3 years. Single copies $10.00. Remit by check, draft, postal or express orders. Other remittances at sender's risk. Address all communications for subscriptions or circulation to NASA Tech Briefs, 41 E. 42nd Street, New York, NY 10017-5391. Second-class postage paid at New York, NY and additional mailing offices.

POSTMASTER: please send address changes to NASA Tech Briefs, 41 E. 42nd Street, Suite 921, New York, NY 10017-5391.

Erratum

In NTB Vol. 13, Num. 8, the subject index incorrectly listed the brief "Adherent Thermal Barrier for Combustion Chambers" as appearing on page 40. The correct title for the brief published on that page is "Optical Interferometric Micrometrology," classified under the following titles: Interferometry, Laser Interferometry, and Metrology.

← **Circle Reader Action No. 303**

Advertiser's Index

***RAC** stands for **Reader Action Card.** For further information on these advertisers, please circle the RAC number on the Reader Action Card elsewhere in this issue. This index has been compiled as a service to our readers and advertisers. Every precaution is taken to ensure its accuracy, but the publisher assumes no liability for errors or omissions.

AMCO ENCLOSURES. THEY'RE LOADED EVEN WHEN THEY'RE EMPTY.

George Sergeena, Quality Control:

"My title is misleading, in a way. 'Cause everyone at AMCO is gung-ho on quality control."

"These enclosures become 'home' to equipment that deserves the best. Some of our enclosures have housed systems that work miracles. Like the modular system we designed for NASA way back in Mercury Project days.

We take your specs and work to improve the results. We know the quality of the product is only as good as the workmanship involved.

And me? I'm seldom in my office waiting for a problem to pop up. I'm out on the floor trying to prevent them. OK quality is a word and anybody can say it. But you spend 30 minutes in our plant, and the quality is so real you can almost *feel* it."

"It's as simple as this: you work at AMCO, you get fanatical about quality."

Call us now for your free full color catalog. #800 shows our general modular enclosure line, #500B is our 5-Work day fast-delivery line.
Dial 1-800/833-3156.
In Illinois 1-312/671-6670.*

*As of November 11, 1989—New Area Code will be **708**.

AMCO®

AMCO Engineering Co.
3801 N. Rose Street
Schiller Park, IL 60176-2190

AMCO GETS THERE FIRST.

See us at the ISA Show 10/22 – 10/26
Philadelphia, PA Booth #7025

Circle Reader Action No. 500

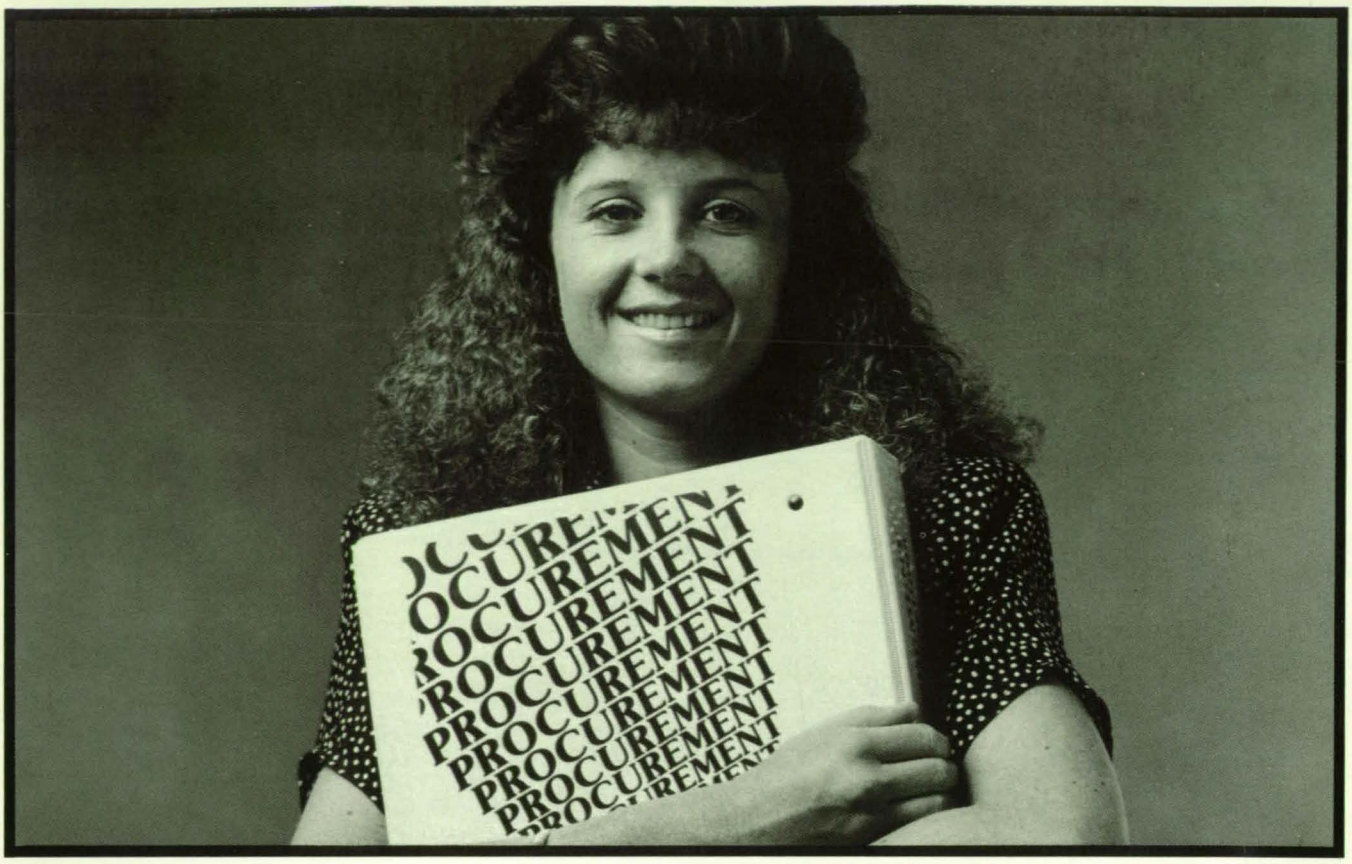

"I didn't want to publish this book until it was finished, until it was perfect.

Putting it together I worked with just about everybody involved in procurement. Getting all of their ideas for what it should include. Organizing their input into sections that made sense. And then going back to everybody again. Together we've developed a manual that really works—a consistent point of reference for old hands and a great tool for newcomers.

It isn't perfect though, because there are always going to be changes—new data to add, new procedures to outline. Sometimes that's a little frustrating, but I still work with perfection as my goal. The people using this book are counting on me for that." *—Lori Pugh, Space Systems Secretary*

MCDONNELL DOUGLAS
A company of leaders.

Circle Reader Action No. 501